

Middle Jurassic to Early Cretaceous tectonic evolution of the western Klamath Mountains and outboard Franciscan assemblages, northern California-southern Oregon, USA

Alan D. Chapman*

Geology Department, Macalester College, 1600 Grand Avenue, St. Paul, Minnesota 55105, USA

Doug Yule

Department of Geological Sciences, California State University Northridge, 18111 Nordhoff Street, Northridge, California 91355-8266, USA

William Schmidt

Department of Earth Sciences, University of Southern California, 3651 Trousdale Parkway, Los Angeles, California 90089, USA

Todd LaMaskin

Department of Earth and Ocean Sciences, University of North Carolina Wilmington, 601 S. College Road, Wilmington, North Carolina 28403, USA

ABSTRACT

The Klamath Mountains province and adjacent Franciscan subduction complex (northern California-southern Oregon) together contain a world-class archive of subduction-related growth and stabilization of continental lithosphere. These key elements of the North American Cordillera expanded significantly from Middle Jurassic to Early Cretaceous time, apparently by a combination of tectonic accretion and continental arc- plus rift-related magmatic additions. The purpose of this field trip is twofold: to showcase the rock record of continental growth in this region and to discuss unresolved regional geologic problems. The latter include: (1) the extent to which Mesozoic orogenesis (e.g., Siskiyou and Nevadan events plus the onset of Franciscan accretion) was driven by collision of continental or oceanic fragments versus changes in plate motion, (2) whether growth involved "accordion tectonics" whereby marginal basins (and associated fringing arcs) repeatedly opened and closed or was driven by the accretion of significant volumes of material exotic to North America, and (3) the origin of the Condrey Mountain schist, a composite low-grade unit occupying an enigmatic structural window in the central Klamaths—at odds with the

^{*}Email: chapman@macalester.edu

Chapman, A.D., Yule, D., Schmidt, W., and LaMaskin, T., 2021, Middle Jurassic to Early Cretaceous tectonic evolution of the western Klamath Mountains and outboard Franciscan assemblages, northern California–southern Oregon, USA, *in* Booth, A.M., and Grunder, A.L., eds., From Terranes to Terrains: Geologic Field Guides on the Construction and Destruction of the Pacific Northwest: Geological Society of America Field Guide 62, p. 73–130, https://doi.org/10.1130/2021.0062(04). © 2021 The Authors. Gold Open Access: This chapter is published under the terms of the CC-BY license and is available open access on www.gsapubs.org.

east-dipping thrust sheet regional structural "rule." Respectively, we assert that (1) if collision drove orogenesis, the requisite exotic materials are missing (we cannot rule out the possibility that such materials were removed via subduction and/or strike slip faulting); (2) opening and closure of the Josephine ophiolite-floored and Galice Formation-filled basin demonstrably occurred adjacent to North America; and (3) the inner Condrey Mountain schist domain is equivalent to the oldest clastic Franciscan subunit (the South Fork Mountain schist) and therefore represents trench assemblages underplated >100 km inboard of the subduction margin, presumably during a previously unrecognized phase of shallow-angle subduction. In aggregate, these relations suggest that the Klamath Mountains and adjacent Franciscan complex represent telescoped arc and forearc upper plate domains of a dynamic Mesozoic subduction zone, wherein the downgoing oceanic plate took a variety of trajectories into the mantle. We speculate that the downgoing plate contained alternating tracts of smooth and dense versus rough and buoyant lithosphere—the former gliding into the mantle (facilitating slab rollback and upper plate extension) and the latter enhancing basal traction (driving upper plate compression and slab-shallowing). Modern snapshots of similarly complex convergent settings are abundant in the western Pacific Ocean, with subduction of the Australian plate beneath New Guinea and adjacent island groups providing perhaps the best analog.

INTRODUCTION

The purpose of this trip is to inspect the rock record of Middle Jurassic to Early Cretaceous continental crustal growth in the Klamath Mountains province (KMP) and adjacent areas (Fig. 1). In this time period, the KMP doubled in width perpendicular to the continental margin and thickened to permit magmatic differentiation at depths greater than 25 km (Snoke and Barnes, 2006). Tectonic (i.e., shortening and underplating) and igneous (i.e., arc plutonism and extensional basin magmatism) processes undoubtedly facilitated expansion of the KMP. However, the relative roles that subduction dynamics (e.g., variations in convergence rate, trajectory, and/or angle of underthrusting) versus collision(s) of far-traveled thickened lithosphere (e.g., microcontinents or oceanic plateaus) played in modulating these processes is less certain (Saleeby et al., 1982; McClelland et al., 1992; Harper and Wright, 1984; Wright and Fahan, 1988; Hacker et al., 1995; Shervais et al., 2005; Sigloch and Mihalynuk, 2013, 2017; Clennett et al., 2020; LaMaskin et al., 2021).

On this trip, we will attempt to shed light on the tectonic mechanisms that drove Middle Jurassic to Early Cretaceous growth of the KMP. Specifically, the trip will focus on the petrologic and structural records of: (1) Middle and Late Jurassic orogenesis (e.g., Siskiyou and Nevadan events); (2) broadly coeval and spatially overlapping extension, ophiolite formation, and marginal basin development; and (3) Early Cretaceous migration of the KMP from the axis of arc magmatism to the forearc and related (?) regional extension and marine transgression. During the trip, we will address several questions pertinent to the tectonic development of the KMP and adjacent provinces. For example, what proportion of KMP growth was driven by accretion of materials formed adjacent to, versus outside of,

North America (Snoke, 1977; Gray, 1986; Burchfiel et al., 1992; Yule et al., 2006; Sigloch and Mihalynuk, 2013; LaMaskin et al., 2021)? How were extension and rifting of the KMP achieved during convergence between North America and the (paleo-) Pacific realm, and can this explain the overlapping magmatic belts like the Rogue-Chetco and Wooley Creek arcs? What is the origin of the Condrey Mountain tectonic window, and how did trench assemblages contained within achieve their far-inboard, and structurally deep, position (e.g., Irwin, 1960; Hotz, 1979)? Finally, what triggered the apparent Early Cretaceous switch from non-accretion to significant accretion in the Franciscan subduction complex (e.g., Dumitru et al., 2010)?

Addressing the above questions permits comparisons with modern continental margins, allowing a global perspective from the western KMP regional example. For example, does this area contain a record of collision and docking (e.g., collision of the Indian subcontinent with Asia or the Ontong-Java oceanic plateau with the Solomon Islands arc), changes in plate motion (e.g., slab steepening beneath New Zealand or shallowing beneath Peru), or some combination thereof (e.g., subduction of alternating rough and smooth patches of seafloor with the margin, like those observed on the Australian plate where it impinges New Guinea, New Britain, New Hebrides, and the Solomon Islands)? Also, did the marginal ocean basin with highly oblique spreading ridge segments envisioned for the Josephine-Galice basin resemble the modern Andaman Sea region? Such comparisons provide valuable insights into how "snapshots" of actively deforming margins will evolve to resemble ancient "processed" margins such as the KMP.

The trip is arranged such that each day has a specific focus. The planned stops bear most significantly on discussions of Middle to Late Jurassic orogenesis and rifting and Early Cretaceous

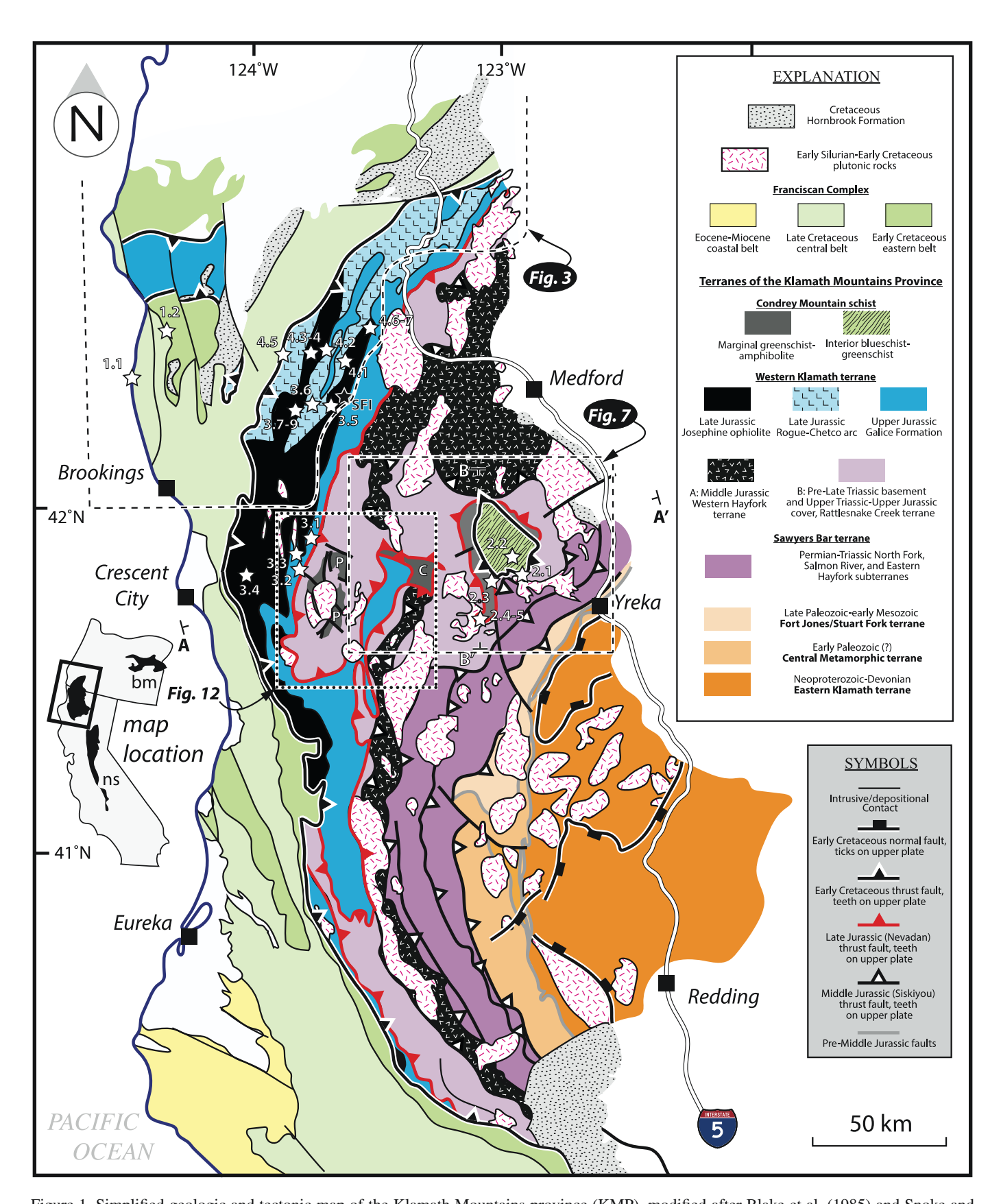


Figure 1. Simplified geologic and tectonic map of the Klamath Mountains province (KMP), modified after Blake et al. (1985) and Snoke and Barnes (2006), with planned field-trip stops (white stars) and Siskiyou Field Institute (SFI, black star) overlain. Traces of cross-sections A–A′ and B–B′ (Fig. 7B) overlain. Inset abbreviations: bm—Blue Mountains; ns—northern Sierra. Map abbreviations: C—China Peak complex; P—Preston Peak complex.

trenchward displacement of the KMP and associated subduction accretion. Day 1 traverses from outboard to inboard portions of the Franciscan subduction complex, examining the Gold Beach and Pickett Peak terranes, respectively. Day 2 will concentrate on the Condrey Mountain schist and associated problems. Days 3 and 4 focus on the products of KMP rifting, including the Josephine ophiolite, Rogue River arc, Galice Formation, and detached Rattlesnake Creek terrane equivalents.

GEOLOGIC BACKGROUND

Paleozoic and Mesozoic Assembly of the Klamath Mountains Province

Numerous long (100s to 1000s of km), parallel, arcuate belts of accreted material comprise the North American Cordillera, resulting from hundreds of millions of years of convergent margin tectonics following Neoproterozoic rifting of supercontinent Rodinia and the development of a passive margin (Burchfiel et al., 1992; Dickinson, 2004; Blakey and Ranney, 2018). Here, we focus on Paleozoic and Mesozoic events germane to construction of the KMP, northern California and southwestern Oregon, and adjacent Franciscan assemblages (Fig. 1).

Neoproterozoic to Devonian basement rocks of the Eastern Klamath terrane, interpreted as dismembered remnants of island arcs of the Paleo-Pacific (i.e., Panthalassa) ocean, are the cornerstone of the Klamath Mountains upon which the remainder of the range was built (Moores, 1970; Speed, 1979; Schweickert and Snyder, 1981; Burchfiel et al., 1992; Wallin and Metcalf, 1998; Wallin et al., 2000; Wright and Wyld, 2006; Grove et al., 2008; Fig. 1). Late Paleozoic docking of the Eastern Klamath terrane with the western margin of North America was preceded by Silurian-Devonian eastward subduction of Panthalassan oceanic lithosphere and derivative upper plate magmatism and underplating of Central Metamorphic terrane oceanic assemblages (Davis, 1968; Irwin, 2003; Barrow and Metcalf, 2006). The resulting composite terrane was conveyed toward, and collided with, the western margin of North America via a west-dipping subduction zone, driving Late Permian-Early Triassic closure of the Golconda-Slide Mountain basin and eastward thrusting of deepwater assemblages atop shallow water passive margin sequences in the Great Basin and adjacent areas (i.e., the Sonoma orogeny; Speed, 1977; Schweickert and Snyder, 1981; Wyld, 1991; Burchfiel et al., 1992; Dickinson, 2000). Transfer of the composite terrane to the North American plate was accompanied by formation of the Fort Jones/Stuart Fork accretionary complex, a possible along-strike equivalent of the Cache Creek assemblage of the Canadian Cordillera (e.g., Johnston and Borel, 2007), and arc magmatism (the "McCloud arc" of Miller, 1987) above the eastward subducting Panthalassa lithosphere (Wright, 1982; Coleman et al., 1988; Goodge, 1989).

The Paleozoic-Early Mesozoic nucleus of the Klamath mountains (i.e., the terranes joined above), now a part of the North American plate, grew significantly during the Middle

Jurassic (ca. 169-161 Ma) Siskiyou orogeny (e.g., Coleman et al., 1988; Wright and Fahan, 1988; Hacker et al., 1995; Snoke and Barnes, 2006). During this event, sequential accretion of three additional "terranes" is interpreted to have occurred, the first and most easterly of which is the Sawyers Bar terrane (Coleman et al., 1988; Ernst, 1990; Hacker and Ernst, 1993; Hacker et al., 1995; Scherer and Ernst, 2008; Scherer et al., 2010; Ernst et al., 2017). Some workers divide this terrane into North Fork, Salmon River, and Eastern Hayfork subterranes, together representing a Permian oceanic arc, overlying Permian-Triassic deep sea and terrigenous sedimentary cover, and outboard accretionary wedge. Accretion of the Western Hayfork and Rattlesnake Creek terranes followed. Respectively, these terranes represent a ca. 177-167 Ma continent-fringing oceanic arc and a dismembered ophiolitic assemblage (Irwin, 1972; Wright, 1982; Harper and Wright, 1984; Coleman et al., 1988; Wright and Fahan, 1988; Wright and Wyld, 1994; Barnes and Barnes, 2020). The latter consists of basal serpentinite matrix mélange, ca. 207-193 Ma mafic volcanic plus plutonic assemblages, and volcaniclastic and hemipelagic cover strata, all of which experienced amphibolite-granulite facies metamorphism. The Rattlesnake Creek terrane is widely regarded to represent the basement of the Western Hayfork terrane (e.g., Wright and Fahan, 1988; Donato et al., 1996).

The Rattlesnake Creek terrane is nonconformably overlain by pre-164 Ma greenschist facies mafic intrusive and volcanic rocks plus hemipelagic sedimentary rocks (the Preston Peak complex; e.g., Snoke, 1977; Saleeby et al., 1982) and tectonically underlain by ca. 172-170 Ma amphibolite facies mafic volcanic rocks and hemipelagic sediments (the China Peak complex; Saleeby and Harper, 1993). Both China Peak and Preston Peak complexes are interpreted as early products of interarc extension that culminated in the ca. 164–162 Ma Josephine ophiolite, the basement of the Western Klamath terrane (Saleeby and Harper, 1993). Lithologic and age similarities between the China Peak and Preston Peak complexes suggest that the former may represent the underthrust equivalent of the latter. Furthermore, these mafic complexes are lithologically similar to, and overlap in age with, the Western Hayfork arc; the possibility that these materials represent tectonically dispersed equivalents is explored on this trip.

The Siskiyou event was immediately followed by oblique rifting of newly accreted Western Hayfork arc and its Rattle-snake Creek terrane basement, forming the ca. 164–162 Ma Josephine ophiolite-floored basin while arc activity broadened to span both sides of the rift zone (represented by the ca. 165–156 Ma Wooley Creek plutonic belt to the east and the ca. 161–155 Ma Rogue-Chetco arc to the west; Saleeby et al., 1982; Harper, 1984; Wright and Wyld, 1986; Wright and Fahan, 1988; Hacker and Ernst, 1993; Harper et al., 1994; Harper, 2003; Allen and Barnes, 2006; Snoke and Barnes, 2006; Yule et al., 2006). Deposition of the Galice Formation (sensu lato) ensued in the submarine Josephine marginal basin, first with ca. 162–157 Ma (Oxfordian) argillite and transitioning to

ca. 153-150 Ma (Kimmeridgian) turbidite, as regional extensional stresses yielded to contractile deformation associated with the ca. 157–150 Ma Nevadan orogeny (Saleeby and Harper, 1993; Harper et al., 1994; Schweickert et al., 1984; Hacker et al., 1995; Miller and Saleeby, 1995; Shervais et al., 2005; MacDonald et al., 2006). The Nevadan event is responsible for thrusting the Western Klamath terrane (including the Rogue-Chetco arc plus consanguineous Josephine ophiolite and nonconformably overlying Galice formation) beneath previously accreted terranes. It should be noted that there is no consensus at this time regarding the driving mechanism(s) for Nevadan and Siskiyou events, with end member models invoking either collisions of oceanic ridges or far-traveled lithospheric blocks such as the Wrangellia-Alexander superterrane (e.g., Schweickert and Cowan, 1975; Wernicke and Klepacki, 1988; McClelland et al., 1992; Saleeby and Harper, 1993; Shervais et al., 2005) and/or changes in relative plate motion (e.g., Wright and Fahan, 1988; Wolf and Saleeby, 1995; Hacker et al., 1995).

In Early Cretaceous time, the KMP moved ~200 km westward to achieve the current position and concave-east arcuate curvature relative to correlative rocks in the northern Sierra Nevada and Blue Mountains (Fig. 1 inset; Jones and Irwin, 1971; Ernst, 2013). During this episode: (1) magmatism in the Klamaths abruptly terminated ca. 136 Ma, in marked contrast to the Sierra Nevada and Blue Mountains where magmatism continued until Late Cretaceous time (Chen and Moore, 1982; Lund and Snee. 1988; Barnes et al., 1996; Allen and Barnes, 2006; Gaschnig et al., 2017); (2) an accretionary wedge, represented by the eastern belt of the Franciscan Complex, formed and grew rapidly along the western edge of the Western Klamath terrane without any intervening forearc basin (Dumitru et al., 2010); (3) the Western Klamath terrane, eastern belt Franciscan rocks, and the Condrey Mountain schist (discussed in the following section) cooled from ~400–200 °C between ca. 135 and 118 Ma (Helper, 1985; Harper et al., 1994; Batt et al., 2010a; Dumitru et al., 2010); (4) low-angle normal faulting commenced in the eastern Klamaths (Cashman and Elder, 2002; Batt et al., 2010b); and (5) topography built up during earlier tectonism was lost during an eastward sweeping Valanginian-Hauterivian marine transgression across the majority of the KMP (Harper et al., 1994; Batt et al., 2010a). These relations strongly suggest that the KMP was affected by a shallow-angle subduction episode. The details surrounding this episode and possible driving mechanisms will be discussed on this trip.

Tectonic "Rosetta stones" of the Klamath Mountains Province

This trip will focus on Mesozoic domains of the Klamath Mountains province (KMP), plus the adjacent Franciscan complex. The petrogenetic histories of each domain are described herein, as these domains provide the necessary cipher to decoding the Mesozoic tectonic development of the province and adjacent areas.

Middle-Late Jurassic Rogue-Galice-Josephine Marginal Ocean Basin

The western Jurassic belt of the Klamath Mountains (Irwin, 1960), also referred to as the Western Klamath terrane (WKT; Blake et al., 1985), is one of Earth's best-preserved, ancient marginal ocean basin systems (Saleeby et al., 1982; Harper and Wright, 1984). It consists of Late Jurassic upper mantle and oceanic crustal rocks that comprise three coeval tectonostratigraphic elements: the Rogue-Chetco volcanic-plutonic oceanic arc (Garcia, 1982), Josephine ophiolite (Harper, 1980, 1984), and Galice hemipelagic and flysch deposits (Wells and Walker, 1953; Garcia, 1979; Harper, 1984; Pessagno and Blome, 1990; Fig. 2). The Galice Formation conformably overlies the Josephine ophiolite and interlayers with the Rogue volcanic rocks (Garcia, 1979; Yule et al., 2006). A fourth element is a Triassic and Middle Jurassic, poly-genetic, block-on-block, and serpentinite-matrix mélange unit—referred to as the Onion Camp complex (OCC) —that forms the wallrocks for the arc and ophiolitic intrusive rocks and the substrate for the arc volcanic rocks and hemipelagic and flysch deposits. Distinct lithologic, structural, age, and geochemical characteristics link the OCC with the Rattlesnake Creek terrane (Yule et al., 2006). The OCC-Rattlesnake Creek terrane linkage crosses the Preston Peak (Orleans) thrust, a major terrane-bounding structure in the Klamath province with 10s to >100 km of displacement (Harper et al., 1994). A fifth element is the Briggs Creek amphibolite (Coleman and Lanphere, 1991), and a sixth is a polylithic breccia and megabreccia unit—known as the Fiddler Mountain olistostrome (Yule et al., 2006)—whose clast provenance identifies both the OCC and Josephine ophiolite as sources. Similar olistostromes are known elsewhere in the Klamaths (e.g., Ohr, 1987; Wyld and Wright, 1988).

The pre-accretion history of the WKT supports a North American margin-adjacent, rift-origin model for the Rogue-Chetco arc and Josephine ophiolite (Snoke, 1977; Saleeby et al., 1982; Harper and Wright, 1984). Basinal sediments provide unmistakable evidence for a close proximity to the continent (see Middle-Upper Jurassic Sedimentation across the KMP section). A "local" rift-origin also predicts that the Rogue-Josephine ocean basin may contain rifted fragments of older (pre-165 Ma) Klamath terranes. The discovery of Rattlesnake Creek terrane-equivalent OCC within the WKT supports the model and documents a linkage between thrust sheets previously considered "exotic" with respect to one another.

Josephine ophiolite. The "Rosetta stone" of Cordilleran ophiolites, the Josephine ophiolite, is exposed over an ~ 900 km² region of the California-Oregon border region (Fig. 1). The Josephine peridotite alone is exposed over 650 km² representing one of the largest peridotite masses in the world (Dick, 1976). In its type location in the Smith River drainage of northern California, the complete ophiolite sequence is preserved and is mildly deformed and metamorphosed to greenschist and subgreenschist grade conditions (Harper, 1984). Radiometric ages obtained from the ophiolite include apparent ages of 162 ± 1.5 Ma (U-Pb zircon) in plagiogranite and 165.3 ± 3.1 Ma (Ar/Ar

78

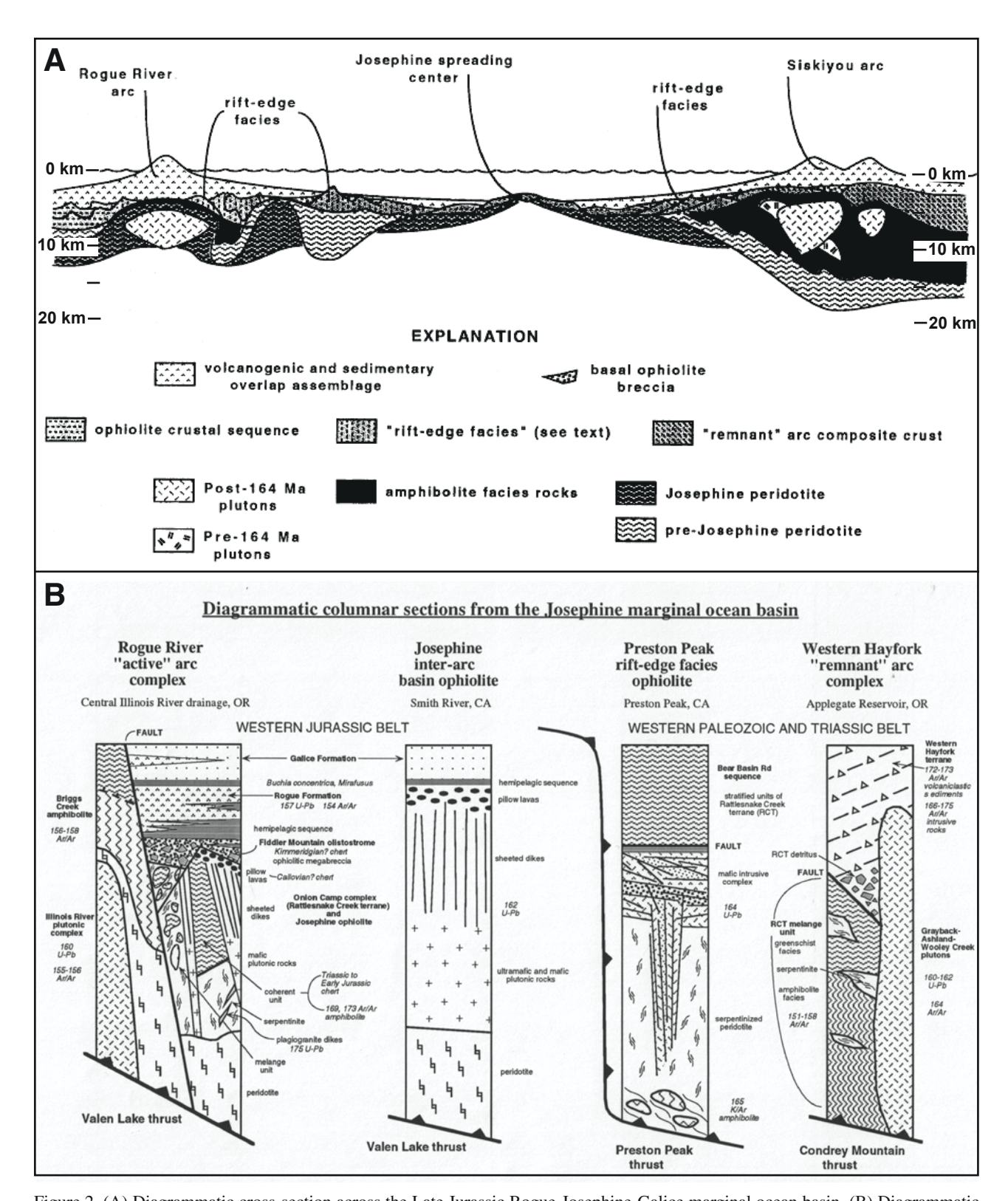


Figure 2. (A) Diagrammatic cross-section across the Late Jurassic Rogue-Josephine-Galice marginal ocean basin. (B) Diagrammatic columnar sections from the Late Jurassic Rogue-Josephine-Galice marginal ocean basin. Sections are modified from Yule (1996; active arc); Harper et al. (1994; inter-arc ophiolite); Snoke (1977; rift-edge facies in remnant "Siskiyou" arc); and Hacker et al. (1995; Middle Jurassic remnant arc). RCT—Rattlesnake Creek Terrane.

amphibole) from meta-gabbro cut by diabase dikes (Saleeby and Harper, 1993; Harper et al., 1994). The geochemical data from crustal rocks of the ophiolite plot in a field transitional between MORB and IAT on trace and REE discrimination diagram plots (e.g., Ti vs Zr) and are consistent with the interpretation that the ophiolite formed above a subduction zone at inter-arc spreading centers (Shervais, 1982; Pearce et al., 1984). Slow- to intermediate-spreading rates are suggested by a number of structural and geometric features exhibited by the ophiolite, including tectonically thinned and rotated crustal sections and abundant oceanic faults (Alexander and Harper, 1992).

Rogue River island arc complex. The Rogue River island arc complex, defined by Garcia (1979, 1982), is a Late Jurassic magmatic arc that formed the fringing arc of the Josephine marginal ocean basin (Snoke, 1977; Saleeby et al., 1982; Harper and Wright, 1984). The Rogue arc consists of an arc volcano-plutonic complex and various highly deformed and metamorphosed mafic and ultramafic rocks interpreted to represent the wallrocks and basement terrane for the arc (Garcia, 1982).

The arc plutonic complex, designated the Illinois River gabbro by Jorgenson (1970) and Illinois River batholith (IRB) by Garcia (1982), is a tholeiitic, reversely zoned, gabbroic to tonalitic plutonic complex (McLachlin, 2011; Weiss, 2014). We use "IRB" when referring to these batholithic rocks in this guidebook. Hotz (1971) defined the "Chetco complex" to include IRB rocks plus the associated Rum Creek meta-gabbro and Pearsoll Peak and Chrome Ridge peridotite bodies (Ramp, 1961). Several K/Ar hornblende ages from the meta-gabbros yield 155-154 Ma ages for the central and northern part of the complex (Hotz, 1971). Two additional K/Ar hornblende ages of ~157 and 160 Ma (Dick, 1976) were determined for hornblende gabbro samples collected from the southern part of the IRB. Yule et al. (2006) report U/Pb zircon ages of 160 ± 0.5 Ma for the main phase gabbro, norite, and gabbro; 160.5 ± 0.5 Ma for dikes that intrude the wallrocks; 157-155 Ma for a late stage tonalite sill; and 40Ar/39Ar hornblende plateau ages from gabbro give ages of ~156-155 Ma.

Basaltic to andesitic, volcaniclastic turbidites and volcanic breccias of the Rogue Formation are interpreted to represent the extrusive equivalents of the IRB based on their similar age (~157 Ma) and similar mineral chemistry signatures (Garcia, 1982; Saleeby, 1984). Additional age control is provided by a 153.4 + 0.6 Ma ⁴⁰Ar/³⁹Ar igneous hornblende age from a lithic tuff breccia collected immediately downstream from the Illinois River falls (Yule et al., 2006). Rocks of the Rogue Formation comprise the northern part of the WKT and occur in relative close proximity to the IRB (Figs. 1 and 3). However, scarce occurrences of thin volcanogenic beds are reported to the south of the main outcrop belt where they are interbedded with strata of the Galice Formation (Harper, 1984).

Peridotite and amphibolite gneiss and schist occupy regions flanking the IRB and in places are thrust over the Dothan Formation (Figs. 1, 3, and 4). The Pearsoll Peak and Chrome Ridge peridotite bodies are considered fragments of the Josephine peridotite, but a definitive linkage is not yet proven. The Briggs Creek amphibolite (BCA) body is interpreted by Coleman and Lanphere (1991) to represent an allochthonous slice of metamorphosed oceanic crust with an ocean island basalt component, and they proposed that the BCA may represent high-grade equivalents to the Franciscan high-grade blocks. Separate occurrences of amphibolite tectonite that are lithologically identical to the BCA are exposed beneath the Madstone Cabin thrust fault (Loney and Himmelberg, 1977; Harper et al., 1994). There, minor and trace element abundances and the occurrence of rhodonite supports linking the Madstone amphibolites with the Rattlesnake Creek terrane. Thus, the metamorphic wallrocks of the IRB appear to have been derived from at least two types of progenitor materials. 40 Ar/ 39 Ar hornblende ages from the BCA give 157.9 + 0.5, 156.3 + 0.5 Ma Ar/Ar (Yule et al., 2006), and 156.4 + 0.9 Ma (Hacker et al., 1995). K-Ar ages range from 155 to 131 Ma (Garcia, 1979, 1982; Coleman and Lanphere, 1971). Several 190–200 K/Ar mineral ages reported by Dick (1976) that once seemed anomalous, may in fact record OCC magmatism consistent with Triassic and Early Jurassic ages common to the Rattlesnake Creek terrane (e.g., Wyld and Wright, 1988).

Galice Formation. Galice Formation strata conformably overlap volcanic rocks of both the Josephine ophiolite and the Rogue Formation (Pessagno and Blome, 1990). In the Josephine section (Harper, 1984; Harper et al., 1988; Saleeby and Harper, 1993), the basal Galice Formation strata consist of Late Callovian pelagic and hemipelagic deposits that grade upward into Oxfordian-Kimmeridgian flysch sediments (Pessagno and Blome, 1990). In the Rogue section (Wells et al., 1949; Irwin, 1966; Coleman, 1972), the pelagic and hemipelagic sediments interfinger with Rogue Formation deposits. Here, Oxfordian-Kimmeridgian flysch deposits conformably overlap the Rogue Formation volcanogenic strata (Pessagno and Blome, 1990). The Rogue and Josephine overlap sections are interpreted to represent lateral facies equivalents (Harper, 1984; MacDonald et al., 2006).

Primary sedimentary minerals contained within the Galice Formation are overprinted by prehnite-pumpellyite to lower greenschist facies metamorphic assemblages (Harper et al., 1988, 1994). Furthermore, sedimentary structures (e.g., cross-bedding, graded bedding, and fluid escape structures) are overprinted by tight-to-isoclinal folds and associated cleavage, LS fabrics, tension gashes, and brittle faults (Kays, 1968; Snoke, 1977; Garcia, 1979; Harper, 1980, 1984, 2006; Norman, 1984; Gray, 1985, 2006; Wyld, 1985). The degree of metamorphism generally tracks with that of deformation, with both increasing from southern Oregon into northern California (Harper, 1980; Harper et al., 1988). Metamorphism and deformation of the Galice Formation is attributed to the Late Jurassic Nevadan orogeny (Harper et al., 1994; Harper, 2006).

Onion Camp complex. The Onion Camp complex (OCC) is named for an association of Late Triassic to Early Jurassic rocks extending along a 40 km-long by 3–4-km-wide, NE-SW belt that extends from west of Cave Junction, Oregon, northward to the Hellgate Canyon of the Rogue River (Figs. 3 and 5). The boggy terrain in upland areas provides an ideal setting for

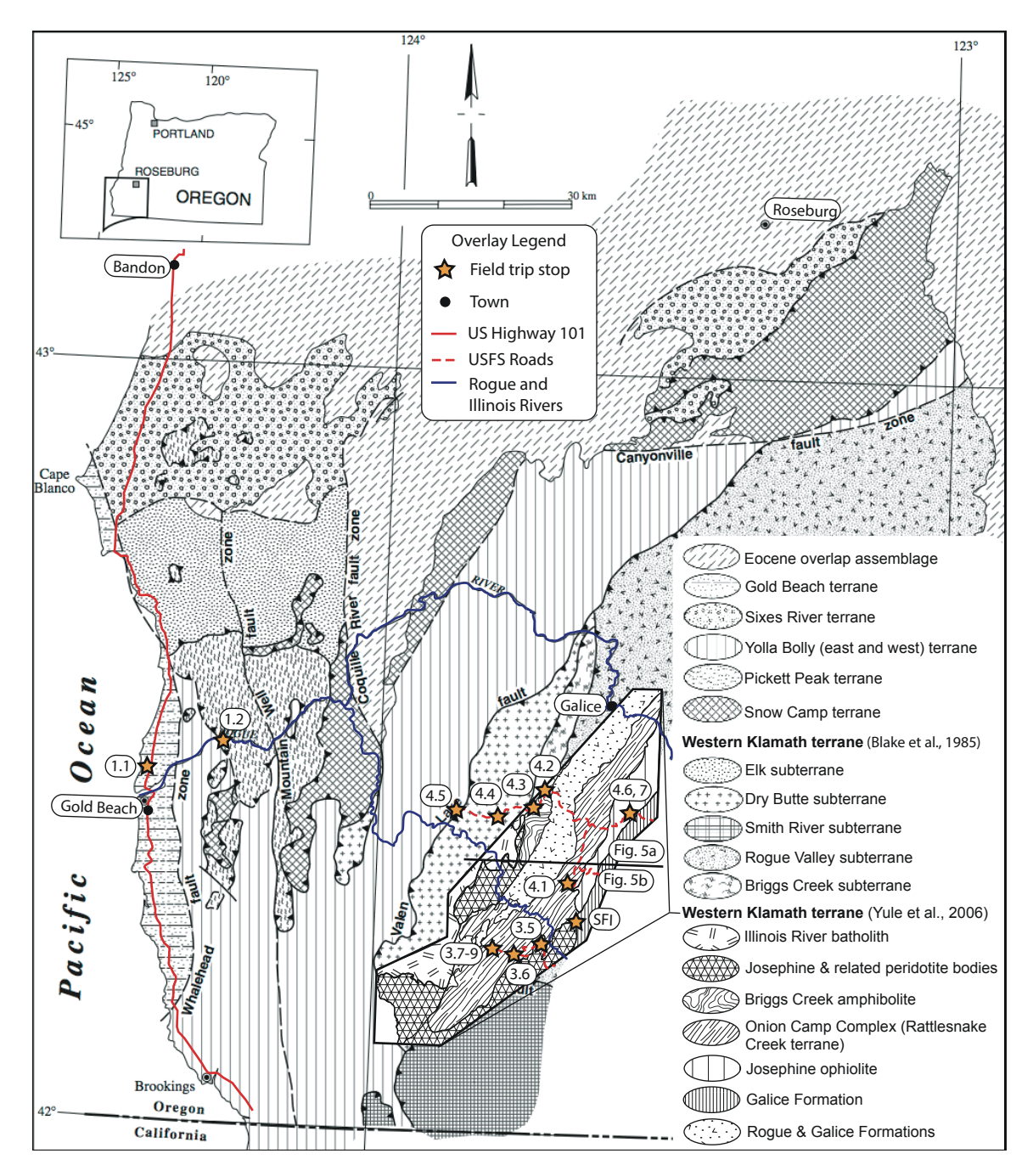


Figure 3. Modified terrane map of Blake et al. (1985) and Snoke and Barnes (2006) with routes and Stops for Days 1, 3, and 4 of this field trip. The area outlined at lower right in the Western Klamath terrane are subdivisions from Yule et al. (2006). The black, east-west line indicates the break between Figures 5A and 5B. SFI—Siskiyou Field Institute.

wild onions, and geographic names like Onion Camp and Onion Mountain led to the selection of "Onion Camp complex" as the unit name. Rocks of the OCC were formerly considered part of the Rogue Formation by Wells and Walker (1953). Subsequent workers noted differences between the type Rogue Formation rocks and the metavolcanic rocks in the region of Onion Camp, but still considered them part of the Rogue Formation rather than

part of a lithologically distinct unit (e.g., Wise, 1969; Dick, 1976; Page et al., 1981; Ramp, 1977, 1984; Ramp and Peterson, 1979). The first suggestion that the OCC belt is distinct from the Rogue arc rocks came from Roure and DeWever (1983) who reported a Triassic age from a chert sample collected near Onion Camp.

The OCC consists primarily of mafic metavolcanic rocks, recrystallized chert, meta-argillite, a heterogeneous mafic intrusive

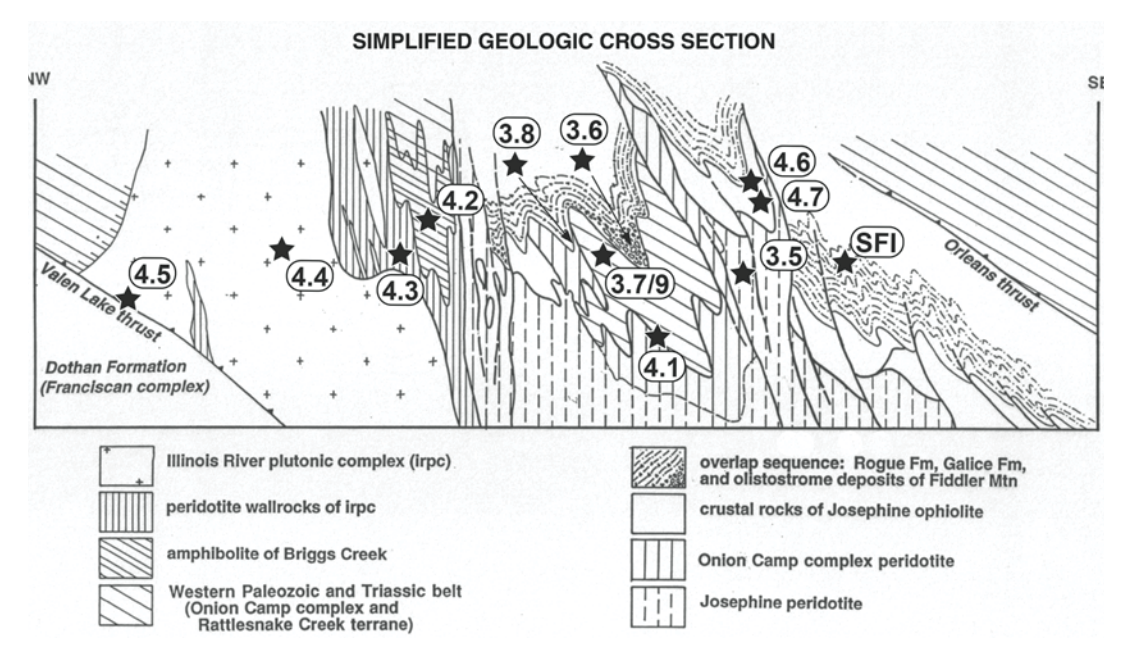


Figure 4. Simplified geologic cross-section of the central Illinois River area (modified from Yule, 1996, fig. 2-41). The section is drawn through the central part of Figure 5 (along line X–X') and perpendicular to the NNE-SSW structural trend. Structures include tight, overturned, NW-vergent folds with faulted limbs. Stars show structural and stratigraphic positions of field-trip stops. SFI—Siskiyou Field Institute.

complex, and serpentinized peridotite. Less common rock types include hornblende schist, amphibolite gneiss, garnet-mica quartzite, and lenses of variably sheared serpentinite. Rocks of the mafic intrusive complex include sheeted mafic dikes and are possibly correlative with the mafic intrusion section of the Josephine ophiolite (Yule et al., 2006). Of the crustal rocks in the complex, metavolcanic and metasedimentary rocks comprise >50% of the exposures, and cross-cutting intrusive rocks of the mafic complex, about one third of the exposures. A small proportion of the OCC consists of amphibolitic rocks that are most common near Squaw Mountain in the central part of the complex.

OCC rocks have experienced several episodes of deformation and metamorphism. The earliest event (D1) produced greenschist to amphibolite grade conditions. Subsequent episodes produced (D2) lower greenschist and prehnite pumpellyite-grade brittle fragmentation and hydrothermal alteration, and (D3) lowest greenschist and sub-greenschist facies regional metamorphism and deformation.

The complex metamorphic and deformational history of the OCC make it challenging to interpret the original stratigraphic sequence. One key observation is that the metavolcanic and metasedimentary rocks generally occur as: (1) metabasalt, sills, and dikes that exhibit MORB geochemical signatures, and lenses and thin intercalations of red chert, and tuffaceous metasediments, and (2) thick sequences of interbedded impure chert, tuffaceous siltstone, and argillite. Both associations are crosscut by a heterogeneous mafic intrusive complex. Amphibolite gneiss, hornblende schist, and impure quartzite occupy regions between serpentinized mantle peridotite and greenschist-facies crustal rocks.

Map patterns show that the serpentinite-amphibolite-greenschist rocks are tightly infolded and share a common axial-planar foliation and hinge-parallel mineral lineation. A metamorphic gradient occurs across the amphibolite/greenschist grade contacts. It remains unclear whether these relations represent a deformed fragment of relatively intact oceanic lithosphere—with a stratigraphic order from shallow to deeper levels of greenschist facies rocks, amphibolites, and peridotite, respectively—or blocks simply subjected to different metamorphic conditions, and possibly at different times, then imbricated at a later time.

The geologic relations define a crude, highly disrupted, block-on-block, and serpentinite-matrix mélange stratigraphy for OCC with: (a) serpentinized mantle peridotite beneath (b) amphibolite-grade mafic sequence that grade into (c) greenschist grade MORB metavolcanic rocks and interlayered metasedimentary rocks. These traits of the OCC bear a strong resemblance to the Rattlesnake Creek terrane (e.g., Wright and Wyld, 1994).

Fiddler Mountain olistostrome (FMO). Named for exposures and greatest mapped extent at Fiddler Mountain to the west of Selma, Oregon, this unit consists of matrix-supported heterolithologic megabreccia, breccia, conglomeratic grit, lithic wacke, and lithic arenite; with secondary impure chert and tuffaceous argillite. Listed in order of decreasing abundance, clast types include: aphyric to phyric green to gray metabasalt, fine- to medium- grained metadiabase, and medium- to coarse-grained gabbro, chert, argillite, serpentinite, and serpentinized peridotite, and rare quartzite, chlorite schist, phyllonite, and amphibolite. The matrix consists of greenschist-grade, sand and pebble-sized

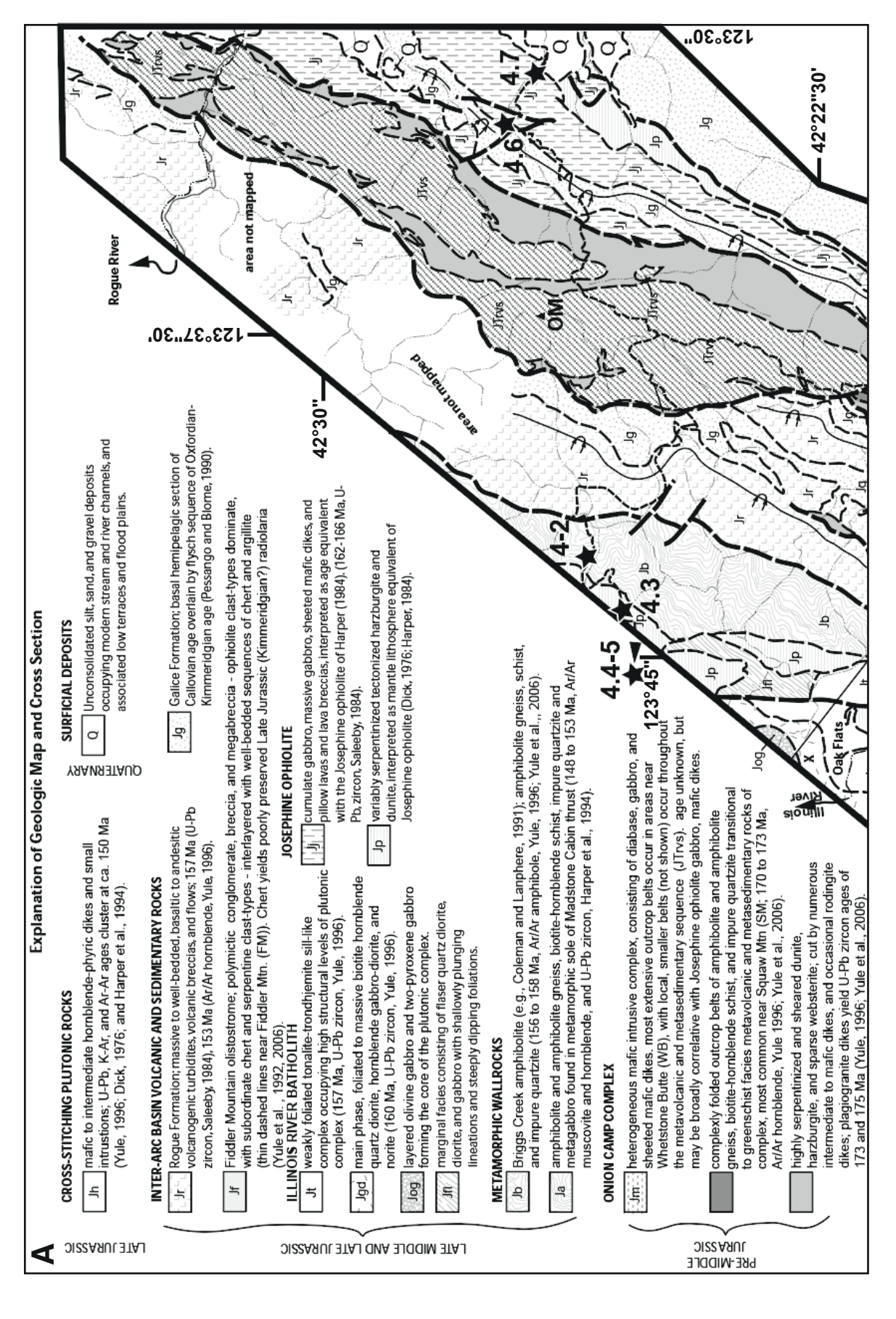


Figure 5. Geologic map and explanation of part of the Western Klamath terrane, Curry and Josephine Counties, Oregon (modified from Yule, 1996, fig. 4-3). (A) North half of geologic map; (B) south half of geologic map. Stars indicate locations of field-trip stops on Days 3 and 4 for this trip. Outline of the geologic map is the same as on Figure 3. SFI—Siskiyou Field Institute. (Continued on following page.)

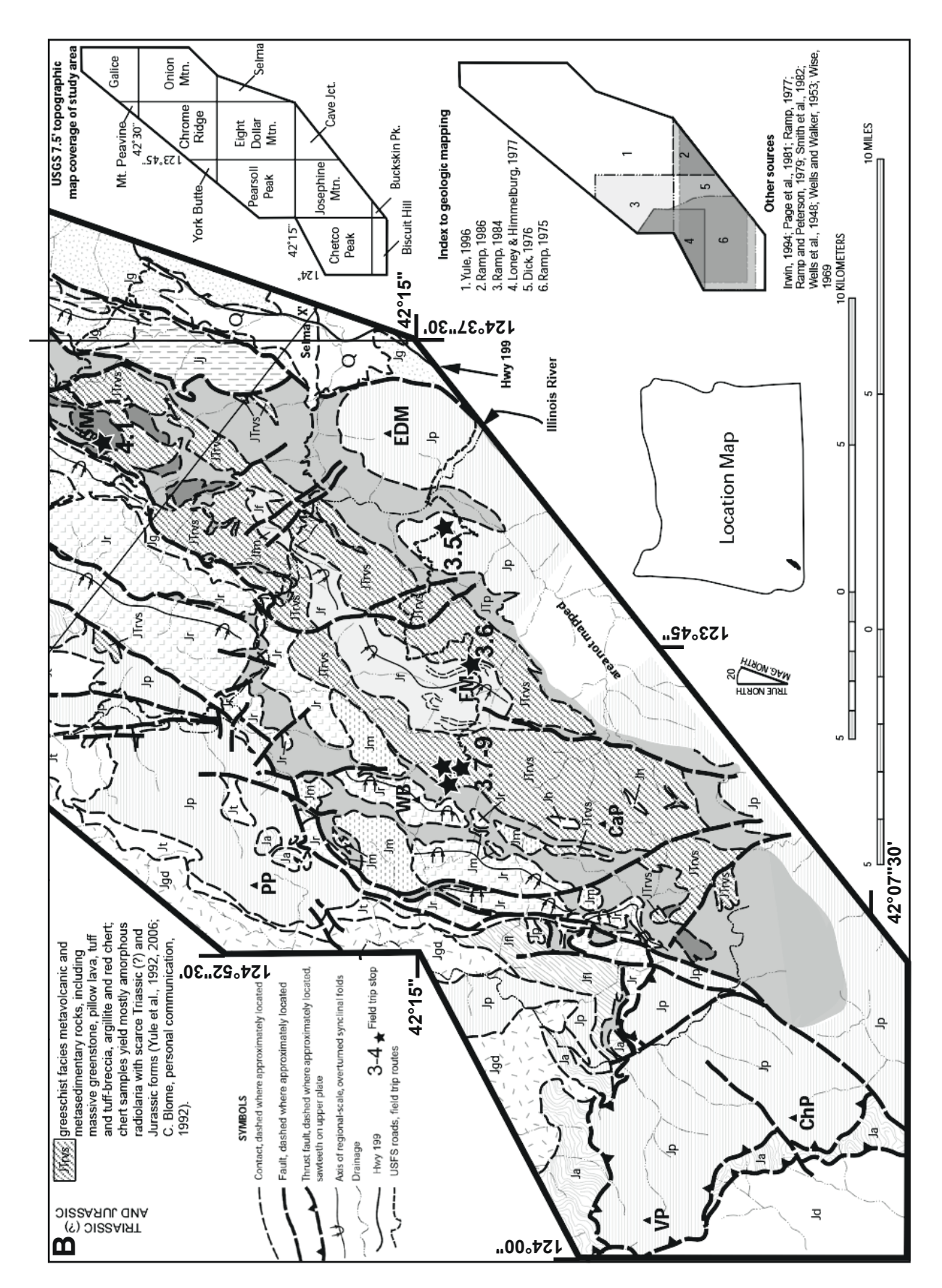


Figure 5 (Continued).

particles and varies depending on locality, ranging from ophiolite-dominant (basalt, diabase, and gabbro) to serpentinite-dominant grains. The most reasonable provenance for these clast types are the Josephine ophiolite and OCC (Yule et al., 2006). Map relations show that FMO deposits unconformably overlie both the OCC and Josephine ophiolite (Fig. 5), and grade laterally with the basal Rogue-Galice section, supporting the clast provenance assessment. When in contact with serpentinized peridotite, the FMO breccia consists entirely of ophicalcitic, serpentinite and peridotite clasts (Yule et al., 2006). Chert samples from the FMO provide its only direct age control, but support the Late Jurassic correlation with other units. Radiolaria from two samples define a poorly constrained Late Jurassic (possible Kimmeridgian?) age (Yule et al., 2006).

Possible correlative units to the FMO occur elsewhere in the Klamath as local basal units within section that overlap ophiolites, e.g., the Lems Ridge olistostrome in the Josephine-Galice basin (Ohr, 1987), and the "rift-edge" facies of the Preston Peak ophiolite (Snoke, 1977). The Devil's Elbow ophiolite section, a southern continuation of the Josephine ophiolite and overlying Galice Formation, also contains an ophiolitic breccia deposit derived from older Klamath terranes (Wyld and Wright, 1988). The FMO and related deposits of the Klamaths are closely associated with the Rattlesnake Creek terrane and the Josephine ophiolite. They indicate that the ophiolite basins contained localized areas of considerable topographic relief, probably as a result of extensional, transfer, and/or transform faulting, and is consistent with the slow-spreading interpretation for the Josephine ocean basin dominated by faulting (Alexander and Harper, 1992). Furthermore, the FMO supports the model of rifting of older Klamath terranes to form the Rogue-Josephine-Galice marginal ocean basin in the Late Jurassic.

Correlating the "rift edges" within the WKT and western Paleozoic and Triassic belt. Work by Snoke (1977), Saleeby et al. (1982), and Harper and Wright (1984) led to the hypothesis that the Late Jurassic Rogue-Josephine-Galice system formed in response to oblique rifting along the western margin of North America, thus disrupting a Middle Jurassic arc constructed on older Klamath terranes. The result produced a triad of the Rogue River active arc, Josephine ophiolite inter-arc basin, and Preston Peak remnant arc. In the Preston Peak area, Snoke (1977) described a "rift-edge" facies within the Preston Peak ophiolite (Rattlesnake Creek terrane equivalent) that supported the "break up" of a polygenetic Klamath terrane (Fig. 2). The rift-edge facies there contains a mafic intrusive complex made of sheeted mafic dikes and gabbro that invade serpentinized peridotite. The intrusive and metamorphic rocks are overlain by a metavolcanic and metasedimentary section containing a distinctive heterolithologic, chert pebble conglomerate with provenance linked to the Rattlesnake Creek terrane. This "rift edge" model to explain relations found in the Preston Peak area predicts that a matching piece resides across the spreading ridges of the ophiolite within the active arc portion of the system. The identification of the OCC and FMO within the WKT has "discovered" this "inferred"

element of the Late Jurassic arc-interarc basin-remnant arc system (Yule et al., 2006).

WKT structure. The regional-scale structure of the WKT is best characterized as a fold belt with faulted limbs rather than a series of eastward dipping, thrust bounded "subterrane" units (Blake et al., 1985; Fig. 4). The WKT is therefore considered to be a relatively intact, though structurally and stratigraphically complex, fragment of composite marginal basin oceanic lithosphere (Yule et al., 2006). Primary Late Jurassic structures control the map outcrop patterns and include: (1) shallowly NE-plunging folds, (2) a pervasive, regional N20–30E-striking, ~60SE-dipping foliation oriented parallel to the axial planes of regional folds, (3) NE-striking, moderately to steeply SE-dipping high-angle faults that are interpreted to truncate the regional fold limbs, (4) moderately E-plunging, late-stage folds that "kink" the regional NE-SW trend, and (5) interference fold patterns in the OCC created by the intersection of Middle Jurassic and older structures with the Late Jurassic folds. When viewed as a fold and thrust belt with regional, shallowly NE-plunging folds, the WKT provides a natural cross-section through composite oceanic lithosphere (Figs. 4 and 5).

Post-Nevadan cross-cutting dikes. Numerous dacitic, acicular hornblende-phyric dikes cut the metamorphic fabrics of older rocks in the WKT. The dikes are unmetamorphosed and are low-dipping with variable strikes. U-Pb zircon ages of these dikes are ~150 Ma (Dick, 1976; Yule et al., 2006) and are the youngest bedrock feature in the WKT. The dikes are interpreted to provide a maximum age constraint for the end of the Nevadan orogeny and accretion of the WKT to western North America.

Middle-Upper Jurassic Sedimentation across the KMP

The Rattlesnake Creek terrane is a polygenetic assemblage that includes a basement of late Paleozoic to Triassic serpentinite-matrix mélange and peridotite massifs and a cover sequence of clastic sedimentary and volcanic rocks. In the southern Klamath Mountains, Wright and Wyld (1994) used radiolaria ages in mélange chert blocks and cross-cutting relationships with a ca. 205–196 Ma early Mesozoic intrusive suite to assign a Late Triassic-Early Jurassic age to the Rattlesnake Creek terrane cover sequence. Irwin and Blome (2004) report multiple locations of Early to Middle Jurassic (Bathonian) radiolaria in the Rattlesnake Creek terrane, and Irwin (2010) and Irwin et al. (2011) suggest that detrital sedimentary rocks in the Rattlesnake Creek terrane may correlate with the Galice(?) Formation. In the west-central Klamath Mountains, Snoke (1977) mapped a conglomerate-grit unit in a coherent metavolcanic and metasedimentary sequence (his Bear Basin Road sequence), which represents the Rattlesnake Creek terrane cover sequence (Bushey et al., 2006; Frost et al., 2006).

New U-Pb detrital zircon data from the Rattlesnake Creek terrane cover sequence suggest maximum depositional ages ca. 167–161 Ma (Middle–early Late Jurassic) and show the presence of 62%–83% Precambrian detrital zircon grains (LaMaskin et al., 2021), interpreted to represent recycled sediment derived from

older terranes of the Klamath Mountains and Sierra Nevada, plus the continental interior. This interpretation matches other lines of evidence suggesting a connection between North America and the Rattlesnake Creek terrane cover sequence, including the presence of quartzose metamorphic detritus (Wright and Wyld, 1994), initial 87 Sr/ 86 Sr of 0.7063–0.7114, initial ϵ Nd from -4.5 to -8.3, and depleted mantle model ages ca. 1.67-1.34 Ga (Frost et al., 2006). Middle Jurassic and early Late Jurassic maximum depositional ages for the Rattlesnake Creek terrane cover sequence presented by LaMaskin et al. (2021) are at least 23 Myr younger than the age of the Late Triassic to Early Jurassic intrusive suite (207-193 Ma) that was interpreted by Wright and Wyld (1994) to cross-cut the cover sequence. LaMaskin et al. (2021) suggest that multiple bodies of sedimentary rock of varying ages—some cut by the Mesozoic intrusive suite (Wright and Wyld, 1994) and some not—may be present in the Rattlesnake Creek terrane.

The Upper Jurassic Galice Formation crops out within the Western Klamath terrane and consists of slate and metasand-stone with volcaniclastic units locally present (MacDonald et al., 2006). The type section conformably overlies the ca. 160–157 Ma Rogue–Chetco volcano-plutonic arc complex and ca. 164–162 Ma Josephine ophiolite (Harper et al., 1994; MacDonald et al., 2006). The Galice Formation *sensu lato* includes a basal hemipelagic sequence ranging from 162 Ma (late Callovian) to 157 Ma (middle Oxfordian; Saleeby, 1984; MacDonald et al., 2006). The Galice Formation sensu stricto is a succession of turbidite sandstone that overlies the hemipelagic sequence and is interpreted to range in age from ca. 157–150 Ma (Harper et al., 1994; Harper, 2006; Pessagno, 2006).

A variety of provenance techniques suggest that the source area for the Galice Formation represents a mix of young volcanic arc and older accreted terrane sources (MacDonald et al., 2006). U-Pb ages of multi-grain zircon fractions from the Galice Formation (Miller and Saleeby, 1995) include two distinct age distributions expressed as average intercept ages ca. 1583 Ma and ca. 215 Ma. Miller et al. (2003) reported ion-microprobe singlecrystal U-Pb detrital zircon ages that included age modes ca. 153 and 227 Ma, as well as lesser quantities of Paleozoic and Proterozoic ages. MacDonald et al. (2006) showed that the source area for rocks of the Galice Formation represents a mix of arc and accreted terranes that was established by ca. 162 Ma. In addition to these Galice Formation studies, Wright and Wyld (1986) reported xenocrystic Paleoproterozoic (ca. 1.7 Ga) zircon grains from the Josephine ophiolite equivalent, Devils Elbow ophiolite, in the southern Klamath Mountains, supporting the input of Precambrian sources into the Western Klamath terrane. New U-Pb detrital zircon ages (LaMaskin et al., 2021; Fig. 6) suggest deposition no older than ca. 158-153 Ma (middle Late Jurassic) and include 15%-55% Precambrian detrital zircon grains with Precambrian ages ca. 2.6-2.3, 1.8-1.7, 1.4, and 1.0 Ga.

Latest Jurassic-Early Cretaceous rocks, locally mapped as the Horsetown Formation and informally known as the "Waldo beds," directly overlie the Galice Formation along an angular unconformity in the northern Klamath Mountains of southeastern Oregon near the town of O'Brien, Oregon (Diller, 1914; Wells et al., 1949). Excellent exposures are found along the Illinois River on Waldo Road, County Road 5560, northeast of O'Brien (443170 E 4658038 N). This succession is ~1000 m thick and consists of a basal unit (~100–200 m thick) of plant-fossil bearing, yellow-weathering gray sandstone and conglomerate that appears to grade upward into a marine-fossil bearing unit (~800– 1000 m thick) of medium gray-weathering dark gray sandstone. These rocks do not bear the cleavage fabric element that characterizes much of the underlying Galice Formation. Use of the name Horsetown Formation for these rocks has been considered questionable (Shenon, 1933; Wells et al., 1949) and subsequent workers have recognized that these rocks correlate in age and lithology to basal rocks of the Late Jurassic Riddle and Knoxville formations (Irwin, 1997; cf. Blake et al., 1985), which are Late Jurassic-Early Cretaceous successions of fluvial- to deep-marine rocks exposed in southeastern Oregon and northern California, respectively. Both the Riddle and Knoxville formations have been considered basal units of the Great Valley Group (Imlay et al., 1959; Jones, 1969; Ingersoll et al., 1977; Ingersoll, 1982; Blake et al., 1985; Ingersoll and Dickinson, 1990; Jayko, 1996; Irwin, 1997).

A detrital zircon sample from the Riddle Formation (Surpless and LaMaskin, 2021, personal commun.) contains a complex, multimodal distribution with ages ranging from Archean to Late Jurassic (Fig. 6). Mesozoic ages dominate the age spectrum with modes at 157, 170, and 205 Ma. The samples bear a relatively continuous distribution of Paleozoic and Neoproterozoic detrital zircon grains with age modes ca. 405, 540, and 630 Ma. Pre-Neoproterozoic grains include abundant Mesoproterozoic ages with a strong age mode ca. 1000-1100 Ma and lesser amounts of 1200-2000 Ma grains. Three grains are Archean in age, older than 2500 Ma. The youngest age mode in our samples of Riddle Formation is ca. 157 ± 1.6 Ma obtained by deconvolution using the mixture-modeling approach of Sambridge and Compston (1994). The maximum depositional age of the sample is 151 \pm 3.5 Ma on the basis of the youngest four grains in the sample (YGC 2s; MSWD 0.119; p = 0.95)

The Franciscan Complex and Onset of Subduction Accretion

Subduction of thousands of kilometers of the Farallon Plate beneath California (Engebretson, 1984) began ~180 Ma (Mulcahy et al., 2018) and was responsible for forming the three main tectonic domains that define California, the Sierra Nevada and Peninsular Range batholiths, the Great Valley Group, and the Franciscan Complex. The batholiths correspond to the magmatic arc, the Great Valley Group to the forearc basin, and the Franciscan to the accretionary wedge (Ernst, 1970; Dickinson, 1970). The E-dipping Coast Range Fault, originally identified as the subduction zone megathrust (Ernst, 1970), but later recognized to have experienced normal-sense reactivation (Platt, 1986; Jayko et al., 1987; Krueger and Jones, 1989; Harms et al., 1992; Wakabayashi and Unruh, 1995), separates the Franciscan from essentially unmetamorphosed ophiolitic rocks and the Great

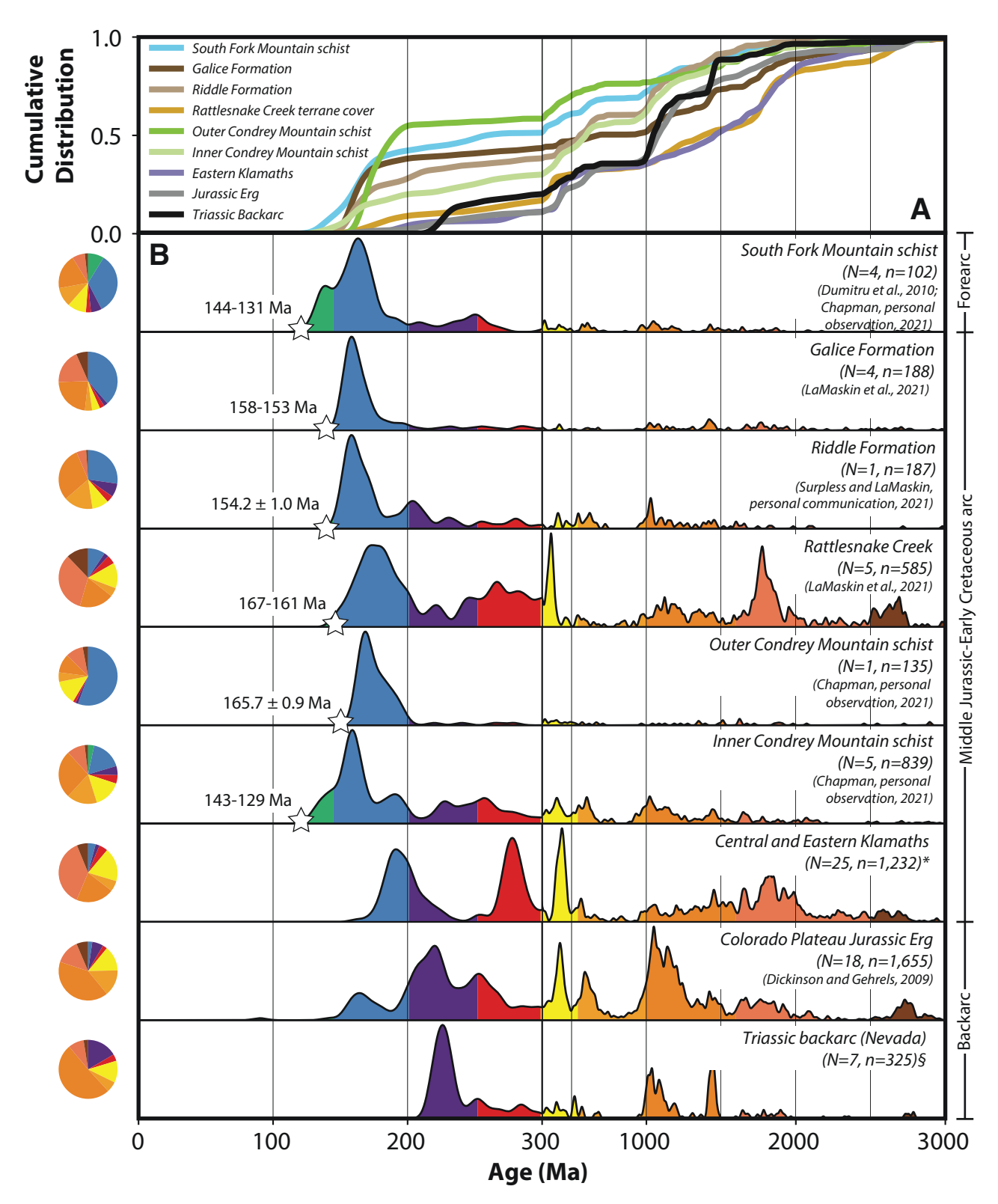


Figure 6. (A) Cumulative probability plot and (B) corresponding non-normalized kernel density estimates (KDE) with 10 Myr bandwidth comparing detrital zircon ages from samples collected from forearc, arc, and backers domains of the Middle Jurassic–Early Cretaceous Klamath Mountains Province. Pie diagram bin colors correspond to those beneath each KDE curve. Numbers (for N = 1) and ranges (for N>1) printed adjacent to stars correspond to calculated maximum depositional ages. Uncertainties provided are 2σ. Abbreviations: N—number of analyzed samples; n—number of concordant analyzed grains. Data from sources listed adjacent to each curve except *, which indicates Gehrels and Miller (2000); Wallin et al. (2000); Grove et al. (2008), Scherer and Ernst (2008); Scherer et al. (2010); Ernst et al. (2017); and §, which indicates Manuszak et al. (2000); Darby et al. (2000); Gehrels and Pecha (2014).

Valley Sequence to the east (Ernst, 1970). In northern California the ophiolitic rocks to the east of the Coast Range Fault belong to the Coast Range Ophiolite (Hopson et al., 2008) and to the Tehama-Colusa Mélange, both deformed ocean floor units that are in fault contact with each other (Hopson and Pessagno, 2005). These units are overlain by the basinal sediments of the Great Valley Group to the east (Dickinson et al., 1996).

For a period of ~50 m.y. after the initiation of subduction, little accretion occurred (Dumitru et al., 2010; Mulcahy et al., 2018). Remnants of this early accreted material occur in two different, broadly seen forms, high-grade blocks in a sedimentary or serpentinite matrix and coherent slabs. The coherent rocks consist of generally intact thrust sheets of metamorphosed volcanic or sedimentary material, ranging in length from hundreds of meters to tens of kilometers and ranging in age of metamorphism from 132 to 168 Ma (Anczkiewicz et al., 2004; Wakabayashi and Dumitru, 2007). The high-grade blocks range in diameter from centimeters to tens of meters and commonly carry blueschist, eclogite, and amphibolite mineral assemblages with metamorphic grains $\geq \sim 0.5$ mm, coarser than that of their enclosing matrix. The ages of these blocks generally range from 141 to 176 Ma (Coleman and Lanphere, 1971; McDowell et al., 1984; Mattinson, 1986; Anczkiewicz et al., 2004; Ukar et al., 2012; Mulcahy et al., 2018). In total, this early accreted material accounts for <1% of Franciscan Complex material (Coleman and Lanphere, 1971; Wakabayashi and Dumitru, 2007). The oldest ages of the high-grade blocks have been taken to approximate the time of subduction initiation (Platt, 1975; Cloos, 1985; Wakabayashi, 1992; Anczkiewicz et al., 2004; Ukar, 2012; Mulcahy et al., 2018) and the oldest obtained age of 176 Ma is the basis for the estimate of ~180 Ma subduction initiation. This oldest age predates the formation of the Coast Range Ophiolite and suggests that the ophiolite formed above an already active east-dipping Franciscan subduction zone (Mulcahy et al., 2018).

Construction of the Franciscan Complex accretionary wedge began in earnest with the ca. 123 Ma accretion of the South Fork Mountain Schist, a package of pelites and graywackes, with lesser amounts of ocean floor basalt and chert. This event marked the end of the non-accretionary period and the beginning of a period of significant accretion that lasted until the Eocene, resulting in the addition of a significant amount of material (Dumitru et al., 2010). The accreted material consists of both coherent units, largely intact thrust sheets with sometimes minor amounts of block-in-matrix material (Wakabayashi, 2015), and of primarily block-in-matrix mélange material (Festa et al., 2010). There are multiple types of Franciscan block-inmatrix material, some with older, higher grade blocks encased in a younger, lower grade matrix of sediments or serpentinite and others with blocks that share an origin and metamorphic history with their matrix. Mélanges are often interpreted as the result of sedimentary processes that deposited recycled older blocks in a younger matrix, or as the result of tectonic mixing. Units with a uniform metamorphic history often consist of interbedded shale and sandstone that was tectonically disrupted, resulting in blocks of sandstone suspended in a shale matrix, though other elements of ocean plate sequences (OPS) can also appear as blocks. Units containing exotic, high-grade blocks are identified as mélange, while units containing isofacial native blocks are identified as OPS mélanges or as broken formation. Sedimentary and tectonic processes are responsible for the formation of the majority of Franciscan mélanges, while diapirism-derived mélanges are rare. For a review of Franciscan mélanges, see Wakabayashi (2015) and Raymond (2019). In northern California, the Franciscan has been divided into three NW-SE-trending belts, the Coastal Belt, Central Belt, and Eastern Belt, based on the timing of accretion, the grade of metamorphism, and the structural style (Berkland et al., 1972; Ernst, 1975). The overall pattern of the Franciscan sees the highest grade and earliest accreted units in the structurally highest positions with a downward decrease in age of accretion, degree of deformation, and metamorphic grade (e.g., Blake et al., 1967; Ernst, 1975; Platt, 1975; Wakabayashi, 1992; Wakabayashi, 2015). While the structurally highest portions of the Franciscan generally lie to the east and structurally lower to the west, in some locations folding and later strike-slip faulting has resulted in a more complicated structure (Wakabayashi, 2015). The Franciscan has been further subdivided into a series of faultbounded terranes (e.g., Maxwell, 1974; Blake et al., 1982, 1984; Jayko et al., 1986).

The Eastern Belt, consisting of primarily coherent terranes, was accreted between 123 and 110 Ma (Dumitru et al., 2010) and experienced peak metamorphic conditions of ~5.5–12 kbar and ~220-377 °C (Jayko et al., 1986; Bröcker and Day, 1995; Ring, 2008; Schmidt and Platt, 2020). It was followed by accretion of the Central Belt between 95 and 88 Ma (Murchey and Blake, 1993), reaching metamorphic conditions of 3-10 kbar and 100-250 °C (Cloos, 1983; Underwood, 1989). In contrast to the Eastern Belt, large portions of the Central Belt are mélange (Hsü, 1968), consisting of pelitic material, which includes highgrade exotic blocks (Berkland et al., 1972). The Coastal Belt was primarily accreted between 65 and 45 Ma (Evitt and Pierce, 1975; Murchey and Blake, 1993; Dumitru et al., 2013) and was scarcely metamorphosed, reaching maximum temperatures close to the closure temperature for fission tracks in apatite (Tagami and Dumitru, 1996) and containing only scattered occurrences of zeolite facies minerals (Bailey et al., 1964). The King Range terrane has recorded somewhat higher temperatures than the rest of the Coastal Belt, but these are interpreted to be the result of a later hydrothermal overprint (Underwood, 1989).

The Eastern Belt has been subdivided into two smaller units, the Pickett Peak terrane to the east and the Yolla Bolly terrane to the west (Jayko et al., 1986). Both terranes were metamorphosed under blueschist facies conditions, as evidenced by the presence of lawsonite, blue amphibole, and sporadic jadeitic pyroxene (Brown and Ghent, 1983; Suppe, 1973; Blake et al., 1969; Ernst, 1971, 2017; Schmidt and Platt, 2020). The Pickett Peak terrane consists of both the South Fork Mountain Schist to the east and the Valentine Springs Unit to the west (Jayko et al., 1986). The South Fork Mountain Schist lies structurally above the Valentine

Springs, which in turn is structurally above the Yolla Bolly terrane to the west; the boundaries between units in this area are east-dipping thrust faults (Worrall, 1981). As with the Franciscan as a whole, degree of metamorphism and deformation generally decreases from structurally higher to structurally lower across the South Fork Mountain Schist and Valentine Springs (Blake et al., 1967; Suppe, 1973; Worrall, 1981; Jayko et al., 1986; Schmidt and Platt, 2018, 2020). They are dominated by graywacke and pelitic material, all affected to some degree by pressure solution. Westernmost rocks are more weakly affected and, while ubiquitously schistose, contain a significant amount of preserved detrital grains. In the South Fork Mountain Schist, the easternmost Pickett Peak unit, pelites have essentially no preserved detrital grains and the rocks have been entirely recrystallized and differentiated into quartz and mica rich bands, and multiple episodes of differentiation and folding are preserved (Jayko and Blake, 1989; Schmidt and Platt, 2018). Detrital zircon data places maximum age of deposition around 123 Ma for the Valentine Springs and between 131 and 137 Ma for the South Fork Mountain Schist (Dumitru et al., 2010; Chapman, 2021, personal observ.). Metamorphic ages for the Valentine Springs and South Fork Mountain Schist, interpreted as approximating the time of accretion, are 117 Ma, based on whole rock 40 Ar/39 Ar analysis (Lanphere et al., 1978), and 121 Ma, based on 40Ar/39Ar step heating of white micas (Dumitru et al., 2010). Peak metamorphic temperatures and pressures across the Pickett Peak range from 240 to 377 °C and ~5.5 to 9.8 kbar (Jayko et al., 1986; Bröcker and Day, 1995, Ring, 2008; Schmidt and Platt, 2020).

The Yolla Bolly terrane in northern California consists of four subsidiary units: the Chicago Rock mélange, the Hammerhorn Ridge metagreywacke, the Devil's Hole Ridge broken formation, and the Taliaferro Metamorphic Complex (Jayko et al., 1986). Degree of deformation and metamorphism is lower than in the Pickett Peak, and metagreywackes of the Yolla Bolly commonly show a weak, anastomosing schistosity (Jayko et al., 1986), while the pelites often have a slaty cleavage that appears to be axial planar to large scale folds. Metasedimentary rocks typically carry albite and lawsonite, although the higher-grade Taliaferro Metamorphic Complex contains jadeitic pyroxene. Portions of the Yolla Bolly have been heavily affected by normal faulting, which is associated with significant decompression (Schmidt and Platt, 2018). Ar-Ar dating of white micas places its time of metamorphism at ~110 Ma, while the age of its deposition is interpreted to have occurred from ~115 to 98 Ma in northern California, based on detrital zircons (Dumitru et al., 2010, 2018). Depositional ages decrease to ~100 Ma in the San Francisco Bay area and to ~89 Ma in the Nacimiento block further to the southeast (Ernst et al., 2009; Chapman et al., 2016; Ernst, 2017). In southern Oregon, the maximum depositional ages range from 102 to 74 Ma (Wiley et al., 2017). Peak temperatures and pressures in the main body of the Yolla Bolly, excluding the higher-grade Taliaferro Metamorphic Complex, are estimated to be 187–293 °C (Jayko et al., 1986; Bröcker and Day, 1995, and references therein; Schmidt and Platt, 2020) and ~7 kbar (Jayko et al., 1986).

Disagreements and reclassification of unit designations have occurred in the Franciscan, due on one hand to the combination of lithologically similar units with complex structure, and on the other hand to issues with naming conventions (Raymond, 2015; Wakabayashi, 2015). The Yolla Bolly is one of the largest terranes of the Franciscan, and it has been the subject of much of this debate. Raymond (2015) notes portions of the central Californian Franciscan that have been alternately assigned to the Yolla Bolly and to the Eylar Mountain terrane. In southern Oregon, early work along the Rogue River placed the Yolla Bolly terrane between the Gold Beach terrane and the Colebrooke Schist (Blake et al., 1985); later mapping interpreted the Gold Beach terrane as being in direct contact with the Colebrooke Schist in this location (McClaughry et al., 2013). Ernst (2017) notes the wide range of depositional ages determined for the Yolla Bolly and argues for its classification as a tectonometamorphic unit, a coherent unit defined by its metamorphic history rather than its depositional history. Conversely, it has been argued that there are insufficient data for determining if the mapped exposures of Yolla Bolly in northernmost California and southern Oregon should actually be grouped with the better studied Yolla Bolly to the south, and that such designations be deferred until they can be made with more confidence (Dumitru et al., 2018). Some workers have argued for methods of unit description other than the traditional terrane designations. Raymond (2018) argues that "Belt" and "terrane" designations should be abandoned entirely, because both as currently defined can contain within them rocks of different ages, metamorphic grades, and lithologies, leading to confusion rather than enhanced understanding. Description of mappable accretionary units (AUs) instead would facilitate a better understanding of Franciscan history, though much of the Franciscan has not yet been mapped in sufficient detail for this. Other workers have focused on grouping units based on time of accretion (Wakabayashi, 1992, 2015; Apen et al., 2021), and Wakabayashi (2015) argues that traditional designations can still be kept so long as their use is clearly defined. We will refrain from commenting on or further describing disagreements over central Californian terrane designations here, as it is beyond the scope of this guide. Here we will consider the Yolla Bolly terrane to extend into southern Oregon, with the understanding that its relationship to the type section of the Yolla Bolly in northern California is debatable and may be revised in the future.

As in California, the rock units of southwest Oregon have been divided into a series of terranes that here include the Gold Beach, Sixes River, Yolla Bolly, and Pickett Peak terranes (Fig. 3). The Pickett Peak terrane in southwest Oregon is represented by the Colebrooke Schist and its underlying serpentinite-matrix mélange (Dott, 1971; Coleman, 1972; Blake et al., 1985). The Colebrooke is a fault-bounded unit resting on an E-dipping, subhorizontal thrust, and it structurally overlies the Yolla Bolly and Gold Beach terranes (Beaulieu and Hughes, 1976; Roure and Blanchet, 1983; Blake et al., 1985; McClaughry et al., 2013),

while the Yolla Bolly and Gold Beach terranes are separated by a steeply dipping right-lateral strike-slip fault (Dott, 1971; Blake et al., 1985; Bourgeois and Dott, 1985; Kelsey and Bockheim, 1994; McClaughry et al., 2013). Whole rock Rb-Sr dating has placed the age of metamorphism of the Colebrooke metasediments at 128 ± 18 Ma (Coleman, 1972), while whole rock K/Ar dating has found the age of metamorphism to be between 142 and 125 Ma (Dott, 1971). The similarity in metamorphic ages, in addition to a similar deformational style, is the primary reason the Colebrooke Schist is thought to be correlative with the South Fork Mountain Schist of California and other Pickett Peak units (Blake et al., 1967; Roure and Blanchet, 1983; Cashman et al., 1986; Brown and Blake, 1987). The Colebrooke Schist is also bound on its east by the Coast Range Fault, which here separates the Franciscan from the Klamath Mountains, rather than from the Great Valley Group. A thin body of sheared serpentinite lies along and parallels the Coast Range Fault, containing blocks of Colebrooke schist within it. The N-S-trending Mountain Well normal fault is a later feature that bisects the Colebrooke Schist (Coleman, 1972).

The northernmost extension of the Yolla Bolly terrane in southern Oregon is locally named the Dothan Formation, and it has been divided into two subterranes based on lithology; the western subterrane is richer in volcaniclastic content, while the eastern subterrane has both detrital muscovite and a greater amount of sandstone (Blake et al., 1985). The western subterrane consists of mudstone, sandstone, and conglomerate turbidites, as well as interbedded radiolarian chert, tuffs, and igneous rocks of basaltic to dacitic composition. Lawsonite and aragonite were documented in the volcanic rocks (Wiggins, 1980, as cited in Blake et al., 1985), though they have not been observed in metasedimentary rocks. The two subterranes are in depositional contact (Aalto, 1989) and the eastern subterrane also consists of metasedimentary turbidite sequences, but volcanic rocks are only present as isolated pillow lavas near the subterrane's upper bounding fault. Sandstones of both terranes commonly contain pumpellyite and in some locations prehnite is present (Blake et al., 1985; Aalto, 1989). South of Oregon, in northernmost California, the Yolla Bolly contains significant portions of mélange and the sandstones here too carry pumpellyite (Aalto, 2014). The dominantly prehnite-pumpellyite assemblages present in southern Oregon and northernmost California are in contrast to the lawsonite-albite facies of the Yolla Bolly in its northern Californian type section, and this decrease in metamorphic grade to the north is gradational (Aalto, 1989).

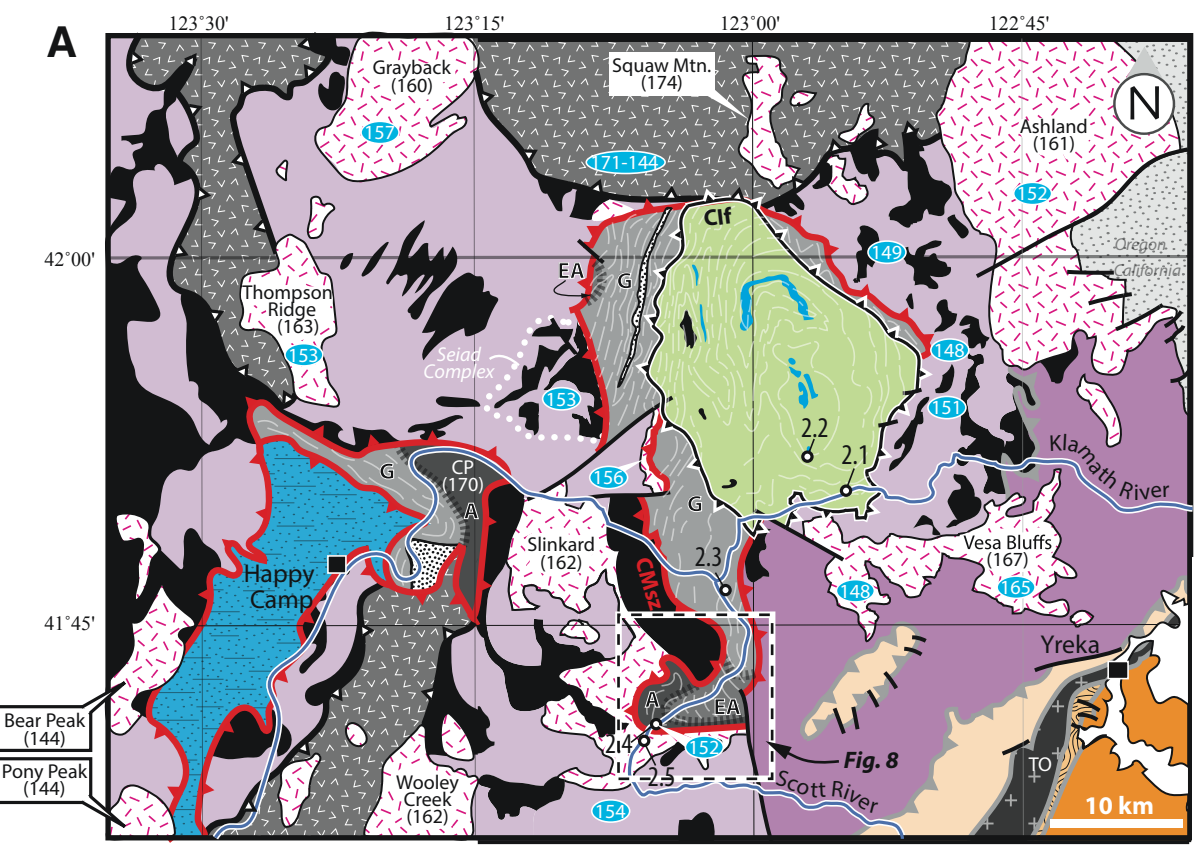
The Gold Beach terrane consists of the Cretaceous Otter Point Formation as well an unconformable overlap of unmetamorphosed Late Cretaceous sediments consisting of the Houstenaden Creek unit, the Cape Sebastian Sandstone, and the Hunter's Cove Formation; these were likely deposited as a result of a Late Cretaceous transgressive episode (Bourgeois, 1980; Bourgeois and Leithold, 1983; Bourgeois and Dott, 1985). The Otter Point Formation is made of sediments and volcanics metamorphosed to zeolite facies, as evidenced by common laumontite veins (Blake

et al., 1985). It crops out along the coast both in the vicinity of the town of Gold Beach and on Cape Blanco to the north. Northeast of Gold Beach it is in fault contact with the overlying Colebrooke Schist, while to the southeast it is separated from the Yolla Bolly terrane by the right lateral, steeply dipping Whaleshead fault (Dott, 1971; Blake et al., 1985; Bourgeois and Dott, 1985; Kelsey and Bockheim, 1994; McClaughry et al., 2013); lensoidal serpentinite and gabbroic bodies crop out in some locations along this fault trace (Roure and Blanchet, 1983). In several other locations in the region, other ultramafic and variably serpentinized bodies are present, commonly outcropping along fault lines. These are interpreted as upper mantle material exhumed via thrust faulting or diapirism, and emplaced at relatively low temperatures (Coleman, 1972; Medaris, 1972; McClaughry et al., 2013). Paleomagnetic and lithologic evidence point to the Gold Beach terrane as originating near southern California and being translated northward by right lateral motion along the Whaleshead Fault (Blake et al., 1985; Bourgeois and Dott, 1985; Jayko and Blake, 1993; Liner, 2005). Emplacement is interpreted to have taken place prior to ~50 Ma (Liner, 2005).

The Sixes River terrane is made of sheared mudstones, sand-stones, and conglomerates, which were initially interpreted as similar in age to Otter Point sediments, based on *Buchia* fossils preserved in concretions (Blake et al., 1985). Laumontite is common in the sandstones, indicating zeolite facies metamorphism. These rocks were originally mapped as belonging to the Otter Point Formation (Dott, 1971; Beaulieu and Hughes, 1976). However, the Sixes River terrane is a mélange containing numerous high-grade and/or exotic blocks, including blueschist, eclogite, and limestone (Coleman and Lanphere, 1971) and, as a result, it has been given its own terrane designation and proposed as correlative with the Central mélange terrane of the northern California Franciscan (Blake et al., 1985). Recent preliminary work has found a maximum depositional age for the graywacke matrix of 90 Ma based on detrital zircon analysis (Waldien and Roeske, 2019).

Condrey Mountain Schist

The Condrey Mountain schist (CMS) is exposed as a domal structural window through the overlying Rattlesnake Creek terrane, beneath the low-angle Condrey Mountain shear zone (Mortimer and Coleman, 1985; Fig. 7). This structural relationship, in addition to the lower metamorphic grade and younger cooling ages of the CMS relative to flanking rocks, makes the CMS the clearest existing violation to the structural "rule" of the Klamaths: an otherwise generally westward-younging stack of eastdipping thrust sheets. Efforts to fit the CMS into the regional puzzle have focused on lithologic and age similarities between the CMS and adjacent rocks, resulting in correlations being drawn with the Central Metamorphic terrane (Irwin, 1960), Stuart Fork terrane (Medaris, 1966), Galice Formation (Klein, 1977; Hotz, 1979; Saleeby and Harper, 1993), China Peak complex (Saleeby and Harper, 1993), and South Fork Mountain schist (the oldest Franciscan unit of significant areal size; Suppe and Armstrong, 1972; Brown and Blake, 1987).



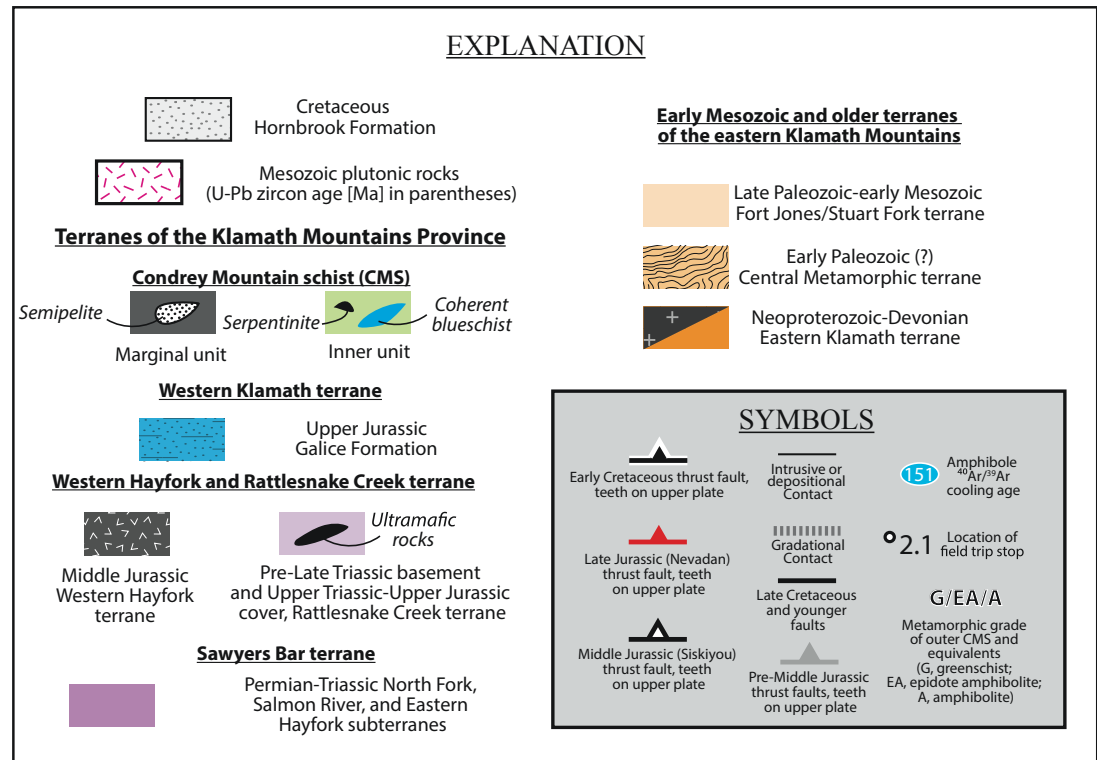


Figure 7. (A) Simplified geologic map of the central Klamath Mountains Province, modified after Hotz (1969), Barrows (1969), Hill (1984), Burton (1982), Helper (1986), and Saleeby and Harper (1993). Note that many faults identified with thrust symbols have been variably reactivated in a normal sense. Amphibole ⁴⁰Ar³⁹Ar ages from Saleeby and Harper (1993), Hacker and Ernst (1993), Hacker et al. (1995), and Donato et al. (1996). Zircon U-Pb ages from Snoke and Barnes (2006). See Figure 1 for map location. Planned field-trip stops (white-filled circles) overlain. Abbreviations: CP—China Peak; TO—Trinity ophiolite; CMsz—Condrey Mountain shear zone. (*Continued on facing page*.)

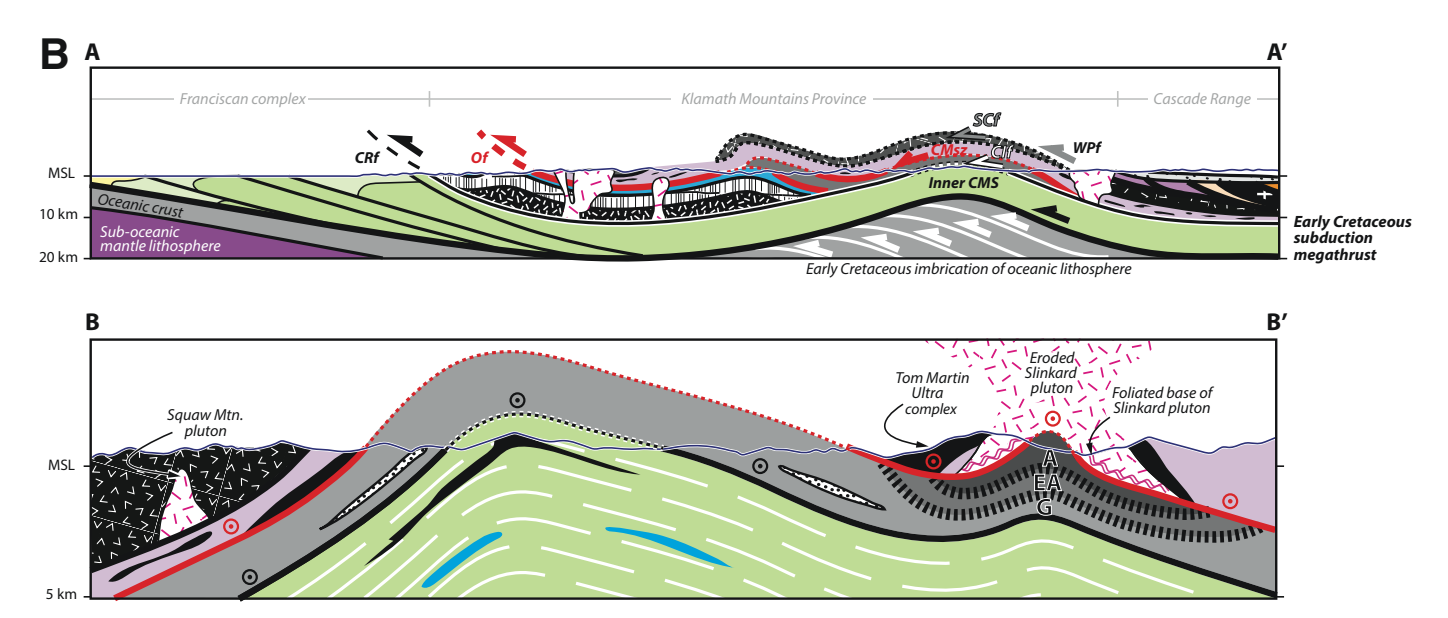


Figure 7 (*Continued*). (B) Cross-sections across the Condrey Mountain schist window (vertical = horizontal scale). Colors and symbols correspond to those used on Figure 7A. See Figure 1 for locations of section lines. Abbreviations: CIf—Condrey Internal fault; CMS—Condrey Mountain schist; CRf—Coast Range fault; MSL—mean sea-level; Of—Orleans fault; SCf—Salt Creek fault; WPf—Wilson Point fault.

The CMS is subdivided into a structurally deeper, relatively low-grade inner unit and structurally higher, relatively high-grade marginal unit, separated by the Condrey Internal fault (Helper, 1986; Saleeby and Harper, 1993; Fig. 7). Both CMS subunits preserve similar prograde ductile non-coaxial deformation and texturally late coaxial flattening fabrics, attributed to subduction-related burial and later structural ascent, respectively (Helper, 1986).

The inner CMS consists chiefly of greenschist to blueschist grade graphitic and quartz-mica schist, likely produced through metamorphism of argillite and chert protoliths, that locally contain meter- to several kilometer-scale lenses and tabular slabs of blueschist (formerly basaltic flows and tuff) and serpentinite (Hotz, 1979; Helper, 1986; Saleeby and Harper, 1993). The array of rock types observed within the inner CMS, and the paucity of clastic material therein, point to sedimentation in an open ocean starved of terrigenous input atop a basement and/or including olistoliths of oceanic lithosphere (e.g., Wakabayashi, 2017).

The outer CMS mantles the inner unit and includes greenschist to amphibolite facies metamorphosed basaltic tuffs, pillow lavas, and rare comagmatic intrusive equivalents and plagiogranite. These igneous protoliths dominate the outer CMS though are locally interrupted by lenses of hemipelagic material (now silicic and graphitic quartz-mica schist) and one prominent (\sim 10 km long \times 0.5 km wide in map view) semi-pelitic horizon exhibiting graded beds, likely representing deep-water turbidite deposits (Hotz, 1979; Helper, 1985). The range of lithologies observed in the outer CMS suggest oceanic deposition proximal to eruptive centers with sporadic input of terrigenous material.

Along the "Scott River appendage" peak metamorphic assemblages preserved in the outer CMS grade smoothly (i.e.,

lacking obvious structural breaks) from greenschist to amphibolite facies as the Condrey Mountain shear zone is approached from below (Saleeby and Harper, 1993; Figs. 7 and 8). Metamorphic grade also increases down-section within the upper plate Rattlesnake Creek terrane, preserving upper amphibolite and locally granulite facies parageneses, as the Condrey Mountain shear zone is approached from above (Hotz, 1979; Mortimer and Coleman, 1985; Garlick et al., 2009). These relations require a sharp inverted metamorphic field gradient spanning structurally deep, low-grade inner CMS and higher-grade outer CMS.

ROAD LOG

We depart from the Oregon Convention Center (777 NE Martin Luther King, Jr. Blvd, Portland, OR 97232, USA), and drive 297 miles to the Otter Point Formation of the Gold Beach terrane, before driving an additional 16 miles to visit the Colebrooke Schist, and finally 117 more miles of driving before reaching the Siskiyou Field Institute.

Universal Transverse Mercator (UTM) coordinates (WGS 84 datum) are given for each field-trip stop. Road log distances are reported in miles.

Day 1

Today, we will focus on the Franciscan Complex. We will begin by visiting the Otter Point Formation of the Gold Beach terrane, where we will see an example of sheared zeolite facies metasediments. Then we will visit Colebrooke Schist metasediments of the Pickett Peak terrane, contrasting its greater degree of metamorphism and deformation with that of the Otter Point

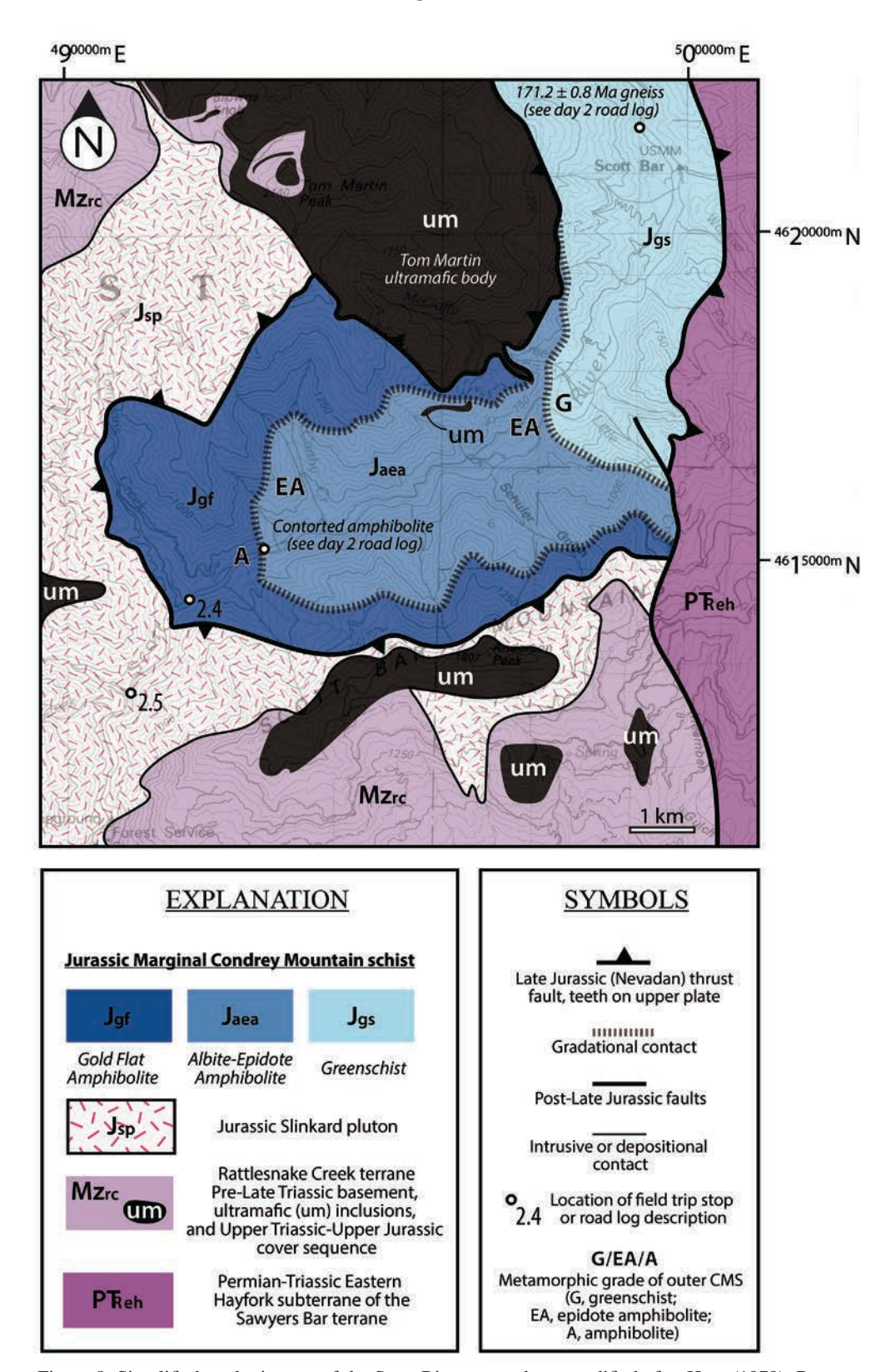


Figure 8. Simplified geologic map of the Scott River appendage, modified after Hotz (1979), Barrows (1969), Cornwall (1981), Burton (1982), Saleeby and Harper (1993). Map base: U.S. Geological Survey 30×60 min series (1:100,000 scale) maps of Yreka (1979) and Happy Camp (1983) quadrangles (The National Geologic Map Database: https://ngmdb.usgs.gov). Planned field-trip stops and road log descriptions (white-filled circles) overlain. See Figure 7A for map location.

Formation; we will also discuss comparisons with the South Fork Mountain Schist of northern California. Stop locations are shown on Figures 1 and 3.

Mileage	Description
0.0	Oregon Convention Center. Drive south and
	follow signs and directions to merge onto I-5
	South. I-5 parallels the Cascade volcanoes to the
	east, a chain extending from northern California
	into Canada. Mt. St. Helens is north of Portland,
	while Mt. Hood is directly to the east.
147	Turn right onto OR-38/W B Avenue.
197.1	Turn left onto U.S101 South.
248	Bandon, Oregon, sits near the northernmost
	boundary of the Sixes River terrane. Several
	high-grade blocks are dispersed over an area
	extending ~5 km south of Bandon.
264	4 km east is a small klippe of Colebrooke Schist
	overlying the Sixes River terrane.
294	The high ground immediately to the east is
	Vondergreen Hill, a major body of serpentinized
	ultramafic material associated with Otter Point
	intraformational faulting.
297.1	Turn right onto Old Coast Road, then continue
	south and look for the right turn into the Otter
	Point State Recreation Area parking lot.
297.5	Park at the Otter Point State Recreation Area and
	walk toward the cliffs at Otter Point, sticking to
	the high ground. On the north side of Otter Point
	is a small path providing access to Otter Point
	Formation rocks. Keep a safe distance away
	from the cliff edge.

Stop 1.1. Lunch and Otter Point Formation (UTM 10T, 382774E, 4702215N)

Otter Point is the type locality of the Otter Point Formation (Koch, 1966), and while much of the ground around the parking area is covered in Quaternary terrace sediments, the cliff sides provide excellent exposures. Rocks visible offshore and somewhat to the south belong to both the Otter Point Formation and to the overlapping Cretaceous deposits of the Gold Beach terrane. The Otter Point Formation primarily consists of interbedded conglomerate, sandstone, and mudstone. Portions of it also include bands of pillow lava and volcanic breccia, while the surface traces of major intraformational faults and shear zones are marked by serpentinite, chert, diorite, and volcanic rocks (McClaughry et al., 2013). While exotic blocks such as these have often been linked to fault and shear zones, it is also possible for them to be associated with olistostromal horizons (e.g., Wakabayashi, 2015) and, as a result, care must be taken with interpretations. The sandstones range from arkosic wacke to lithic wacke and have a chloritic matrix (Koch, 1966; Aalto, 1989). Otter Point sandstones are compositionally distinct from Yolla Bolly sandstones to the east, being richer in plagioclase and volcanic rock fragments, as well in some detrital minerals, including clinopyroxene (Aalto, 1989). Conglomerates and sandstones are seen to contain a significant amount of volcaniclastics, and the sediments are interpreted to have been sourced from an island arc located west of the present-day coastline (Dott, 1971; Coleman, 1972; Walker, 1977). The presence of commonly found *Buchia piochii* suggests an age of deposition in the Late Jurassic and Early Cretaceous (Koch, 1966; Dott, 1971). However, *Buchia* fossils in the Franciscan have frequently been found to be reworked when detrital zircon analysis reveals much younger ages of deposition (Ernst et al., 2009; Dumitru et al., 2018). While there is no existing detrital zircon data for the Otter Point Formation, it is possible that the depositional age is significantly younger than the *Buchia piochii*.

The Otter Point Formation has experienced extensive deformation and asymmetric folds are common. Folding is interpreted to have occurred in two episodes, with originally N-S-trending folds refolded about an E-W axis, resulting in fold axes that dominantly plunge to the N and to the S. Thick sandstones are folded with longer wavelengths than thinly interbedded sandstone and shale sequences (McClaughry et al., 2013).

Bedding in the vicinity of Otter Point ranges from steeply dipping to overturned and in places graded bedding is preserved, as is cross bedding in sandy layers. A boudinaged layer of whitish sandstone is evidence of intense shearing, and veins that crosscut the boudins point to an episode of veining that either predated or was coeval with deformation. Later veins cut all layers at a high angle.

Return to vehicles, reset odometers to zero, and proceed to Stop 2.

Mileage	Description
0.0	Follow Old Coast Road back to the highway and
	turn right onto U.S101 South.
5.2	Turn into the Conoco gas station in the town of
	Gold Beach and refuel, then drive north on
	U.S101.
6.2	Turn right onto Jerry's Flat Road.
16	Turn left onto Lobster Creek Road.
16.2	Immediately after crossing the bridge, carefully
	do a U-turn and park along the west side of the
	road. Follow the footpath below the bridge and
	onto the Colebrooke Schist exposures.

Stop 1.2. Colebrooke Schist (UTM 10T, 393691E, 4706564N)

The bulk of the Colebrooke Schist consists of schistose metapelite and sandstone with lesser amounts of isolated metavolcanic, metaplutonic, serpentinite, and talc-schist blocks. The metavolcanic blocks are almost all basaltic and many contain preserved pillow structures (Katrib, 2005). The metapelites contain quartz, chlorite, phengite, albite, lawsonite, and epidote, and have a chemical composition similar to that of the Galice Formation (Coleman, 1972). In some places lawsonite and epidote coexist and this has been interpreted as evidence that the Colebrooke Schist is transitional between greenschist and blueschist facies, metamorphosed at 200–250 °C and 5–6 kbar

(Coleman, 1972). Other workers have interpreted this to be the result of blueschist facies metamorphism followed by a higher temperature event (Roure and Blanchet, 1983). The absence of massive sandstones and the generally fine-grained nature of the Colebrooke is interpreted as evidence of deep-water deposition (Coleman, 1972).

Colebrooke Schist metasediments have been differentiated by pressure solution into alternating quartz and phyllosilicate rich bands, forming the main foliation, S1, which is parallel to bedding. This foliation has been affected by at least two subsequent episodes of folding, resulting in a younger S2 foliation that is parallel to fold axial planes. Fold axes are reported to trend N-S, with axial planes dipping to the west, indicating eastvergent folding (Coleman, 1972). Later work in the southern portion of the Colebrooke Schist reported fold vergences toward the west or the northwest rather than to the east (Roure and Blanchet, 1983), and this discrepancy may be due to local variations in orientations. Plake (1989) noted variations in F2 fold axes based on location within the Colebrooke and interpreted them to be the result of rigid block rotation about vertical axes, an explanation also invoked to explain scatter of structural measurements in the Pickett Peak's Redwood Schist Formation in northern California (Cashman et al., 1986). In the South Fork Mountain Schist of northern California folds were found to be dominantly NW vergent and to be hierarchical in nature, with smaller cm-scale folds occupying the limbs of larger folds with amplitudes of dozens to hundreds of meters. Small-scale folds on the overturned limbs of larger folds showed an eastward vergence, opposite the dominant orientation (Schmidt and Platt, 2018).

The Colebrooke Schist is exposed at the intersection of the Rogue River and Lobster Creek, close to the thrust fault separating it from structurally lower units to the west. Two key observations attest to the intensity of deformation here. First, rafts of sandstone suspended in matrix (i.e., broken formation) are preserved on the south bank of the Rogue River. Second, alternating quartz- and phyllosilicate-rich bands point to differentiation by pressure solution. This pressure solution foliation is folded into asymmetric folds, some of which verge to the NW-NNW. Foliation parallel quartz veins are present, and in places are boundinaged.

The pressure solution—derived foliation points to the importance of this deformation mechanism in the development of the Colebrooke Schist. Previous work on the possibly correlative South Fork Mountain Schist has found that pressure solution was the dominant deformation mechanism during subduction and close to the time of accretion, while dislocation creep dominated after the sediments were transferred to the overriding plate and during the early stages of exhumation. Phyllosilicates increase pressure solution rates, and dislocation creep is more favored where they are sparse or absent. As pressure solution differentiates rocks into quartz and phyllosilicate rich bands dislocation creep becomes more favored in the quartz-rich domains, potentially leading to a switch in deformation mechanism. In the Nevada-Filabride Complex

of southern Spain, another way to suppress pressure solution and promote dislocation creep was documented. Retrogressive metamorphism removed free water from pore spaces and sequestered it in newly grown hydrous minerals like chlorite (Behr and Platt, 2013). The result of the deformation mechanism switch in the South Fork Mountain Schist is a main, pressure solution—derived foliation visible at outcrop scale while dynamically recrystallized grains are ubiquitous in thin sections. The recrystallized grain sizes are smaller in the vicinity of the bounding faults, reflecting a local increase in stress and localization of strain during cooling and exhumation. A similarly detailed history of the deformation and exhumation of the Colebrooke Schist has not yet been obtained.

Return to vehicles, reset odometers to zero, and proceed to Siskiyou Field Institute.

Mileage	Description
0.0	Drive south on Lobster Creek Road over the
	Rogue River.
0.2	Turn right on Jerry's Flat Road.
10	Turn left onto U.S101 South.
31.2	This is where U.S101 crosses the Whaleshead
	fault, separating the Gold Beach terrane to the
	NW from the Dothan to the SE.
45.1	Oregon-California border.
55.4	Turn left onto CA-197 South.
62.1	Turn left onto U.S199 North.
63.3	This is where U.S199 crosses the E-dipping
	Coast Range Fault, separating Franciscan rocks
	to the west from the ultramafic rocks of the Jose-
	phine Ophiolite to the east.
77.3	Note the large serpentinized cliff exposures of
	Josephine Ophiolite on the south side of the
	road.
93.8	Oregon-California border.
115.2	Turn left onto Illinois River Road
116.7	Arrive at Siskiyou Field Institute.

End Day 1.

Day 2

Today we will focus on the Condrey Mountain schist and related tectonic problems. We will begin by exploring rocks that crop out at the deepest structural levels of the Condrey Mountain schist (CMS), contrast predominantly metasedimentary rocks of the inner CMS with predominantly metavolcanic rocks of the outer CMS, showcase the well-developed inverted metamorphic field gradient displayed by the outer CMS, and investigate rocks that comprise the regional upper plate to the CMS. The locations of all Day 2 stops are shown on Figures 7 and 8.

Mileage	Description
0.0	Depart Siskiyou Field Institute at 8 a.m. and drive east 1.5 miles to the intersection of U.S.

73.8

79.8

89.6

Hwy 199 and Illinois River Road in Selma, Oregon. Turn left (north) on Hwy 199 toward Grants Pass, Oregon. Continue 22 miles until the intersection with Interstate 5. Merge onto Interstate 5 south toward Medford, Oregon.

From Medford to the vicinity of Mt. Ashland (~6 miles north of the California-Oregon border) Interstate 5 follows Bear Creek Valley, which contains basement rocks of the KMP nonconformably overlain by forearc strata of the Early (?) to Late Cretaceous Hornbrook Formation and Upper Eocene coarse clastics (McKnight, 1984; Wiley et al., 2011). Beginning at the southern city limits of Medford (south of milepost 27) are roadcuts, adjacent to northbound lanes, of turbidite belonging to the Hornbrook Formation (Campanian (?) Rocky Gulch Sandstone Member; Nilsen, 1984). These exposures consist chiefly of medium- to coarse-grained bedded sandstone with lower proportions of conglomerate, siltstone, and shale. Detrital zircon U-Pb ages and geochemistry are more closely aligned with a Sierran, rather than the more proximal KMP, source for Hornbrook detritus (Surpless and Beverly, 2013; Surpless, 2015). Furthermore deposition of deep-water turbidite atop the KMP indicate that Late Cretaceous subsidence affected this region, while the Sierra Nevada was prominent enough to be prone to erosion. An excellent roadcut on the east side of north-

bound Interstate 5 (stop 10 of Nilsen, 1984), exposing a northeast-striking fault juxtaposing the Hornbrook Formation with fluvial conglomerate of the Payne Cliffs Formation. Paleocurrent data from, and the array of clast lithologies contained in, the Payne Cliffs Formation suggest derivation from the KMP (McKnight, 1984). Hence, the KMP likely emerged from the floor of the Pacific Ocean to become a prominent topographic feature in early Cenozoic time. After passing through Ashland and beginning to climb from the southern terminus of Bear Creek Valley, note exposure of the nonconformity separating the deeply weathered Late Jurassic Ashland pluton from the overlying Hornbrook

Formation. Fresher fine- to medium-grained bio-

tite diorite of the Ashland pluton are observed in

roadcut over the next mile.

Exposures of folded marble plus quartz-biotite gneiss and schist of the KMP framework, most likely belonging to the structurally lower portion of the Applegate Group of the Late Triassic to Early Jurassic Rattlesnake Creek terrane (Donato et al., 1996).

Roadcuts in the vicinity of Siskiyou Summit expose the nonconformity separating the Ashland pluton from a section of the Hornbrook Formation containing its lower three members (the Klamath River Conglomerate, Osburger Gulch Sandstone, and Ditch Creek Siltstone). The nonconformity itself is a ~4 m thick grus horizon containing chiefly disaggregated granitic material with subordinate cm- to 10 cm-scale clasts of quartzite, chert, and metavolcanic material. Overlying Hornbrook Formation members record a progression from fluvial and alluvial sedimentation to slope and deep basin plain deposits. These relations are interpreted to reflect southward transgression of the Late Cretaceous ocean across the subsiding KMP (McKnight,

Approximately 1/2 mile south of this location, the SW-striking Siskiyou Summit fault places Oligocene nonmarine volcaniclastic and pyroclastic rocks of the Colestin Formation (excellent exposures adjacent to "Rocks" sign at Siskiyou Summit) above diorite belonging to the Ashland pluton, without intervening Hornbrook or Payne Cliffs formations. The prevailing explanation for these relations suggests that uplift along the Siskiyou Summit fault led to erosional removal of the Hornbrook and Payne Cliffs units, and normal-sense reactivation of this structure formed a graben filled by the Colestin Formation (Bestland, 1987).

1984; Nilsen, 1984; Surpless, 2015).

At the Oregon-California border, the Stateline fault marks the southern boundary of the Colestin graben and the northern edge of Cottonwood Creek Valley. This west-striking fault juxtaposes hanging wall Colestin Formation with the uppermost (Blue Gulch Mudstone) member of the Hornbrook Formation in the footwall.

On the west side of Interstate 5 lie roadcuts into the type section of the Klamath River Conglomerate of the Hornbrook Formation, and derivative placer mine workings (stop 2 of Nilsen, 1984). Exposures here consist primarily of clast- and matrix-supported conglomerate containing cobbles of subangular to subrounded metavolcanic rocks. Where observed, clast imbrication suggests southeastward transport. Based on these relations, Nilsen (1984) interprets these exposures as debris flow deposits derived from local sources in the Klamath Mountains. The prevalence of Jurassic plus Early Cretaceous detrital zircons with juvenile hafnium isotopic compositions from the Klamath River Conglomerate, and absence of Late Cretaceous grains, are

compatible with this view (Surpless and Beverly, 2013). Highly sheared basement rocks of greenstone, argillite, and chert of the North Fork terrane lie in nonconformable contact beneath the Hornbrook Formation here and in roadcuts preceding our upcoming stop at the Collier Rest Area in 1.9 miles.

Take exit 786 for CA-96 toward Klamath River Highway and follow signs for Randolph E. Col-

lier Rest Area. Bathroom break.

Return to vehicles, reset odometers to zero, follow signs for Klamath River Highway, and turn left (west) onto CA-96.

Mileage	Description
0.0	Continue west on CA-96/Klamath River Hwy 23.3 miles. From Interstate 5, CA-96 follows the Klamath River and traverses down structural section from the Sawyers Bar terrane, into the Rattlesnake Creek terrane, and finally into the inner metasedimentary unit of the Condrey Mountain schist.
7.7	Approximately one mile west of the turnoff to Tree of Heaven Campground, note roadcuts along the north side of the highway of feebly recrystallized pillow basalt mapped as Eastern Hayfork terrane (e.g., Barnes and Barnes, 2020).
14.5	A series of roadcuts on the north side of the highway into Rattlesnake Creek terrane mélange containing roughly subequal proportions of amphibolite and ultramafic rocks, each recrystallized at amphibolite grade.
23.3	Park on shoulder and prepare to examine Stop 2.1 exposures along CA-96 (be mindful of traffic along this busy road). We will spend at least 30 min at this stop and will stay close to the vehicles so there is no need to gear up. If stopping along a lower traffic road is desirable, similar exposures may be accessed along Walker Road, which parallels CA-96 on the south side of the Klamath river. To visit these exposures, cross the Walker Bridge at the unincorporated community of Klamath Falls, turn right (west), reset odometer, and continue to good exposures at 1.9–3.6 miles. Exposures of serpentinite and amphibolite belonging to the Rattlesnake Creek terrane begin west of the Oak Bar Lodge.

Stop 2.1. Inner Metasedimentary Condrey Mountain Schist (UTM 10T, 508728E, 4632525N)

The inner metasedimentary unit of the Condrey Mountain schist is exposed here in roadcut along California Highway 96. The inner unit of the CMS consists chiefly of dark quartz-mica schist (~95%), with subsidiary proportions of metabasalt exhibit-

ing transitional blueschist-greenschist facies parageneses (~3%), metaserpentinite (~1%), and metachert (<1%). Gradational, foliation-concordant contacts separating these subunits and local preservation of mappable relict stratigraphy (Helper, 1986) suggest that the lithologies contained in the inner CMS were introduced via sedimentary (i.e., not tectonic) mechanisms. Metaserpentinite also occurs along the Condrey Internal fault, which separates the inner and outer domains of the CMS.

The quartz-mica schist component of the CMS, on display at this location, is a homogenous, fine- to medium-grained foliated schist consisting chiefly of quartz and phengitic to paragonitic white mica, with subsidiary albitic plagioclase, chlorite, and carbonaceous material. The light gray to steely gray/green banding of this schist results from alternating quartz plus albite and white mica plus chlorite folia, respectively (each layer containing significant carbonaceous material). Minor amounts of pyrite, garnet, stilpnomelane, clinozoisite, titanite, apatite, tourmaline, cymrite, and calcite are locally present (Hotz, 1979). Volumetrically insignificant quantities of detrital zircon (5 or fewer grains/thin section) were observed in ~25% of petrographically analyzed samples.

Quartz-mica schist of the inner CMS likely formed via metamorphism of (hemi)pelagic protoliths. This inference is based on the small metaclastic component contained within quartz-mica schist and the association of these rocks with metamorphosed basalt, serpentinite, and chert, strongly suggesting that these materials accumulated on the ocean floor.

While an oceanic setting is envisioned for deposition of inner CMS protoliths, the spectra of U-Pb ages determined from detrital zircon grains of this unit indicate non-negligible terrigenous input and a strong affinity to western North America (Chapman, 2021, personal observ.; Fig. 6). Five samples, collected from the base to the top of the exposed inner CMS section, yielded a total of 839 concordant analyses and the following relations: (1) the youngest analyzed grains (~3% of all analyses) are Early Cretaceous in age, permitting calculation of maximum depositional ages that young downsection from 143.4 ± 3.2 to 128.7 ± 2.4 Ma (2σ , calculated from the youngest cluster of two or more ages with overlapping 15 uncertainties; Sharman et al., 2018); (2) the most prominent age peak occurs at ca. 160 Ma, with Middle and Late Jurassic ages making up 12% of all analyzed grains; (3) scattered Neoproterozoic and younger peaks of diminishing prominence occur at ca. 260, 400, and 600 Ma; (4) 21% of all analyses are "Grenville-age" (i.e., 950–1300 Ma); (5) older grains make up ~20% of all analyzed grains, with discernible peaks at ca. 1450 and 1660 Ma.

Observation 1 strongly suggests derivation of Early Cretaceous grains from ca. 142–136 Ma volcanic and/or exhumed plutonic rocks of the KMP. Given that these are the youngest igneous materials preserved in the province, detrital zircon grains younger than 136 Ma contained within the CMS must have originated from elsewhere, presumably from the still-active Sierra Nevada arc. Downsection-younging trends of maximum depositional ages (where such ages are demonstrably linked to the

independently known "true" depositional age and/or metamorphic age) are consistent with sequential underplating of progressively younger trench materials, an observation reported from subduction accretion assemblages around the world (e.g., Grove et al., 2008; Knittel et al., 2014; Dumitru et al., 2015; Chapman, 2017; Ducea and Chapman, 2018). It is important to note, however, that Observation 2 likewise suggests a significant contribution of regionally derived detrital zircon grains, as Middle and Late Jurassic (ca. 177–151 Ma) igneous rocks are abundant in the KMP (e.g., the Western Hayfork arc, the Wooley Creek belt, and the Rogue-Chetco arc; Saleeby et al., 1982; Harper, 1984; Wright and Wyld, 1986; Wright and Fahan, 1988; Hacker and Ernst, 1993; Harper et al., 1994; Harper, 2003; Snoke and Barnes, 2006; Yule et al., 2006; Barnes and Barnes, 2020).

Pre-Middle Jurassic detrital zircon populations contained in the inner CMS (i.e., Observations 3–5), do not overlap significantly with those of the central and eastern Klamaths (Fig. 6), suggesting that these grains originated from outside the KMP. This observation also suggests that basement rocks of the KMP were not exposed during Early Cretaceous deposition of inner CMS protoliths, and instead the province was blanketed with volcanic rocks at that time. The Sierran-Klamath backarc is the next most proximal inboard region from which pre-Middle Jurassic grain populations may have originated. Indeed, Jurassic eolianites (and, to a lesser extent, underlying Upper Triassic basinal strata) exposed east of the Sierran-Klamath arc overlap pre-Middle Jurassic detrital zircon populations contained within the inner CMS quite well (Fig. 6). We suggest that incorporation of pre-Middle Jurassic inner CMS components involved Jurassic erosion in the backarc region, perhaps within the Luning-Fencemaker thrust belt (e.g., Wyld, 2002; Wyld et al., 2003) or the Mogollon Highlands (Mauel et al., 2011), and westward routing of resulting detritus into the trench.

A comparison of U-Pb detrital zircon age spectra derived from the inner CMS with units of the western KMP and adjacent areas is illustrated in Figure 6. As noted previously, determining the origin of the CMS is of critical importance to accurately determining the magnitude and timing of late Mesozoic shortening in the KMP. With this in mind, several attempts have been made at correlating the inner (and outer) CMS with other late Mesozoic units in the region, with most tying the inner CMS to Late Jurassic rift clastics (e.g., the Galice Formation; Klein, 1977; Hotz, 1979; Saleeby and Harper, 1993) or Early Cretaceous trench deposits (e.g., the South Fork Mountain schist; Suppe and Armstrong, 1972; Brown and Blake, 1987). The majority of samples analyzed by Chapman (2021, personal observ.) yield Early Cretaceous maximum depositional ages and age spectra closely overlapping those of the South Fork Mountain schist. However, one sample collected from the inner CMS directly beneath structurally overlying outer CMS yields a Late Jurassic (ca. 160 Ma) maximum depositional age and a spectrum of ages closely overlapping the Galice Formation and Rattlesnake Creek terrane cover sequence. Furthermore, a sample of clastic material analyzed from the outer CMS (see Stop 2.3) also yields a Late Jurassic (ca. 164 Ma) maximum depositional age and spectrum overlapping the Galice Formation and Rattlesnake Creek terrane cover strata. In aggregate, U-Pb detrital zircon relations from the CMS strongly suggest that the unit was assembled from Late Jurassic to Early Cretaceous time, beginning with underplating of rift products and culminating with underthrusting of trench deposits. This significant finding will be echoed throughout the remaining Day 2 stops.

At least four generations of rock fabrics are recognized in both metasedimentary and metabasaltic units of the inner CMS, suggesting that these subunits were deformed together (Figs. 9 and 10). The oldest fabric preserved at this location (hereafter F0) is recognized as alternating light (quartz \pm albite) and dark (chlorite + carbonaceous matter \pm white mica) intervals, possibly representing primary sedimentary layering. This fabric is asymmetrically folded and transposed nearly beyond recognition into a second foliation (F1) of subhorizontal orientation, the most prominent fabric observed here. Detailed structural analysis by Helper (1986) revealed an additional asymmetric fabric (F2) in metabasaltic rocks (see optional blueschist quarry stop), and to a lesser extent in metasedimentary lithologies, that formed parallel to the dominant F1 fabric. A final F3 fabric, again better represented in metabasalt, is marked by the development of boudins adjacent to quartz-rich domains, where ductility contrast with adjacent micaceous material is high. In aggregate, the sequential development of asymmetric F1 and F2 features, followed by symmetric F3 boudinage is linked to burial within a noncoaxial regime followed by coaxial structural ascent (Helper, 1986).

Integration of observations made at this location and elsewhere provide key insights into the significance of the inner CMS: (1) the array of rock types contained in the inner CMS were introduced via sedimentary processes and point to abyssal deposition with limited terrigenous input, probably in an ocean trench; (2) inner CMS sedimentary protoliths (~95% of the inner CMS) were sourced from the western margin of North America, specifically from the Sierran-Klamath arc and backarc; (3) transitional blueschist-greenschist parageneses preserved in mafic volcanic inner CMS protoliths (see optional blueschist quarry stop), and the development of noncoaxial F1-F2 fabrics, suggest that these rocks were buried in a subduction zone to >20 km paleodepth (>6 kbar); (4) calculated maximum depositional ages require that burial began no earlier than ca. 143 Ma and continued with underplating of progressively younger slices until at least ca. 131 Ma; (5) ca. 128-118 Ma K-Ar amphibole and white mica ages suggest that burial-related metamorphism and cooling from peak conditions occurred in this time frame; (6) coaxial F3 fabrics and associated retrograde mineralization developed during Neogene structural ascent and associated doming (Mortimer and Coleman, 1985).

These relations, plus the observations that the inner CMS resides ~100 km inboard from the inferred Early Cretaceous paleotrench and no mantle intervenes between it and upper plate rocks, lead us to assert that the inner CMS is a product of a previously unrecognized shallow-angle subduction episode.

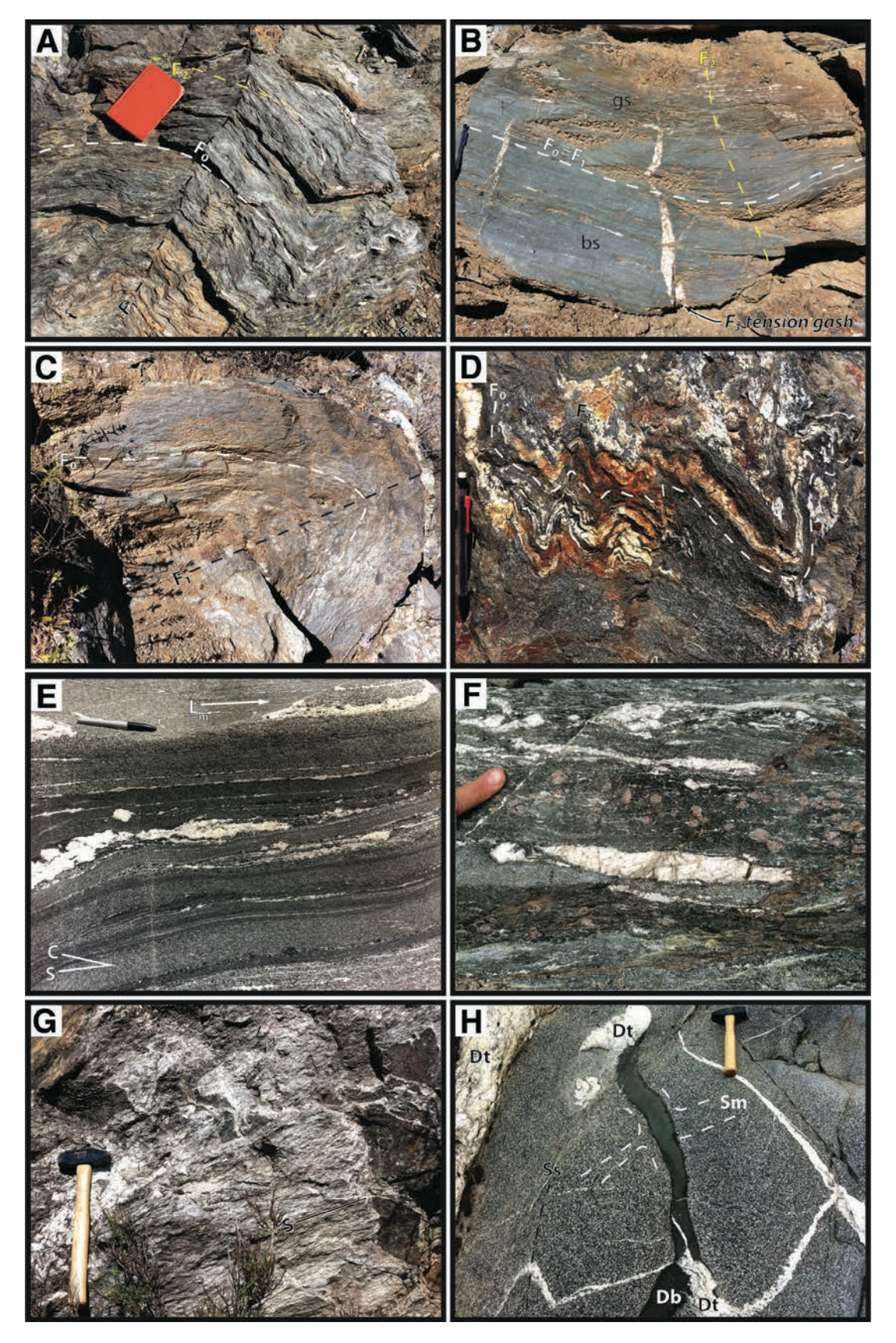


Figure 9.

Return to vehicles, reset odometers to zero, and proceed to optional blueschist quarry stop, if time allows.

Mileage	Description
0.0	Turn the vehicles around, drive east on CA-96
	for 1.4 miles, and take a sharp left at Doggett
	Creek Road.
1.4	Continue on Doggett Creek Road for 1.2 miles and
	turn left on 12 Road/Forest Route 46N52. Note
	small exposures of inner CMS metasedimentary
	rocks near this intersection (most notably folded
	examples at UTM 10T, 509494E, 4633168N).
2.6	Continue for 6.9 miles, turn right on an
	unmarked road. Continue for 0.4 miles and
	arrive at Stop 2.2.

Stop 2.2 (Optional). Inner CMS Blueschist Quarry (UTM 10T, 504588E, 4635456N)

This stop was originally showcased as stop 6 in the guidebook of Kays and Ferns (1980). At this location, fine-grained blueschist of the inner CMS is exposed in a small quarry. Contact relations between this blueschist and surrounding metasedimentary assemblages are not clear at this location. However, ~3 km along strike (north) of this location the contact is an ~1–20 m thick succession wherein blueschist is sequentially overlain by fine-grained greenschist, metalliferous chert and schist (with rare pelitic blueschist), and chlorite-rich greenschist, before entering graphitic schist like that exposed at stop 1 (Helper, 1986). The consistency of this succession, the gradational and interfingering nature of individual contacts, and the lack of block-in-matrix

Figure 9. Field photographs of petrologic and structural features relevant to Day 2 stops. (A) Quartz-mica schist of the inner Condrey Mountain Schist (CMS) displaying F0, F1, and F2 fabrics (see text for discussion), exposed ~3 km SE of Condrey Mountain peak (14-cmlong field notebook for scale). (B) Stop 2.2 transitional blueschist (bs)greenschist (gs) displaying F0, F1, F2, and F3 fabrics (see text for discussion; 14-cm-long mechanical pencil for scale). (C) Stop 2.3 outer CMS greenschist displaying F0 and F1 fabrics (see text for discussion; 14-cm-long pen for scale). (D) Exposure within the gradational contact of outer CMS albite-epidote amphibolite with Gold Flat amphibolite. The "contorted nature" of folding (note F0 and F1 fabrics) is invoked by Barrows (1969) as evidence for a cryptic shear zone along the gradational contact, which we dispute (14-cm-long mechanical pencil for scale). (E) Foliation-perpendicular, lineation parallel section of Gold Flat amphibolite (Stop 2.4) showing S-C fabrics suggesting top \rightarrow right (east) sense of shear. Note asymmetric porphyroclasts of sheared light-colored (plagioclase-rich) transposed vein material (14-cm-long marker for scale). Lm—mineral stretching lineation. (F) Garnet (~1 cm round red porphyroblasts)-bearing Gold Flat amphibolite exposed at Stop 2.4 (human finger for scale). (G) Leucogneiss (S annotation approximates gneissic foliation) exposed north of Scott Bar (see road log; 38-cm-long hammer for scale). (H) Exposure of Slinkard Pluton and cross-cutting basaltic (Db) and trondhjemitic (Dt) dikes, Stop 2.5. Note magmatic foliation (Sm, defined by elongate felsic and mafic phenocrysts) formed synchronously with mafic dikes while solid-state (Ss) foliation and associated folding deforms both dike populations.

relations strongly suggest a sedimentary origin for these features and that tectonic processes did not introduce blueschist to the inner CMS. This sequence resembles the basalt-chert-clastic variety of oceanic plate stratigraphy commonly preserved in the Franciscan complex (e.g., Wakabayashi, 2017).

Blueschist here consists chiefly of fibrous sodic amphibole (crossite to glaucophane) and epidote, with minor chlorite, albite, phengitic mica, titanite, calcite, garnet, and stilpnomelane (Figs. 10C and 10D). Lawsonite has not been reported at this, or any other, exposure in the CMS. Similar peak metamorphic parageneses, reported near Condrey Mountain Peak (\sim 3 km north of this location), imply equilibration at temperature-pressure conditions of 380 \pm 40 °C and 6.3 \pm 1.2 kbar (Helper, 1986).

Also apparent at this location are several centimeter- to millimeter-scale intercalations of greenschist that display the same assemblage, though contain calcic (actinolite) instead of sodic amphibole and a higher modal abundance of chlorite (Figs. 10C and 10D). The intercalations apparent here may reflect the influence of fine-scale variations in bulk rock composition as the inner CMS equilibrated under transitional blueschist-greenschist facies conditions (Donato et al., 1980). Alternatively, actinoliterich domains, in contrast to those containing sodic amphibole (as discussed in the following paragraph), do not display strong mineral preferred orientations and thus may represent zones of static greenschist facies retrograde overprinting (Helper, 1986), modulated by the limited availability of fluids.

At least four generations of rock fabrics are apparent at this location. The oldest fabric preserved at this location (F0) is recognized as alternating felsic (albite+quartz) and mafic (amphibole ± epidote ± titanite) intervals, possibly representing primary volcanic layering (Figs. 9B and 10C).

The F0 fabric is asymmetrically folded and transposed nearly beyond recognition into a second foliation (F1) of sub-horizontal orientation, the most prominent fabric observed here. The phase of deformation that formed F1 and related fabrics was also accompanied by growth of sodic amphibole and white mica. The long dimensions of each mineral lie within the prominent foliation and an amphibole lineation is apparent within foliation planes. In aggregate, the large strain magnitudes, asymmetric aspect of transposed F0 fabrics, and linked prograde metamorphic recrystallization point to simple shear associated with tectonic burial.

A third fabric, recognized by open-to-isoclinal folds with N-S-trending, shallowly plunging, and locally crenulated fold hinges (F2), overprints F1. Detailed structural analysis of the inner CMS indicates that F2 folds tightened progressively, leading Helper (1986) to distinguish an additional set of identically oriented structures. Helper (1986) attributes the difference in fold style associated with F2 fabrics to reflect strain localization (i.e., a dominance of distributed flow versus flexural slip implied by F1 versus F2 features, respectively), perhaps during the early stages of structural ascent.

The fourth and final deformation phase (F3) formed boudins that pinch-and-swell the F1 foliation, quartz-filled tension gashes

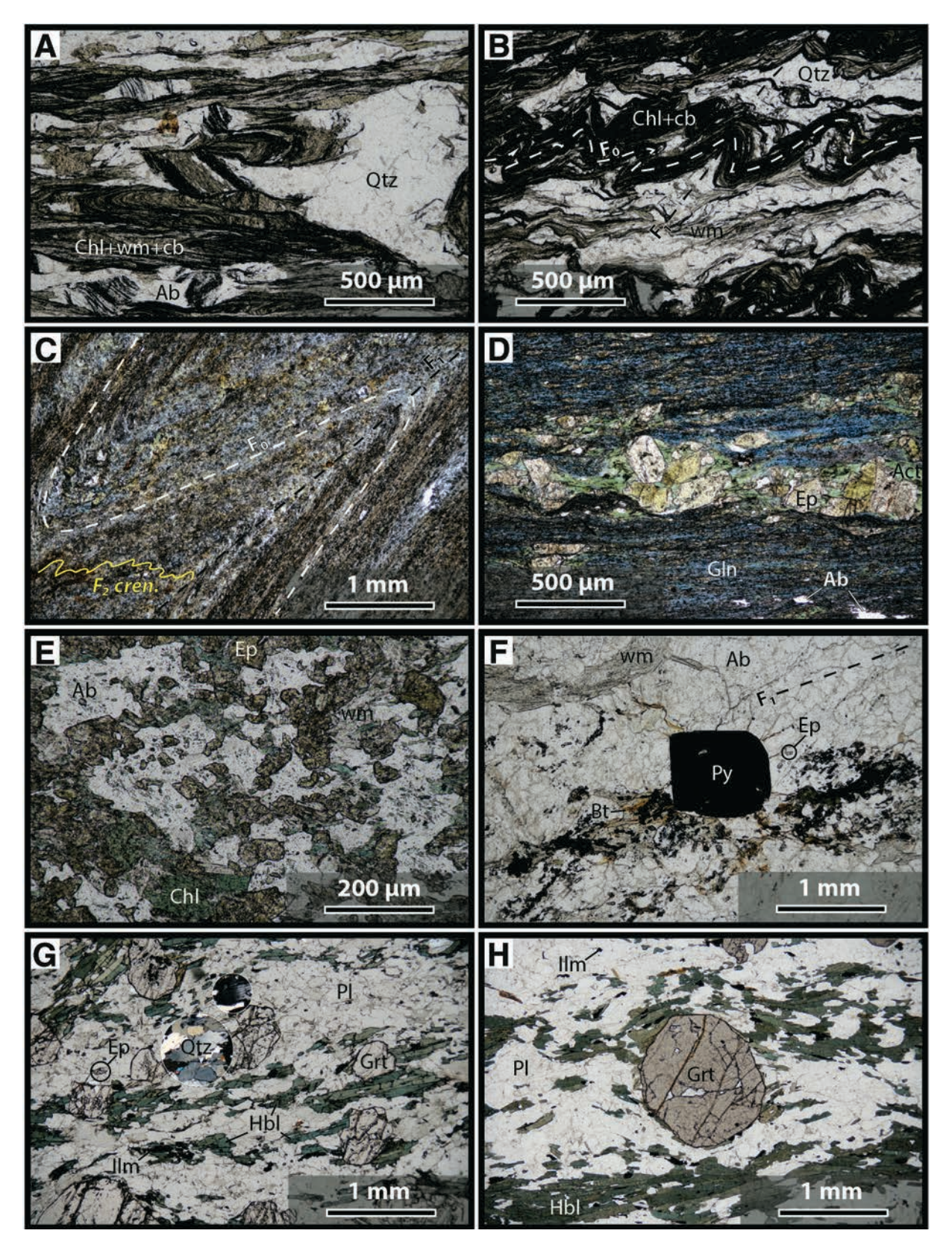


Figure 10.

that cut F1 at high-angle, and a crenulation cleavage oriented at high-angle that of F2. These features most likely formed within an extensional, pure shear regime associated with structural ascent of the inner CMS through the ductile-brittle transition zone. Isostatic rise of buoyant CMS relative to overlying rock types, perhaps during the Neogene doming event proposed by Mortimer and Coleman (1985), provides a working explanation for F3 fabrics.

The timing of deposition, metamorphism, deformation, and cooling of inner CMS blueschists are all poorly constrained. One sodic amphibole 40 Ar/ 39 Ar age of 167 ± 12 Ma is reported on the geologic map of Coleman et al. (1983) and one K-Ar amphibole age of 127.4 ± 6.3 Ma is reported in the unpublished Ph.D. thesis of Helper (1985) from the same area. White mica K-Ar data are available from two inner CMS blueschist locations, yielding ages of 127.9 \pm 2.0 Ma (Helper, 1985) and 118 \pm 2 Ma (Coleman et al., 1983). In light of contact relations suggesting that inner CMS blueschist and metasediments were part of a stratigraphic package, and therefore experienced metamorphism en masse, ⁴⁰Ar/³⁹Ar and K-Ar ages derived from either unit must postdate the timing of sedimentation. As mentioned at Stop 1, detrital zircon U-Pb maximum depositional ages derived from metasediment collected adjacent to blueschist in the deepest exposed portions of the Condrey Mountain window fall in the ca. 141-129 Ma range (Fig. 6). The ca. 167 Ma age reported by Coleman et al. (1983) is therefore irreconcilable with new detrital zircon geochronology and perhaps suffered from excess argon.

Figure 10. Plane-polarized light photomicrographs of petrologic and structural features in inner (A-D) and outer (E-H) Condrey Mountain Schist. All thin sections oriented perpendicular to dominant macroscopic foliation (F1) and parallel to mineral stretching lineation. (A) Stop 2.1 quartz-mica schist containing isoclinal folds severed via pressure solution. (B) Less deformed equivalent of A from the summit of Condrey Mountain peak. (C) Stop 2.2 transitional blueschistgreenschist displaying mm-scale folding of primary volcanic layering (F0). Crenulations (F2) are common in fold hinge zones. (D) Coarsergrained blueschist-greenschist from the same location. Note coarsegrained transposed vein running from left to right of the photo containing epidote and pale green actinolite, the latter growing at the expense of blue amphibole. (E) Albite-chlorite-epidote-white mica greenschist exposed at Stop 2.3. (F) Leucogneiss (F1 annotation approximates gneissic foliation) exposed north of Scott Bar (see road log) showing plagioclase- and mica-dominated assemblage. (G) Garnet-bearing Gold Flat amphibolite exposed at Stop 2.4. Note inclination of asymmetric garnet porphyroblasts to the right (west), suggesting top \rightarrow west (i.e., burial-related) kinematics. Also note tapered deformation twins in plagioclase plus amoeboid grain boundaries in undulose quartz (both shown in circular cross-polarized light "spotlights"), suggesting deformation at elevated shear stress and temperature. (H) Large garnet porphyroblast in Gold Flat amphibolite, Stop 2.4 (note garnet in this unit locally achieves diameters of ~1 cm). Mineral abbreviations: Ab—albite; Act—actinolite; Bt—biotite; cb—carbonaceous material; Chl—chlorite; Ep—epidote; Gln—sodic amphibole (glaucophane/ crossite); Grt—garnet; Hbl—hornblende; Ilm—ilmenite; Pl—plagioclase; Py—pyrite; Qtz—quartz; wm—white (phengitic) mica.

Remaining amphibole and white mica ages fall in a much tighter ca. 128–118 Ma cluster, though it should be emphasized that the quality of these unpublished data is uncertain as detailed argon systematics of individual samples are unavailable. Interpretation of these data requires three key assumptions: (1) that these unpublished ages are robust, (2) that amphibole and white mica closure temperatures of 530 ± 40 and 350 ± 50 °C (e.g., McDougall and Harrison, 1999), respectively, are valid for these rocks, and (3) that these rocks experienced peak metamorphism at 380 ± 40 °C. If these assumptions are valid, then amphibole and white mica ages should be interpreted as dating burial-related metamorphism and cooling from peak temperatures, respectively.

These ages are identical, within uncertainty to 126–120 Ma ⁴⁰Ar^{/39}Ar white mica total gas ages derived from the South Fork Mountain schist of the Franciscan complex (Dumitru et al., 2010). Furthermore, the inner CMS and South Fork Mountain schist share a similar range of lithologies, yield identical maximum depositional ages, and exhibit overlapping U-Pb detrital zircon age specta, strongly suggesting that the inner CMS represents inboard equivalents to the SFMS (Fig. 6). In aggregate, deposition, metamorphism, and cooling the inner CMS occurred in a 140–120 Ma window. This window significantly postdates the Nevadan orogeny and therefore burial of the SFMS-inner CMS must be related to a previously unrecognized phase of Early Cretaceous underthrusting beneath the KMP.

This time window also corresponds with the ca. 136 Ma termination of arc magmatism in the KMP (e.g., Snoke and Barnes, 2006), the separation of the KMP from its northern Sierra Nevada/Blue Mountains counterparts (e.g., Ernst, 2013), low-angle normal faulting in the eastern Klamaths (Cashman and Elder, 2002; Batt et al., 2010b), and the development of a Valanginian-Hauterivian marine transgression across the KMP (Harper et al., 1994; Batt et al., 2010a). We posit that tectonic switching (e.g., Collins, 2002) from shallow-angle to steeper downflow of an ~300-km-wide segment (i.e., the approximate width of the KMP) of subducting Farallon lithosphere, over an ~10 Myr timeframe in the Early Cretaceous, drove upper plate extension and trench retreat. Subduction of an inactive spreading ridge, hypothesized to explain anomalously high-temperature metamorphism of the South Fork Mountain schist (Wakabayashi, 2015), may have driven inferred changes in slab dip.

Return to vehicles and proceed to Stop 2.3.

Mileage	Description
0.0	Return to Stop 2.1, reset odometers to zero, and
	continue west on CA-96.
2.5	After 2.5 miles, we cross over the Condrey
	Mountain shear zone and enter upper plate rocks
	of the Rattlesnake Creek terrane. Roadcuts over
	the next ~1.8 road miles feature interlayered
	quartz-biotite schist and amphibolite gneiss,
	each cut by mafic dikes, all metamorphosed and
	deformed en masse.

2.9 Roadcut of medium-grained quartz monzonite cutting basement rocks of the Rattlesnake Creek terrane. These intrusives presumably originated from the ca. 167 Ma Vesa Bluffs pluton of the Wooley Creek suite, the main mass of which occurs ~200 m south of this location.

5.1 CA-96 crosses a truss bridge to the south side of the Klamath River. Approximately one mile west of the bridge, CA-96 crosses the Condrey Mountain shear zone again within the unincorporated community of Horse Creek, reentering the Condrey Mountain schist at the approximate location of the Condrey Internal fault. The outer metavolcanic and inner metasedimentary subunits lie on the south and north side of CA-96 within Horse Creek, respectively.

10.9 Turn left (south) on the Scott River Rd and park at the pullout adjacent to LDMA camp.

Stop 2.3. Outer Metavolcanic Condrey Mountain Schist (UTM 10T, 497107E, 4624875N)

The structurally higher, hence outer, unit of the Condrey Mountain schist is well exposed here in a roadcut directly south of the intersection between CA-96 and the Scott River Road, also the confluence of Klamath and Scott rivers. This stop corresponds to the location of stop 8 in the guidebook of Kays and Ferns (1980).

The outer unit of the Condrey Mountain schist consists chiefly of albite-chlorite-quartz assemblages that vary in mafic mineral content (primarily chlorite, amphibole, and epidote) and range from pale to dark green, as a result (Fig. 10E). Pale green varieties typically exhibit compositional banding defined by chlorite content, while more mafic assemblages tend to be more massive though locally preserve flattened pillow structures. The compositions and textures preserved in these rocks point to a volcanic origin with protoliths ranging from spilitized basaltic tuffs to lava flows (Hotz, 1979; Helper, 1986).

A subordinate (<5% by area) metasedimentary component, mainly gray to brown semipelitic to pelitic schist, locally interleaves with metavolcanic rocks of the outer CMS. These rocks are distinguished from mafic schists described above by a higher proportion of quartz plus white mica, a lower proportion of mafic minerals, and the presence of small amounts of garnet and finely disseminated carbonaceous matter. Graded bedding is locally apparent, based on subtle variations in the abundance of carbonaceous matter. (Semi)pelitic schist is distributed throughout the outer CMS as thin intercalations with mafic schist, though occurs most prominently as an ~150 m-thick interval within the core of a synform on the western flank of the Condrey Mountain window (Fig. 7).

The contact zone separating mafic from (semi)pelitic schists is marked by (1) a gradation in the former to a more felsic, mainly quartz-albite-white mica, schist with local pyrite, epidote, chlorite, amphibole, calcite, and chloritoid, and (2) the appear-

ance of thin, finely laminated, and resistant quartzite (presumably metamorphosed chert) beds. The relative abundance of sulfides in these "white schists" was exploited during the 1905–1930 operations of the Blue Ledge mine. The legacy of this operation continues in the form of acid mine drainage, leading the U.S. Environmental Protection Agency to classify the Blue Ledge mine as a Superfund site in 2006.

In aggregate, the above relations suggest that the outer unit of the CMS represents a disrupted section of mafic-to-felsic pyroclastic material, submarine basalt flows, and deep marine hemipelagic plus chert sediment. Furthermore, the absence of calcareous material from, the presence of metachert in, and the limited clastic component of this unit point to deposition in a deep though continental margin-flanking basin.

At this location, a fine- to medium-grained compositionally layered schist is exposed. These rocks preserve a greenschist facies assemblage of chiefly quartz, chlorite, and albite, with minor quantities of actinolite, epidote, pale-pink grossular-spessartine-almandine garnet, and trace amounts of dark carbonaceous material and bright-green phengitic mica (Fig. 10E). An increase in carbonaceous material from the north to south end of this road-cut results in darker hues to the south. Though modern quantitative thermobarometry has not been done at this location or in greenschist facies assemblages elsewhere in the outer CMS, peak metamorphism at conditions of 400 ± 50 °C and 4.5 ± 2.5 kbar likely occurred, based primarily on textural equilibration of the above assemblage, the local preservation of chloritoid, and the absence of pumpellyite and Na-amphibole (Helper, 1985).

At this location, quartz veins are injected parallel to compositional layering; together these domains are isoclinally and ptygmatically folded with west-dipping axial planar cleavage. Respectively, these structures are referred to by Helper (1985) as D1 (shown as F0 on Fig. 9C), interpreted as a pseudostratigraphy formed through isoclinal folding and transposing original beds of tuff, and D2 structures (F1 on Fig. 9C). The latter structures commonly achieve amplitudes and wavelengths of several meters. These two fabrics apparently preceded and/or overlapped peak metamorphism and record contraction and shearing; as such, we refer to these as "prograde" or burial-related fabrics and argue that these fabrics developed during the Nevadan orogeny.

Two additional "retrograde" fabrics superimpose the prograde fabrics discussed above. The first (D3 of Helper, 1985) is restricted to within ~500 m of the unit-bounding Condrey Mountain shear zone and thus is not apparent at this locality. This fabric apparently formed during and/or slightly following peak metamorphism, and is recognized by boudinage of earlier formed prograde structures, the development of a mineral stretching lineation, and open folding. The second retrograde fabric (D4 of Helper, 1985) is marked by brittle-ductile features including kink banding, mode 1 fractures, and the development of several eastwest–striking faults. Retrograde D3 and D4 fabrics may record the initial stage of structural ascent of the outer CMS, presumably associated with Neogene doming that formed the Condrey Mountain window (Mortimer and Coleman, 1985).

New U-Pb analysis from one sample of semipelite collected ~18 km NNW of this location yielded concordant ages from 135 detrital zircon grains. Ages range from 161.4 ± 4.8 to $2898.3 \pm 12.0 \text{ Ma}$ (1 σ ; Fig. 6). The majority of analyzed grains (54%) yield Jurassic ages, with the most pronounced peak centered at ca. 168 Ma. The weighted average of the youngest ten grains from this sample (that overlap within uncertainty) constrains the depositional age to no older than 164 Ma (Callovian). The true depositional age of this sample must lie between its maximum depositional age (ca. 164 Ma, as constrained above) and ca. 152 Ma (an Ar-Ar hornblende age determined from Stop 2.4 and inferred to coincide with the waning stages of thrusting along the Condrey Mountain shear zone; Saleeby and Harper, 1993). Significant overlap between this ca. 164-152 Ma interval, in which the analyzed sample was deposited and underthrust beneath the Rattlesnake Creek terrane, and the ca. 157-150 Ma Nevadan orogeny lead us to assert that burial of the outer CMS occurred during this event. One unpublished K-Ar age of 142.1 \pm 2.3 Ma (white mica; Helper, 1985) may reflect additional cooling of the outer CMS below ~350 °C following underthrusting. An additional unpublished K-Ar age of 125 ± 3 Ma (actinolite; Coleman et al., 1983) is not readily interpretable.

This sample contains a significant proportion of pre-Jurassic detrital zircon. Paleozoic populations (21% of the total) exhibit minor peaks occurring at 268, 320, 329, 390, and 486 Ma. Timanian/Pan-African-age grains make up 5% of the total. Proterozoic populations include a broad swath of Grenvilleage grains (7%) plus distinct peaks at 1350 Ma, 1500 Ma, and 1630 Ma, corresponding to 5%, 3% and 5% of analyzed grains, respectively. Four isolated Archean grains range from 2500 to 2900 Ma. The full age spectrum derived from outer CMS semipelite significantly overlaps those of the Salt Creek and Dubakella Mountain assemblages and Galice Formation, all inferred to have been deposited in extensional/rift basins flanking the western KMP between Middle to Late Jurassic time. Furthermore, the abundance of pre-Jurassic detrital zircon grains contained within outer CMS semipelite and the degree of age spectrum overlap between this sample and Mesozoic strata deposited along the western margin of North America (Fig. 6) corroborate models suggesting that these materials formed adjacent to North America (e.g., Snoke, 1977; Wright and Wyld, 1994; Yule et al., 2006; LaMaskin et al., 2021). Models suggesting that these materials formed far from North America and were transported across the Panthalassan ocean before colliding with North America during the Nevadan event (e.g., Sigloch and Mihalynuk, 2017; Clennett et al., 2020) are not supported by the data.

Return to vehicles, reset odometers to zero, and proceed to Stop 2.4.

Mileage	Description
0.0	Continue south on Scott River Road.
2.6	Roadcuts on the right (west side of Scott
	River Road) of a small (a few 10s of meters
	wide) coarse-grained leucocratic igneous

rock within the outer metavolcanic CMS unit, ~0.4 miles north of the unincorporated community of Scott Bar (UTM 10T, 499157E, 4622064N). Gneissic layering of this chiefly plagioclase+chlorite+white mica+biotite+quartz+ epidote+pyrite assemblage (Fig. 10F) is concordant with the dominant foliation of the outer metavolcanic CMS (labeled S on Fig. 9G). This structural relationship led Saleeby and Harper (1993) and Helper (1985) to interpret leucocratic gneiss exposed at this location as a sill that invaded the outer CMS. An unpublished concordant U-Pb zircon TIMS age of 170 +/- 1 Ma was also determined from this location, which the same workers interpret to reflect the timing of sill injection. By this interpretation, the protoliths of the outer CMS must be older than ca. 170 Ma. However, intrusive relationships such as injections into the host or contact metamorphism between leucocratic gneiss and outer CMS greenschist are not observed at this location. Furthermore, the structural concordance between, and overlapping greenschist facies grade of, leucocratic gneiss and the outer CMS strongly suggests that both materials were deformed and metamorphosed together. These relations lead us to interpret that leucocratic gneiss exposed here originated as a felsic tuff erupted ca. 170 Ma. Recent U-Pb zircon analyses from this location corroborate previously mentioned unpublished ages, yielding a concordia age of 171.8 ± 0.8 Ma (2σ; Chapman, 2021, personal observ.; Fig. 11B).

- 6.1 Continuing south, we approach the core of a broad, shallowly west-plunging anticlinorium (Barrows, 1969; Fig. 8). Peak metamorphic parageneses preserved in the outer CMS transition from greenschist into albite-epidote amphibolite facies assemblages.
- 10.0 Metamorphic grade continues to increase as we traverse southward, here transitioning from albite-epidote amphibolite to upper amphibolite facies assemblages. At the Townsend Gulch River Access (UTM 10T, 4922994E, 4615154N; Fig. 8), folded and banded gneiss of the outer CMS crop out along the Scott River and roadcuts along the Scott River road, a short walk (<500 feet) from the river access (Fig. 9D). From Stop 2.3, the metamorphic grade of the outer CMS has increased from greenschist to upper amphibolite facies without any clear structural breaks (e.g., mylonite or brittle fault rocks). Despite the lack of obvious discontinuities, the outer CMS-Rattlesnake Creek terrane fault

contact has traditionally been placed at this location, based primarily on the "contorted nature of the foliation and fold axes" found here (Barrows, 1969, p. 91). At Stops 2.4 and 2.5, we suggest that the upper-lower plate contact be placed at the base of the Slinkard Pluton and that the Gold Flat Amphibolite, traditionally assigned to the Rattlesnake Creek terrane, is the structurally

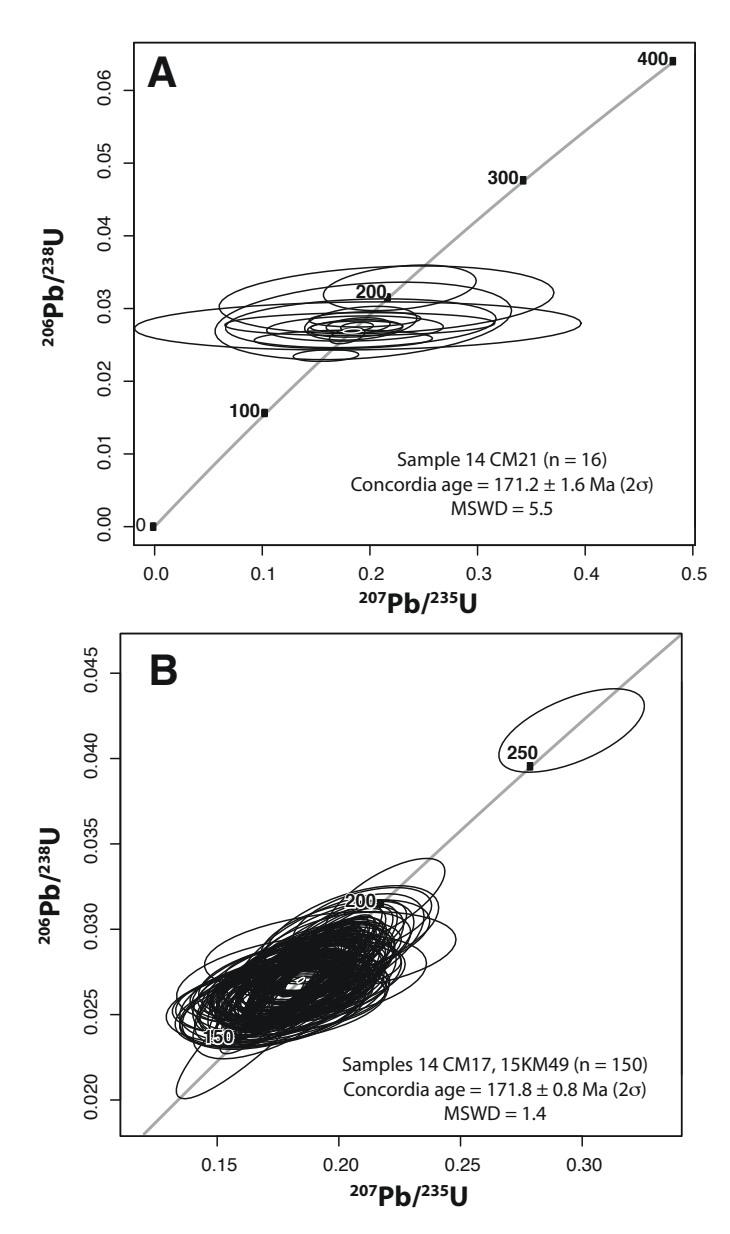


Figure 11. U-Pb zircon concordia plots (from laser ablation inductively coupled plasma mass spectrometry analysis) from (A) Gold Flat amphibolite melanosomes collected from Stop 2.4 and (B) leucogneiss collected from ~0.4 miles north of Scott Bar (see Day 2 road log description at cumulative mileage = 138.6). Individual analyses shown as unfilled black ellipses; calculated concordia ages shown as white ellipses with black fill. MSWD—mean square of weighted deviates.

highest and highest grade portion of the outer CMS.

10.8 Prepare to pull over and park on the left side of Scott River Road at the wide pullout marked by the Tompkins Creek River Access sign. Take care when descending to river level down a steep and poison oak—choked path.

Stop 2.4. Gold Flat Amphibolite: Rattlesnake Creek Terrane or Outermost CMS? (UTM 10T, 491966E, 4614462N)

From Stop 2, we traversed south along the "Scott River appendage" of Saleeby and Harper (1993), a south-trending projection from the main domal mass of CMS, to its southern terminus—the east-west-trending and shallowly (west) plunging Scott River antiform (Barrows, 1969; Burton, 1982; Fig. 8). In doing so, we ascended ~3 km structurally, witnessing outer CMS lithologies grade up from greenschist, through epidote amphibolite, and to garnet-bearing upper amphibolite facies assemblages (Barrows, 1969; Burton, 1982; Saleeby and Harper, 1993). A gradational textural upgrade from schist to migmatitic gneiss occurs in tandem with mineralogical changes.

Barrows (1969) infer a structural break between amphibolite and epidote-amphibolite facies assemblages, based on abundant ptygmatic folds overlapping the boundary (Fig. 9D). However, no evidence of significant ductile shearing (e.g., mylonite) is observed within this zone, leading us to assert that the contact is truly gradational. Instead, we recognize that feldspathic veins abundant in upper amphibolite facies rocks (described in detail below) first appear at the gradational epidote amphibolite-upper amphibolite unit boundary and posit that the viscosity contrast between leucocratic and melanocratic domains led to buckling of the former and the development of ptygmatic folds.

These relations indicate that the outer CMS preserves an inverted metamorphic field gradient on the order ~75 °C/km. The Gold Flat amphibolite, named by Burton (1982) for excellent exposures at this location along the Scott River, represents either the basal domain of the Rattlesnake Creek terrane or the upper amphibolite facies culmination of the inverted metamorphic field gradient preserved in the outer CMS. The affinity of the Gold Flat amphibolite will be a focal point of this stop.

Detailed petrographic and structural analysis of the Gold Flat Amphibolite was first completed by Barrows (1969), who distinguished this "Amphibolite unit" from "pre-Mesozoic older metamorphic rocks" (Rynearson and Smith, 1940). Barrows (1969) described these rocks as a medium- to coarse-grained gneiss consisting chiefly of pargasitic hornblende and albitic to labradoritic plagioclase, with accessory ilmenite and apatite. Garnet, colorless clinoamphibole (cummingtonite), and clinopyroxene are rare in these rocks though are locally abundant within ~100 m of the contact with the Slinkard pluton and ultramafic bodies that occupy the same structural position above the Gold Flat unit (Figs. 9E, 9F, 10G, and 10H). Hornblende and plagioclase compositions also appear to vary in space, becoming more tschermakitic and anorthitic, respectively, with proximity to overlying

units. Hornblende is commonly zoned, with brown cores and green rims, adjacent to overlying rocks. Quartz and rutile are also rare in the Gold Flat amphibolite though their occurrence does not appear to vary with proximity to other rock units.

Peak amphibolite facies parageneses described above equilibrated at 630 ± 50 °C and 7.3 ± 1.0 kbar, corresponding to transitional albite-epidote amphibolite/upper amphibolite conditions and overlapping the $\rm H_2O$ -saturated solidus for the bulk composition of outer CMS metabasalt (Klapper and Chapman, 2017). Peak assemblages are locally overprinted by retrograde growth of chlorite, epidote, titanite (as mantles on rutile), and the development of pale green rims (actinolite?) on dark green or brown hornblende cores, presumably as these rocks cooled through the greenschist facies.

The Gold Flat amphibolite exhibits a well-developed gneissic to blastomylonitic foliation with thin (typically < 1 cm wide) feldspathic veins (hereafter "leucosomes") oriented parallel, and at shallow angles, to the foliation ("melanosomes"). At this location, the foliation (S on Fig. 9E) strikes ~north-south and dips moderately to the west. A well-developed lineation (Lm on Fig. 9E), marked by the long dimension of amphibole within the foliation plane, plunges approximately down-dip, subparallel to the trend of the Scott River antiform. The macroscopic L-S fabric apparently resulted from flattening and stretching of felsic vein material and mafic host rocks as each are isoclinally folded. Limited kinematic analyses of sections oriented parallel to the lineation and perpendicular to the foliation do not yield a consistent shear sense (Coons, 2017). Chevron folds locally overprint L-S fabrics and appear to be associated with greenschist facies retrograde parageneses. Thus, the sequence of structural events preserved in the Scott River antiform involved: (1) deposition of mafic volcanic protoliths, (2) partial melting, fracturing, and injection of felsic vein fill coeval with burial and development of prograde L-S fabrics, and (3) retrograde chevron-style refolding of L-S fabrics.

The contact between the Gold Flat Amphibolite and overlying Slinkard Pluton and ultramafic rocks is concordant with the foliation of each unit. As noted at the next stop (Stop 2.5), the Slinkard pluton is also well-foliated within ~100 m of the contact with the Gold Flat Amphibolite (Fig. 9H); this foliation yields to hypidiomorphic-granular textures >100 m from the contact. (It should be noted that petrography is generally needed to determine the location of the contact since foliated hornblende-plagioclase assemblages are present on either side.) These textural relationships, and the lack of intrusive relationships (e.g., no dikes originating in the Slinkard pluton are observed in the Gold Flat unit), strongly suggest that contact between the Gold Flat amphibolite is a shear zone several hundreds of meters thick.

The Gold Flat amphibolite was assigned by Burton (1982) to the base of the Rattlesnake Creek terrane, in the upper plate of the Condrey Mountain shear zone, on the basis of structural position and the presence of garnet-bearing amphibolite facies assemblages. However, it is conceivable that the Gold Flat amphibolite represents the amphibolite facies culmination of a documented

north-to-south field metamorphic gradient, beginning in greenschist facies outer CMS assemblages near the confluence of the Scott and Klamath rivers (Barrows, 1969; Saleeby and Harper, 1993). Indeed, U-Pb data from oscillatory zoned zircon core domains from Gold Flat amphibolite melanosomes point to igneous crystallization of these domains at 171.2 ± 1.6 Ma (Chapman, 2021, personal observ.; Fig. 11A), ~20 Myr younger than the youngest dated igneous protoliths from the Rattlesnake Creek terrane (cf., Wright and Wyld, 1994) and overlapping ages from igneous protoliths of the outer CMS. The "Scott River granophyre" of Saleeby and Harper (1993), a relatively large leucosome sampled from the Gold Flat amphibolite, yielded a slightly discordant multi-fraction age of 157 +3/-2 Ma, which these workers attributed to some combination of inheritance plus open system behavior. New results from single zircon crystals extracted from the same leucosome material yield U-Pb ages of 155.3 ± 0.3 Ma (Gates et al., 2019; Dailey et al., 2019). Amphibole from this location yields 40 Ar/ 39 Ar ages of 150.1 \pm 4.6 Ma and 152 \pm 1 Ma (Saleeby and Harper, 1993; Hacker et al., 1995). We interpret the array of ages determined from the Gold Flat amphibolite to reflect ca. 170 Ma eruption, ca. 155 Ma metamorphism, and ca. 150 Ma cooling from peak metamorphic conditions.

The above petrologic, structural, and geochronologic relations strongly suggest that the Gold Flat unit does not belong to the Rattlesnake Creek terrane, in the upper plate of the Condrey Mountain shear zone, and instead represents migmatitic amphibolite facies equivalents to the outer CMS. According to this interpretation, the outer CMS erupted ca. 171 Ma, was buried beneath the ca. 162 Ma Slinkard pluton and its Rattlesnake Creek terrane framework during the Nevadan orogeny ca. 155 Ma, and cooled through amphibole Ar-Ar closure in the waning stages of that event. The Slinkard pluton therefore supplied the heat required for metamorphism of the Gold Flat amphibolite as the latter came into contact with the former via underthrusting rather than conventional contact metamorphism associated with intrusion.

Return to vehicles, reset odometers to zero, and proceed to Stop 2.5.

Mileage	Description
1.3	Continue south on Scott River Road. Pull onto a short unmarked gravel road accessing Middle
	Creek, prior to crossing the bridge over the
	creek. Prepare to view road and river exposures
	of the Slinkard Pluton.

Stop 2.5. Slinkard Pluton (UTM 10T, 490890E, 4612946N)

As noted at Stop 2.4, the most well-developed mylonitic fabrics in the Scott River antiform are observed at the top of the amphibolite unit and in the lowermost ~100 m of the upper plate. For this reason, we place the contact between lower plate CMS and upper plate rocks, the Condrey Mountain shear zone, in this interval. From Stop 2.4, we ascended structurally across the Condrey Mountain shear zone into definitive upper plate assemblages.

The upper plate of the Condrey Mountain shear zone is quite heterogeneous, consisting of Rattlesnake Creek terrane ophiolitic mélange (locally containing large alpine-type peridotite massifs e.g., the ~40 km² Tom Martin ultramafic complex; Fig. 8), cover strata, and plutonic rocks of the Wooley Creek suite that intrude this framework. At this location, the Slinkard pluton—the inferred basal domain of the Wooley Creek plutonic suite (Barnes et al., 1986a)—is exposed along the Scott River.

River- and roadcuts at Stop 2.5 consist of rounded blocks, produced via joint weathering, of quartz diorite consisting chiefly of subequal proportions of hornblende and plagioclase (variably altered by chlorite, clinozoisite, and sericite). Clinopyroxene and orthopyroxene are locally observed in hornblende cores. Minor phases include quartz, biotite, clinopyroxene, and orthopyroxene, while accessory epidote, apatite, titanite, Fe-Ti oxides, and zircon are common. The main quartz diorite constituent displays welldeveloped magmatic fabrics, characterized by coplanar hornblende and deformation-twinned plagioclase. Magmatic fabrics are cut by multiple populations of dikes (an early basaltic population with well-developed chill margins and more widespread cross-cutting trondhjemitic pegmatite) and folded together (Fig. 9H). Magmatic fabrics (Sm on Fig. 9H) and cross-cutting dikes are each locally overprinted by solid-state fabrics (Ss on Fig. 9H) recognized by elongate quartz grains, chloritized biotite fish, and folding of dikes.

The magmatic foliation exhibited by quartz diorite at this location is concordant with that of the Rattlesnake Creek terrane that it intrudes and structurally underlying Gold Flat amphibolite. Furthermore, the curvilinear appearance of the Slinkard pluton on geologic maps (Figs. 7 and 8) is likely a reflection of its overall tabular or "sill-like" (Barnes et al., 1986a) geometry with respect to adjacent units. This geometry is tilted ~30° to the WSW, exposing the deepest (>8 kbar, based on local preservation of magmatic epidote) and most mafic portions of the Wooley Creek suite adjacent to the CMS. This observation strongly suggests that the event that formed the Condrey Mountain dome also affected Wooley Creek suite.

Elsewhere, the Wooley Creek suite exhibits a wide range of rock types and compositions from ultramafic and gabbroic cumulates to tonalitic and two-mica granitic assemblages. The compositional diversity of the Wooley Creek suite points to a composite origin, though intriguingly these intrusives yield a narrow (<5 Myr) range of U-Pb zircon ages (Barnes et al., 1986a; Allen and Barnes, 2006; Coint et al., 2013). This field trip stop is the location of sample II from Barnes et al. (1986a), which yielded a concordant U-Pb age of 160.6 ± 0.94 Ma.

Whole-rock O (7.8% $< \delta^{18}$ O < 12.2%) and time-corrected Sr (most analyses 0.7035 $< {}^{87}$ Sr/ 86 Sr < 0.705) and Nd (most analyses +2.1 $< \epsilon$ Nd <+5.5) isotopic values span wide ranges, mirroring the lithologic diversity observed in the Wooley Creek suite (Allen and Barnes, 2006). These wide ranges in isotopic values are observed even in the most primitive rocks of the Wooley Creek suite, strongly suggesting that crustal contamination of mantle-derived mafic melts occurred deeper than emplacement level (Barnes et al., 1992; Allen and Barnes, 2006). Given that

the Wooley Creek suite is structurally underlain by the Condrey Mountain schist and portions of the Rattlesnake Creek terrane, the original roots of this magmatic system, including its crustal contaminant(s), have been tectonically excised. Most inherited zircon grains contained within the Wooley Creek suite yield U-Pb ages from 164 to 200 Ma (Allen and Barnes, 2006; Coint et al., 2013). These ages overlap those derived from the Western Hayfork arc and Rattlesnake Creek terrane, suggesting that these materials may be partially responsible for contamination of the Wooley Creek suite.

Modern thermochronologic data from the Slinkard pluton are not available, though hornblende and biotite K-Ar ages (157 ± 5 Ma and 151 ± 5 Ma, respectively; Lanphere et al., 1968) fall in the 167–148 Ma range of ⁴⁰Ar/³⁹Ar hornblende and mica ages determined from other intrusives of the Wooley Creek suite (Hacker et al., 1995). In aggregate, these data are interpreted to reflect upper plate cooling associated with underthrusting of lower plate outer CMS. Later tilting of the Slinkard and adjacent plutons (SW of the Condrey Mountain window) to the SW and the Ashland pluton (NE of the Condrey Mountain window) to the NE was presumably related to the same Neogene doming event that formed the Condrey Mountain window (Barnes et al., 1986b).

End Day 2. Return to vehicles, reset odometers to zero, and return to Siskiyou Field Institute.

Mileage	Description
10.6	Carefully back out onto Scott River Road, and continue south and east toward Fort Jones, California. At Meamber Gulch (odometer: 10.6 miles), Scott River Road crosses an east-side up reverse fault separating Rattlesnake Creek terrane assemblages to the west from the Sawyers Bar terrane to the east. This structure cuts an earlier, lower-angle thrust that branches out of the high-angle structure to the north; rocks of the Eastern Hayfork terrane intervene
	between fault branches.
19.8	Optional stop in Fort Jones for bathrooms, gas, and/or snacks at the intersection with California State Route 3. Turn left (north) on CA-3 and continue north toward Yreka, California.
24.9	From Fort Jones, CA-3 follows Scott Valley ~6.4 miles before ascending to Forest Mountain summit (4097'). Approximately 5.1 road miles from Fort Jones, at the intersection with Bear Springs Road, we cross a thrust fault buried in Scott Valley alluvium separating the Sawyers Bar terrane to the west from serpentinized peridotite, dunite, and minor gabbro to the east. The climb up and over Forest Mountain summit (4097') begins ~1.3 miles east of this location and features excellent roadcuts of these ultramafic rocks, which most likely represent

an extension of the Ordovician Trinity ophiolite (TO on Fig. 7), the main mass of which crops out ~25 km SE of this location (Hotz, 1977).

31.8 As we descend along CA-3 into Yreka, we traverse an ~1/4 mile section of fault-bounded Central Metamorphic terrane before entering the Eastern Klamath terrane. From Yreka, navigate toward Interstate 5 north and retrace the route followed this morning to Siskiyou Field Institute.

Day 3

Today, we will focus on the Preston Peak terrane (PPT; Rattle-snake Creek terrane [RCT] correlative) and elements of the West-ern Klamath terrane (WKT). Today's transect will cross elements that comprise a Late Jurassic accreted arc-inter-arc basin-remnant arc system. Stops will visit the PPT/RCT remnant arc, Josephine ophiolite inter-arc basin, and active arc rocks (Rogue Formation and Fiddler Mountain olistostrome) and their substrate (Onion Camp complex [OCC], correlative with the PPT/RCT). Maps with today's stops are shown in Figures 1, 3, 5B, and 12.

Depart Siskiyou Field Institute and drive east on the Illinois River Road to U.S. Hwy 199. Reset odometers to zero.

Mileage	Description
0.0	Selma, Oregon. Intersection of U.S. Hwy 199
	and Illinois River Road. Drive south toward
	Cave Junction, Oregon. The route parallels the
	Illinois Valley fault. This late Quaternary struc-
	ture marks a distinct topographic break between
	rugged topography to the west, underlain by the
	Josephine peridotite, from gentle topography on
	the east, underlain by Galice Formation.
8.6	Cave Junction, Oregon. Intersection of U.S.
	Hwy 199 and Caves Highway (State Hwy 46).
	Oregon Caves National Monument and Pre-
	serve is located ~20 miles to the east. The caves
	occur in marble within the Rattlesnake Creek
	terrane (RCT).
21.0	Oregon-California state line. Continue on U.S.
	Hwy 199 for 6.2 miles.
27.2	Turn left onto Bear Basin Road (USFS 18N07),
	continue 1.8 miles and park at Stop 3.1.

Stop 3.1 (Optional). Structurally High Galice Formation (UTM 10T, 438656 E, 4642238 N)

This forest roadcut, adjacent to the Middle Fork of the Smith River, is the location of sample GALI4 of Frost et al. (2006; Figs. 1 and 12). This location lies within the upper turbidite subunit of the Galice Formation, ~3 km beneath the Preston Peak fault and overlying Preston Peak ophiolite (Snoke, 1977), and ~2 km above nonconformably underlying Josephine ophiolite (Yule et al., 2006). Here, river gravels lie in angular unconformable contact above the Galice Formation.

The Galice Formation exposed at this location are typical of the turbidite sequence, consisting of alternating thinly laminated siltstone and shale protoliths, the former commonly grades upward into the latter, preserving partial Bouma sequences. Siltstone and slate are best classified as lithic wacke, containing chiefly lithic fragments and plagioclase with minor carbonaceous material (Harper, 1980; Norman, 1984; Wyld, 1985; MacDonald et al., 2006). Most lithic fragments are of siliceous argillite, with lesser amounts of andesitic lava and chloritized volcanic glass clasts (Harper, 1980). The relative proportions of quartz, feldspar, and lithic fragments suggest derivation of Galice detritus from an undissected to partially dissected arc. Primary sedimentary assemblages are overprinted by mica (sericite plus chlorite) plus pumpellyite (?) and a feebly developed slaty cleavage oriented parallel to bedding.

Detrital zircon is a ubiquitous accessory constituent of the turbiditic portion of the Galice Formation and yields a remarkably uniform distribution of U-Pb ages across the region (LaMaskin et al., 2021; Fig. 6). A maximum depositional age of 157 ± 2 Ma (2σ) was calculated from this location (LaMaskin et al., 2021), consistent with middle Oxfordian to late Kimmeridgian biostratigraphic ages provided by bivalve *Buchia concentrica* and ca. 150 Ma cross-cutting dikes (Imlay et al., 1959; Harper et al., 1994, 2002; MacDonald et al., 2006). This sample exhibits a prominent ca. 160 Ma age peak (Jurassic grains comprise 27% of all ages) with auxiliary Mesozoic peaks at ca. 186, 200, and 235 Ma.

Late Jurassic detrital zircon grains were most likely sourced from ca. 165–156 Ma plutons and ca. 156–152 Ma late-stage intrusives of the Wooley Creek belt (Barnes, 1986a; Hacker et al., 1995; Irwin and Wooden, 1999; Snoke and Barnes, 2006; MacDonald et al., 2006), with probable additional input from the ca. 161–155 Ma Rogue-Chetco arc and underlying Josephine ophiolite basement (Harper et al., 1994). Incorporation of Josephine ophiolite-derived detritus may also explain whole-rock isotopic evidence for a young, mantle-derived source component plus Cr-spinel as an accessory detrital mineral in some samples of the Galice Formation. Incorporation of disaggregated materials within, and adjacent to, the ophiolite-floored basin is consistent with paleocurrent and petrographic data suggesting dispersal of Galice detritus to the north and west (present-day coordinates, Harper, 1980; MacDonald et al., 2006).

The majority of detrital zircon grains contained within this sample are pre-Mesozoic in age and are generally more rounded than Mesozoic grains (LaMaskin et al., 2021), consistent with whole-rock isotopic data requiring significant terrigenous input (Frost et al., 2006). Pre-Mesozoic populations include significant proportions of "Grenville-age" (i.e., ca. 1.3–0.95 Ga; 22% of all analyses), ca. 1.4 Ga grains (14%), Paleozoic grains with peaks at 290 and 420 Ma (13%), and scattered proportions of Neoproterozoic, Paleoproterozoic, and Neoarchean grains. The spectrum of pre-Mesozoic detrital zircon ages contained within the Galice Formation does not match those published from older strata of the central and eastern Klamaths (Grove et al., 2008; Scherer and Ernst, 2008; Scherer et al., 2010; Ernst, 2017),

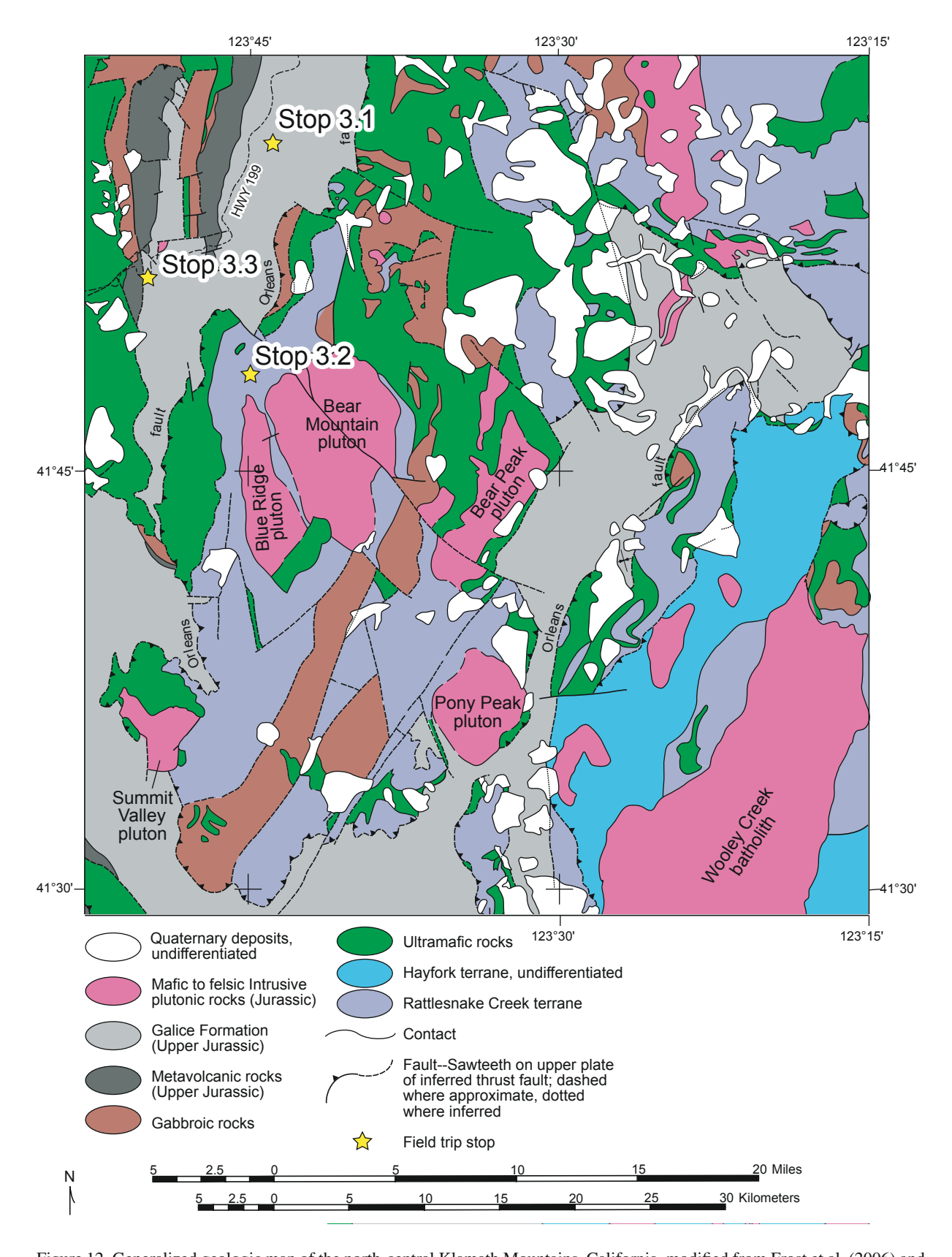


Figure 12. Generalized geologic map of the north-central Klamath Mountains, California, modified from Frost et al. (2006) and showing the locations of Stops 3.1, 3.2, and 3.3. The base for this map is Wagner and Saucedo (1987).

strongly suggesting that a significant portion of Galice detritus must have originated outside of the Siskiyou orogenic highlands. Recycled Triassic backarc basin strata of Nevada and eastern California (Manuszak et al., 2000; Darby et al., 2000; Gehrels and Pecha, 2014; Dickinson and Gehrels, 2008; LaMaskin et al., 2011) and/or Jurassic erg materials of the Colorado Plateau and adjacent areas (e.g., Dickinson and Gehrels, 2003, 2009) are excellent candidates for the extraregional input(s) required to fully explain detrital zircon age spectra of the Galice Formation (Fi. 6). Incorporation of one or both of these components likely involved Jurassic erosion in the backarc region, perhaps within the Luning-Fencemaker thrust belt (e.g., Wyld, 2002; Wyld et al., 2003), and westward routing of resulting detritus along the flanks of the elevated Klamath–northern Sierra Nevada before entering the Josephine ophiolite-floored basin.

It is important to note that some models for Nevadan closure of the ophiolite-floored marginal basin call on collision of the southern flank of the Wrangellia-Alexander composite terrane (e.g., Tipper, 1984; Wernicke and Klepacki, 1988; McClelland et al., 1992). This model predicts some detrital contributions from the Wrangellia-Alexander terrane to the Galice and related formations (see discussion below) during its approach. Recent detrital zircon geochronology from late Paleozoic strata of the southern Wrangellia-Alexander terrane, exposed on Vancouver Island (British Columbia, Canada), reveals abundant Carboniferous ages (ca. 344-317 Ma) and very few pre-400 Ma grains (Alberts et al., 2021). This Carboniferous component is not recognized in the Galice formation, suggesting either that Paleozoic strata of the Wrangellia-Alexander terrane were not exposed during collision or that the terrane did not collide at the paleolatitude of the Klamath Mountains in Late Jurassic time.

Return to vehicles and drive back to U.S. Hwy 199. Reset odometers to zero.

Mileage	Description
0.0	Turn left (south) on U.S. Hwy 199 and continue
<i>5 5</i>	for 5.5 miles.
5.5	Turn left onto Bear Basin Road (USFS 17N05) and continue to Stop 3.2.
11.0	Preston Peak fault / Orleans thrust emplacing
	serpentinite-matrix mélange of the Preston Peak
	terrane over Galice Formation metasedimentary
	rocks of the Smith River subterrane. Proceed
	3.2 miles (14.2 miles since Stop 3.1) and park at
	Stop 3.2.
42.0	Optional stop. Take a left turn to Bear Basin and, weather permitting, take a short hike to a spectacular overview at Bear Basin Lookout Cabin.

Stop 3.2. Metasedimentary and Metavolcanic Rocks, Including Chert-Clast Conglomerate, Meta-Argillite, and Metavolcanic Rocks (UTM 10T, 437651 E 4629331 N)

Snoke (1977) mapped a coherent metavolcanic and metasedimentary sequence of rocks along the Bear Basin Road that

were believed to be of Permian-Triassic age and recognized four broad units including: (1) lower metavolcanic rocks, (2) siliceous argillite, (3) conglomerate-grit, and (4) upper metavolcanic rocks (Figs. 1 and 12). The Bear Basin Road sequence forms a right-side-up homocline dipping 40° to 60° to the southeast. The lower contact of the succession is faulted against underlying sheared serpentinite. The uppermost rocks in the succession are intruded and metamorphosed by the Bear Mountain and Blue Ridge plutons (151–147 Ma; Chamberlain et al., 2006). Saleeby et al. (1982) noted that this succession lacks the metamorphic and deformational features of the structurally underlying ophiolitic rocks, and that similar strata to the north contained Jurassic radiolaria. Bushey et al. (2006) specifically correlated Snoke's (1977) Bear Basin Road sequence with the Rattlesnake Creek terrane cover sequence (Wright and Wyld, 1994) and considered the succession to be Late Triassic-Early Jurassic in age. Bushey et al. (2006) described the unit as being composed of fine-grained, tan to dark gray metasiltstone, siliceous meta-argillite, and metachert, locally including interlayered metavolcaniclastic rocks, metabasaltic rocks, and lenses of serpentinite. Frost et al. (2006) analyzed meta-argillite, including samples from the Bear Basin Road sequence (i.e., Rattlesnake Creek terrane cover sequence), which yielded initial ⁸⁷Sr/⁸⁶Sr of 0.7063–0.7114, initial ɛNd from -4.5 to -8.3, and depleted mantle model ages 1.67-1.34 Ga. The results led Frost et al. (2006) to suggest that the isotopic composition of the cover sequence was comparable to major river systems in North America and thus that cratonic sediment was delivered to the depocenter of the Rattlesnake Creek terrane arc. LaMaskin et al. (2021) obtained detrital zircon U-Pb ages from a sample of chert-rich lithic arenite collected along Bear Basin Road from the Rattlesnake Creek terrane cover sequence (see Fig. 6 for Rattlesnake Creek terrane cover sequence composite). The sample yielded a small number of usable ages (n = 65) consisting of 83% Precambrian, 5% Paleozoic, and 12% Mesozoic ages with dominant subdistributions ca. 2700-2550, 1850-1730, 1075, and 175 Ma. The low number of Mesozoic ages did not allow for calculation of a maximum depositional age; however, other samples of Rattlesnake Creek terrane cover sequence yielded maximum depositional ages of 170–161 Ma (Fig. 6). LaMaskin et al. (2021) suggested that the Rattlesnake Creek terrane cover sequence is a Middle to Late Jurassic succession representing the rifting stages of marginal-basin formation and that sediment was likely sourced from the older terranes of the Klamath Mountains and Sierra Nevada, as well as active-arc sources, with some degree of contribution from sources in the continental interior.

Return to vehicles. Time and weather permitting, take a left turn to Bear Basin and take a short hike to a spectacular overview at Bear Basin Lookout Cabin (optional stop listed above). Return to Hwy 199. Reset odometers to zero.

Mileage	Description
0.0	Intersection of Bear Basin Road and Hwy 199. Turn left (west) onto U.S. Hwy 199. Proceed 0.9 miles to Stop 3.3.

Stop 3.3. Basal Galice Flysch atop Josephine Pillow Lavas (UTM 10T, 430987 E, 4635590 N)

This is the type section of the pillow lava unit of the Josephine Ophiolite and overlying pelagic-hemipelagic sequence that grades upward into the overlying turbidite sandstone deposits (Harper, 1984; Pessagno and Blome, 1990; Harper et al., 2002; same location as stop 2 in Harper, 1989, and stop 5 in Harper et al., 2002; Figs. 1 and 12). Here, biostratigraphic and radiometric ages indicate that the exposed rocks at this locality range from ~162 Ma (pillow lavas) to 157 Ma. Light gray sills and dikes belonging to the 151–146 Ma suite of syntectonic calc-alkaline intrusives cut this section (Harper et al., 1994, 2002).

Park in the parking area on the south side of the road and walk south to the beginning of the guardrail. Continue carefully walking south along the highway for ~120 m and descend down a steep embankment of loose rock to the river; the place to descend is upriver from the mouth of a creek that is visible on the other side of the river (Harper et al., 2002). Once at river level, walk downstream to outcrops across from the mouth of the creek visible on the other side of the river. Observe cross-sections of pillows in the walls of large potholes overlain by a thick massive lava flow (Harper et al., 2002). Next, proceed upriver to where the top of the massive flow is exposed and can be seen grading into a pillow breccia. Metersize pillows with paleomagnetic drill holes overlie this pillow breccia.

Climb back up to the highway and walk back (north) toward the parking area. Near the end of the guardrail, drop down to the river to an exposure of the contact between the pillow unit and the overlying hemipelagic-pelagic sequence (Harper, 1984; Harper et al., 2002). The contact is much easier to see if the rocks are wetted. Pillows below the contact are lobate, but look for dark chilled pillow margins and triangular shaped junctions filled with light-green chert and dark elongate glass fragments (Harper et al., 2002). These pillows are also highly fractionated Fe-Ti basalt and have abundant microphenocrysts of plagioclase and clinopyroxene. The basal 45 m of sediments overlying the pillows consist of chert, tuffaceous chert, siliceous argillite (black), and rare nodules and layers of gray limestone, as well as several sills (Harper, 1989; Harper et al., 2002). At ~35-40 m above the contact, bedding in the hemipelagic sequence is disrupted, likely due to soft-sediment deformation that predates dike intrusion (Harper, 1989; Harper et al., 2002). A volcanic pebbly mudstone bed can be observed in this zone. At 45 m above the contact, observe two beds of thick-bedded lithic wacke (i.e., graywacke) that mark the beginning of turbidite sandstone deposition. These beds are overlain by silty radiolarian argillite and a small number of turbidite sandstone beds (Harper, 1989; Harper et al., 2002). Return to vehicles and continue driving south on U.S. Hwy 199. Note: mileage is cumulative.

Mileage	Description
2.6	Fault, up-on-the-west, separating volcanic rocks (mainly pillow lavas) of Josephine ophiolite on
	east from Josephine peridotite on west. Patrick's

Creek Lodge is an historic building located 0.1 mile to the west.

Gasquet Market. The town of Gasquet, California, occupies fluvial terraces developed along

10.5

nia, occupies fluvial terraces developed along the Smith River. Steep canyon walls here expose Josephine peridotite. The canyon narrows dramatically to the west of Gasquet across a downto-west fault separating Josephine peridotite from gabbros and sheeted dikes.

14.1 Carefully turn left across traffic and park in the large, paved turnout. Walk to the east end of turnout and climb down to the river. Walk upstream ~100 m to outcrops that expose sheeted mafic dikes and gabbro screens.

Stop 3.4. Sheeted Mafic Dikes and Gabbro Screens (UTM 10T, 414073 E, 4632454 N)

At this location, we observe a transition from mostly gabbro to nearly 100% sheeted dikes (same location as stop 4 in Harper, 1989, and stop 6 in Harper et al., 2002; Fig. 1). Exposures on the opposite side of the river and upstream on the highway side represent sheeted dikes that transition downstream into gabbro (Harper, 1989; Harper et al., 2002). Subparallel dikes with chilled margins and gabbro screens are present, and here, plagiogranite cut by sheeted dikes yields a 162 ± 1 Ma U-Pb zircon age (Harper et al., 1994). This outcrop has been studied extensively, including the nature of the dike-gabbro transition, dike intrusion, hydrothermal metamorphism, and oceanic faulting (Harper, 1989; Alexander and Harper, 1992). Here, the rocks bear amphibolite-facies mineral assemblages interpreted to result from high-temperature subseafloor hydrothermal metamorphism; however,

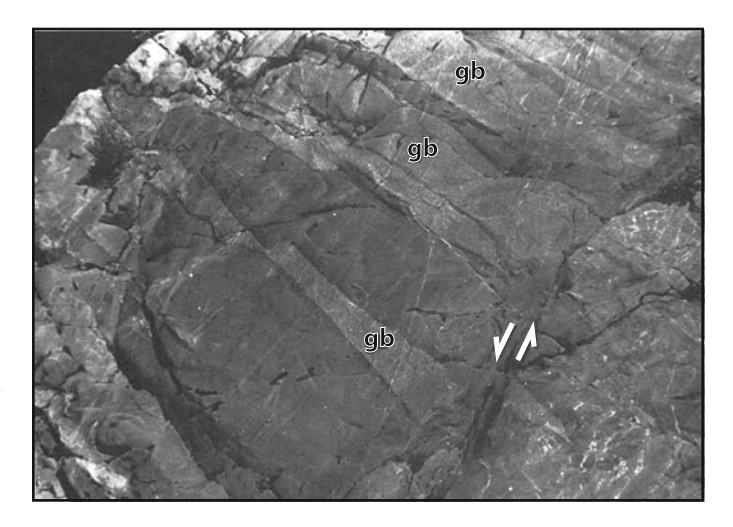


Figure 13. Sheeted dikes and gabbro screens (gb) at Stop 3.4. Figure modified after Harper (1989). The center dike is ~0.4 m wide. In the right foreground is a probable oceanic normal fault; the lowermost gabbro screen is displaced 30 cm as shown by arrows. Prehnite veins (white), some with small offsets, occur on either side of the fault.

a retrograde greenschist facies metamorphic assemblage is also present (Harper, 1989). Also observable are epidote veins and abundant white prehnite veins as well as quartz veins or quartz-matrix breccias (Harper, 1989)

Begin by walking back up the road (north) to where trees begin and descend to prominent outcrops along the river (Harper et al., 2002). Observe sheeted dikes dipping ~40° with wall rock exposed between dikes (i.e., screens) of gabbro and other coarsegrained plutonic rocks, including some ultramafic cumulates (Harper, 1989; Harper et al., 2002).

Walk back up to the highway shoulder and walk downriver (west) 0.1 miles to just before the location of several small trees close to the road. Look across the river at sheeted dikes dipping to the right (south) ~ 40° . This outcrop is in the core of a syncline so that we are seeing the actual dip of the sheeted dikes. Tilting of the sheeted dikes is interpreted to have occurred at the ridge axis, probably as a result of normal faulting (Alexander and Harper, 1992; Harper et al., 2002). Note the thick, "soft" looking, steeply dipping dike across the river. This late dike is a Fe-TI basalt related to the upper pillow lava (Harper et al., 2002).

Return to vehicles and drive 31.6 miles north on U.S. Hwy 199 to USFS Rd 4201 (Eight Dollar Road) just to the north of Kerby, Oregon. Reset odometers to zero. Refer to maps in Figures 3 and 5B for the remainder of today's stops. Stops 3.5–3.9 and tomorrow's stops will visit tectonostratigraphic elements of the WKT. Together these elements comprise the Late Jurassic Rogue-Chetco active arc and its Triassic–Middle Jurassic underpinnings (Fig. 14).

Mileage	Description
0.0	Intersection of U.S. Hwy 199 and USFS Rd 4201
	(Eight Dollar Road). Turn west onto USFS Rd
	4201 and proceed to Stop 3.5. The route is plot-
	ted on Figure 5B. En route, the conical-shaped
	mountain to the north is Eight Dollar Mountain,
	most likely named for a gold nugget worth \$8
	(~\$275 in 2021) mined from a placer deposit
	along the west flank of the mountain in the nine-
	teenth century. Eight Dollar Mountain exposes
	Josephine peridotite and is bounded on the east
	by the Illinois River Valley fault (Ramp, 1986).
2.8	Turn left to cross the Illinois River bridge.
	Immediately to the southwest of the bridge, the
	road passes beneath a strath terrace 100-
	200 m beyond the bridge with cemented, boul-
	dery gravels above Josephine peridotite. In
	places the strath terraces have been worked for
	placer deposits. One such placer working is vis-
	ible in the roadcut as the pavement ends.
3.8	Bear right at the fork in the road, continuing on
	USFS Rd 4201.
6.1	Park at a turnout on the east side of the road and
	cross the road to view roadcut exposures of Jose-
	phine peridotite.

Stop 3.5. Josephine Peridotite (UTM 10T, 441695 E, 4677705 N)

Stop 3.5 (see Figs. 4 and 5B) is located at the northern extent of the Josephine peridotite massif, the largest peridotite massif in North America, covering >1000 km² (Dick, 1976). Here, outcrops of peridotite consist of moderately serpentinized harzburgite (olivine + orthopyroxene) and subordinate dunite. Magnetite replacing spinel defines a weak L-tectonite fabric. Across the valley to the east, note the distinct vegetation change on the west flank of Eight Dollar Mountain (Fig. 15). This change marks a boundary between sheared and serpentinized peridotite at lower elevations from relatively unaltered peridotite at higher elevations. The reason for this change is not well understood. Possible explanations include: (1) pre-accretion serpentinization beneath an oceanic fault or fracture zone, (2) accretion-related serpentinization along fault or shear zone, and (3) two-phase generation of peridotite formation, one phase of Middle Jurassic or older age and a second Late Jurassic phase associated with formation of the Josephine ophiolite (Yule, 1996).

Squaw Peak (Stop 4.1) is evident to the northeast (Fig. 15). Return to vehicles and continue west on USFS 4201.

Mileage	Description
7.5	High-angle fault separating metabasalt and chert
	of the Onion Camp complex (OCC) to west
	from the Josephine peridotite to east (UTM 10T,
	440211 E, 4677307 N).
9.1	Roadcut exposes a shallowly dipping, post-
	Nevadan 150 Ma dacitic dike (U-Pb zircon age;
	Yule et al., 2006) cutting foliated metavolcanic
	and metasedimentary rocks of the OCC (UTM
	10T, 438762 E, 4678111 N). Road crosses a
	recent landslide 0.3 mi west of the dike outcrop.
12.1	Park on the left at turnout.

Stop 3.6. Fiddler Mountain Olistostrome (UTM 10T, 437500 E, 4675927 N)

Refer to Figures 4 and 5B for location. This area provides the relations similar to those depicted as the "Sixmile Creek" columnar section in Figure 14. Start across from the parking turnout and walk west along the exposures to examine slaty meta-argillite with subvertical to steeply SE-dipping foliation and kink bands. The meta-argillite is locally interbedded with white-weathering, light-gray chert. Chert collected nearby has yielded Late Jurassic (Kimmeridgian?) radiolaria (Yule et al., 2006).

West of the argillite along the roadcuts, one will encounter a conformable contact between slaty meta-argillite and poly lithologic, ophiolite-clast breccia and conglomerate (Fig. 16). Particle sizes at these outcrops range from coarse sand to small cobbles. Elsewhere, clast sizes in this unit can reach ~100 m in size (!). The best outcrops to view the "mega" clasts are located atop Fiddler Mountain where 10–100-m blocks of gabbro and basalt are encased in a matrix of cobble- and boulder-sized ophiolite clasts with local sandy interlayers. Many boulders

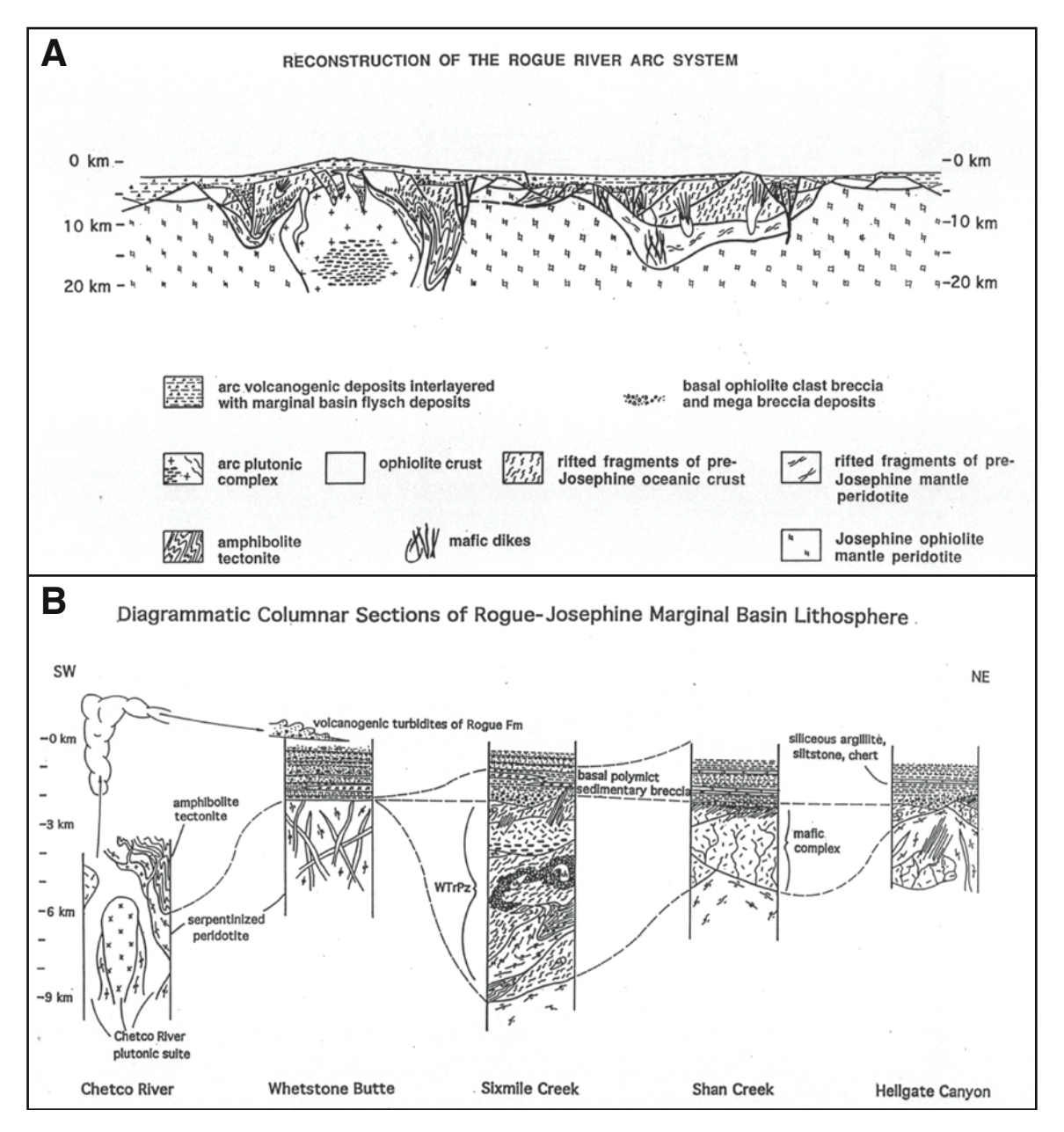


Figure 14. (A) Pre-accretion (pre-Late Jurassic Nevadan orogeny) schematic reconstruction of the Rogue River arc system, Illinois River area, Oregon (from Yule, 1996, fig. 4-6). (B) Diagrammatic columnar sections illustrating the generalized stratigraphy at five key locations in the Illinois River area, Oregon (from Yule, 1996, fig. 4-5). This trip will visit four of the sites, from SW to NE on B: Stops 4.2–4.5 at the Illinois River batholith and wallrocks, equivalent to the Chetco River plutonic complex column; Stop 3.8 near Whetstone Butte; Stop 3.7 at Fiddler Mountain, equivalent to the Sixmile Creek column; and Stop 4.6 at Shan Creek. WTrPz, western Paleozoic and Triassic belt, depicted in the Sixmile Creek column is equivalent to the Onion Camp complex in this area and Rattlesnake Creek terrane to the east in the hanging wall of the Orleans fault (Fig. 12).

are internally brecciated and cut by epidote-chlorite-quartz vein networks.

Clasts are subangular to angular and consist of a variety of rock types, including: gray-green metabasalt, metadiabase, medium- to coarse-grained gabbro, with secondary chert, argillite, serpentinite, and serpentinized peridotite. Scarce clast types include quartzite, chlorite schist, phyllonite, and amphibolite. The clast lithologies correlate with rock types that comprise the Josephine ophiolite and OCC.

The poorly sorted, brecciated, altered nature of clasts suggest a local environment of deposition near a high-relief, faulted and fractured, hydrothermally altered source. This unit is informally referred to as the Fiddler Mountain olistostrome (FMO) (Yule et al., 2006).

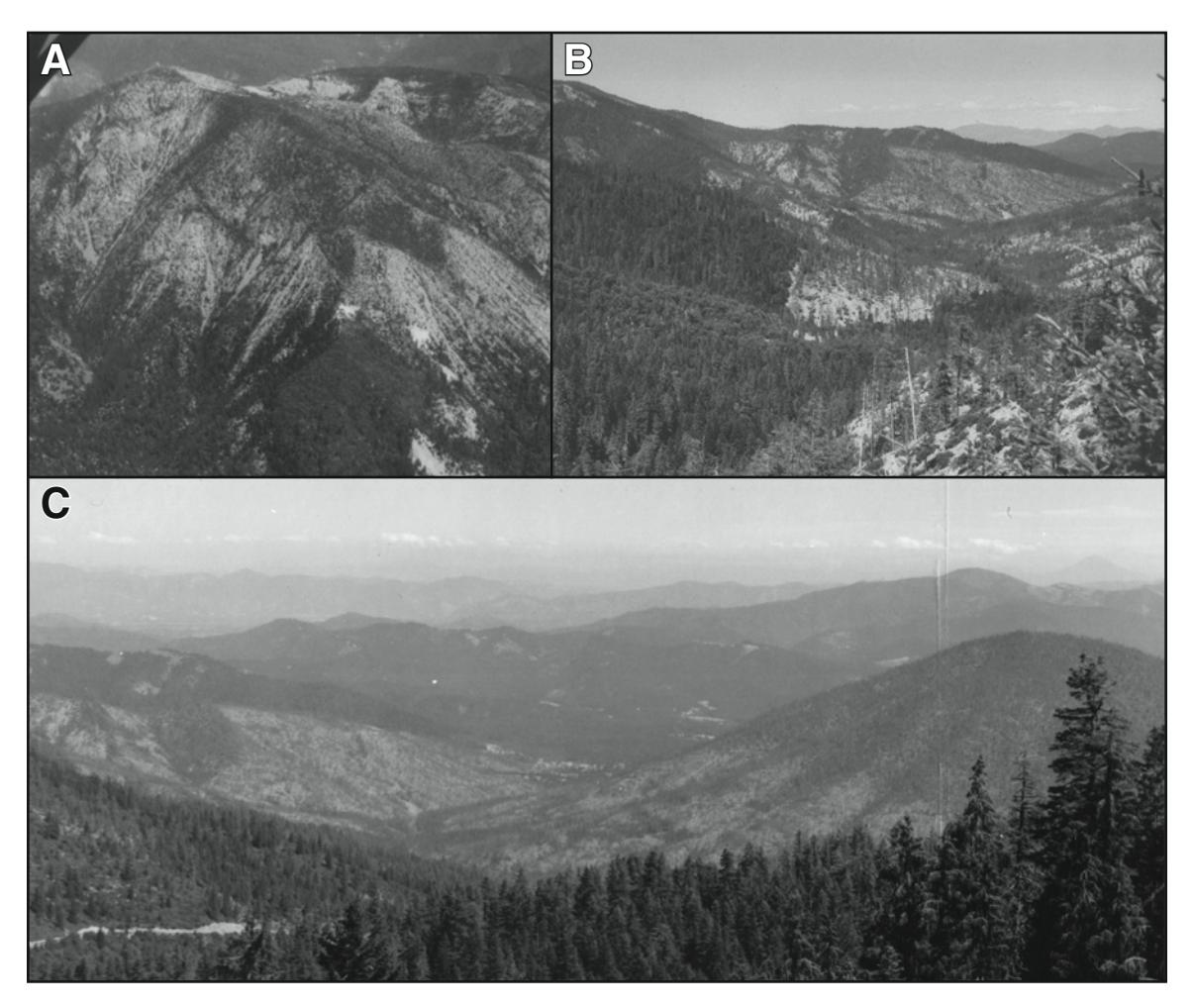


Figure 15. (A) Photograph from airplane looking northeast at west flank of Pearsoll Peak, with relatively unvegetated upper slopes underlain by peridotite, and forested lower slopes underlain by tonalite-trondhjemite and hornblende gabbro of Illinois River batholith. (B) Photograph taken from USFS Road 4201 with view to NE along contact separating metavolcanic and sedimentary rocks on left (forested) from serpentinite-matrix mélange, comprising a natural cross-section through the Onion Camp complex. The flat mountain in the center-right of the photo is Squaw Peak, the location of Stop 4.1 of this trip, and is underlain by polydeformed serpentinite and amphibolite bodies. (C) View to the east from Fiddler Mountain with metavolcanic rocks of the Onion Camp complex in the foreground, and Eight Dollar Mountain at the right, Squaw Peak at left, and Selma in center of photograph. The vegetation change on the flanks of Eight Dollar Mountain occurs where serpentinized peridotite changes to unaltered peridotite upslope. This marks a contact between the serpentinite-matrix mélange of the Onion Camp complex to "fresh" Josephine peridotite.

Bedding attitudes in sandy lenses, slaty argillite, and chert define a tight NE-SW-trending synform centered on Fiddler Mountain. The NW and SE margins of the FMO are in nonconformable contact with the underlying OCC, and suggest that the unit cores a regional syncline (Figs. 4 and 5).

Similar units are known throughout the WKT, e.g., the Lems Ridge olistostrome (Ohr, 1987), and breccias associated with the Preston Peak ophiolite (Snoke, 1977), Coast Ranges ophiolite near Paskenta, California (Blake et al., 1985), and Devil's Elbow ophiolite (Wyld and Wright, 1988). Due to the predominance of ophiolitic clasts, the WKT olistostrome/breccia units are referred to as "ophiolite-clast breccia" (e.g., Ohr, 1987). These strata interfinger with pelagic and hemipelagic strata of and overlie pil-

low lavas of their respective Late Jurassic ophiolite sequences. With the exception of the Paskenta example, the ophiolite-clast gravels are in fault or depositional contact with the Rattlesnake Creek terrane and closely-related units (OCC). In some cases, the breccias contain Rattlesnake Creek terrane–like rock clasts (e.g., Wyld and Wright, 1988).

The WKT olistostromes/breccias were probably deposited in ocean basins along fault scarps with considerable relief. This setting supports the model of Snoke (1977) where older accreted oceanic terranes (like the RCT) rifted apart to form Late Jurassic ophiolites (Josephine, Coast Ranges). The Lau Basin in the SW Pacific may represent a modern analogy.

Return to vehicles and continue west on USFS 4201.

Mileage	Description
14.6	Bear right at fork, staying on USFS 4201.
14.9	Park at the large pullout on the left.
	Walk northwest to view outcrops in the road
	metal quarry.

Stop 3.7. Metabasalt of the Onion Camp Complex (UTM 10T, 434270 E, 4676257 N)

Refer to Figures 4 and 5B for location. The quarry across and to the north of the pullout exposes purple-gray weathering metabasalt with a weakly developed NE-striking, SE-dipping

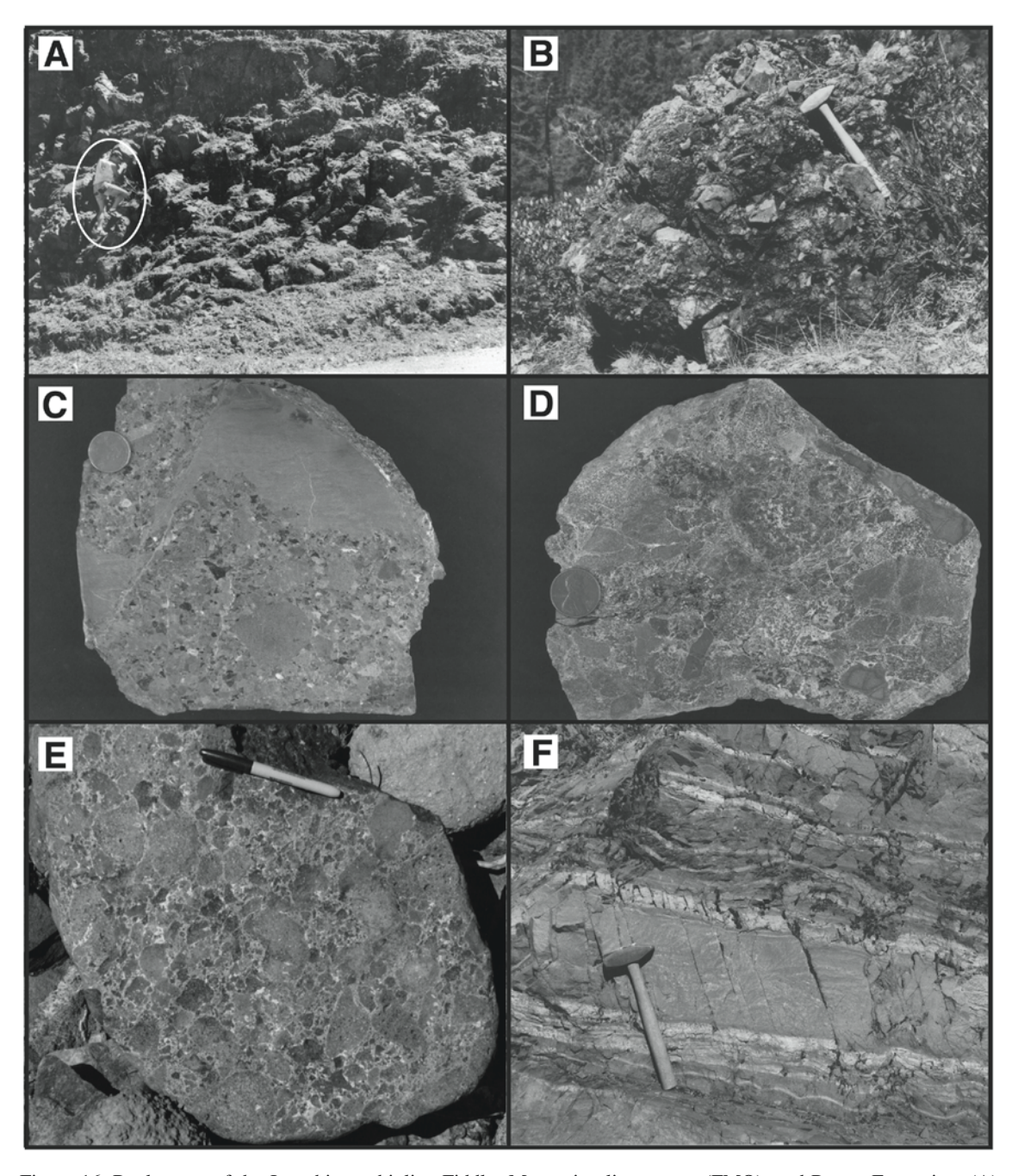


Figure 16. Rock types of the Josephine ophiolite, Fiddler Mountain olistostrome (FMO), and Rogue Formation. (A) Steeply overturned Josephine pillow lavas at Shan Creek, Stop 4.6 (person for scale). (B) Serpentinite-clast breccia of the FMO near Chetco Pass (30-cm-long hammer handle for scale). (C, D) Slabbed hand samples of the ophiolite-clast conglomerate (C) and breccia (D) of the FMO, Stop 3.6 (2 cm coin for scale). (E) Boulder of Rogue Formation volcanic breccia (14-cm-long pen for scale). (F) Outcrop of Rogue Formation volcaniclastic turbidites, Stop 3.8 (30-cm-long hammer handle for scale).

foliation. Rocks here (Fig. 17) consist of a greenschist-facies mineral assemblage including epidote + chlorite + albite + calcite + titanite + actinolite + quartz, with secondary Fe-oxide and pyrite. Prehnite, prehnite + quartz, and quartz + calcite veins are common, cutting most outcrops. Small bodies of red chert and black serpentinite are common in this area. Float of red chert and sheared serpentinite can be found on the hillsides surround-

ing the quarry. A bedded red chert fossil locality occurs nearby (see optional Stop 3.9 below). In places the serpentinite has a polished, glassy-black luster, presumably due to intense shearing. Elsewhere in the Onion Camp complex, metabasalt seen at this stop is associated with slaty tuff and argillite, and scarce basalt breccia with relict clinopyroxene-rich clasts. In places these greenschist-facies rocks grade into amphibolite-facies

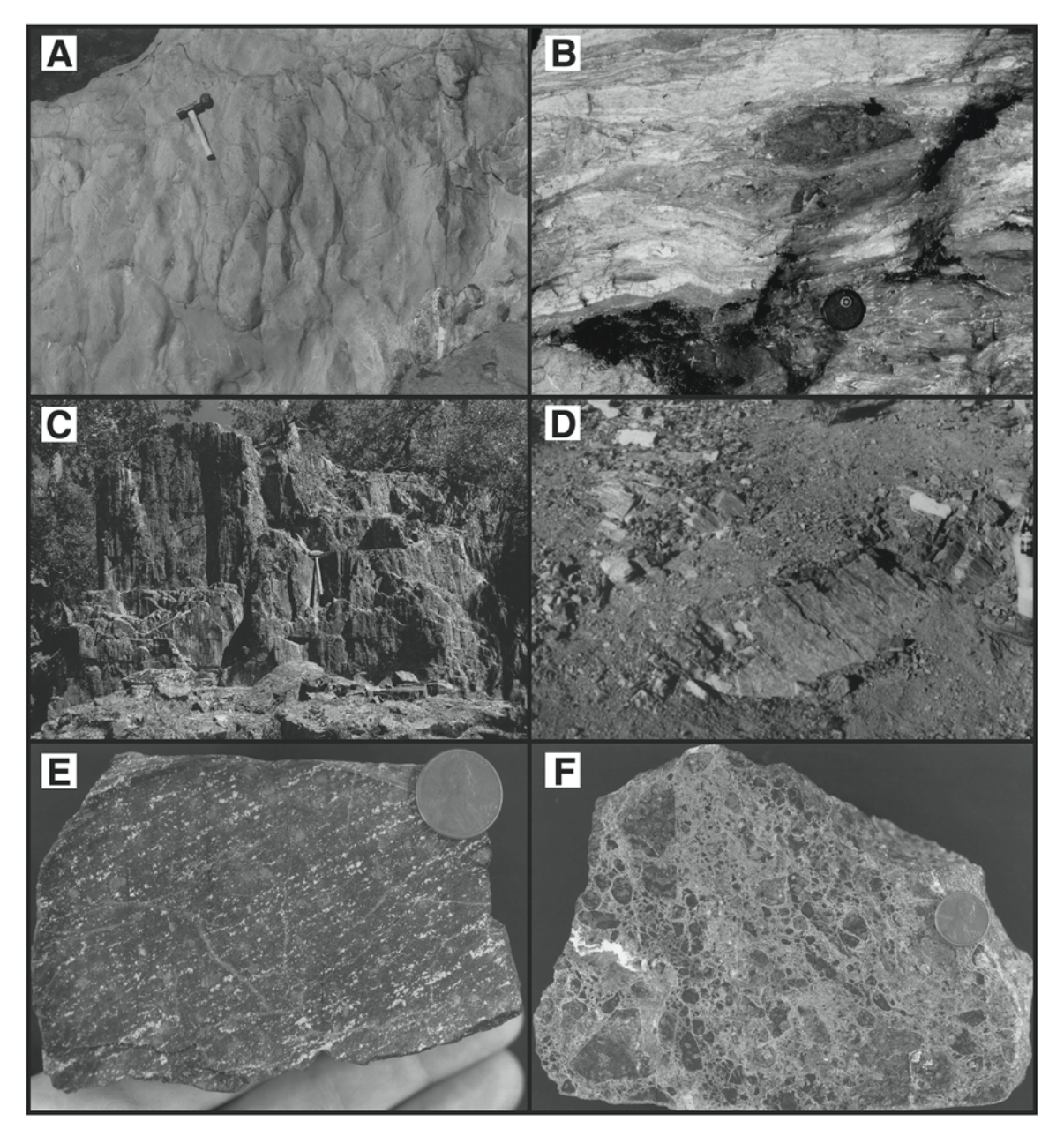


Figure 17. Photographs of rock types from the Onion Camp complex. (A) Outcrop of pillow lava, with tubes parallel to 30-cm-long hammer handle. (B) Foliated meta tuff with lens of chert in upper right center of photo (camera lens is 4 cm in diameter). (C) Outcrop in meta chert with prominent, subvertical foliation perpendicular to view, and down-dip lineation (30-cm-long hammer handle for scale). (D) Triassic (?) red chert locality (Optional Stop 3.9) with layering dipping moderately to the right. (E) Slabbed hand specimen of foliated serpentinized peridotite from Squaw Mountain, Stop 4.1 (2 cm coin for scale). (F) Slabbed hand specimen of brecciated serpentinized peridotite from Squaw Mountain, Stop 4.1 (2 cm coin for scale).

equivalents (amphibolite gneiss and schists with local quartzites [metachert]).

Major element analyses of metabasalt from this and other locations in the Onion Camp complex range in composition from 46% to 55% SiO₂ and display a wide range of FeO/MgO values and generally high TiO₂ concentrations. Trace and rareearth element (REE) data span normal mid-oceanic-ridge basalt (N-MORB), eruption of mid-oceanic-ridge basalt (E-MORB), and alkaline within-plate basalt (WPB) (Yule et al., 2006). Chemically the Onion Camp complex metabasalts correlate with the lower mélange metabasalts of the type Rattlesnake Creek terrane section described by Wright and Wyld (1994). Return to vehicles and continue west on USFS 4201.

Mileage Description

15.3 Park in Kalmiopsis Wilderness trailhead parking area, with pit toilets available.

Stop 3.8. Nonconformity between Late Triassic to Jurassic Onion Camp Complex and Late Jurassic Rogue Formation (UTM 10T, 433985 E, 4676734 N)

Refer to Figures 4 and 5B for location. This area provides the stratigraphic relations depicted as the "Whetstone Butte" columnar section in Figure 14. The purpose of this stop is to examine OCC-type peridotite, which is distinctly different from the Josephine peridotite seen at Stop 3.5, and to examine the nature of the contact between the OCC and Rogue Formation. This stop involves an ~3-km round-trip hike along an exposed ridgeline. Plan to spend ~two hours away from the vehicles.

Point of interest: The massive Biscuit Fire (2002) burned over 500,000 acres and scorched most of the Kalmiopsis wilderness to the west, including the outskirts of Brookings, Oregon. The fire produced a massive pyrocumulous cloud whose collapse was centered in this area and incinerated all life here. I (D. Yule) collected charred bones of deer and bears on a backpack trip into the wilderness there in summer 2003. An ash layer 10-20 cm thick still blanketed the ground in protected areas beneath fallen tree trunks. Needles on scorched, old-growth trees defined a radiating "blast" pattern that located the center of the collapsed pyrocumulus column. Salvage logging approved by the Bush administration removed most of the scorched old-growth trees on USFS land, but left them inside the wilderness boundary. In the years since the salvage, numerous articles have been published criticizing the practice. Two recent fires, the 2017 Chetco Fire and 2018 Klondike Fire, reburned southern and northern areas, respectively, within the Biscuit Fire perimeter. Stops 3.7-3.9 occur along the eastern limit of the Chetco Fire.

Begin the hike by walking west from the parking area on the wilderness trail for ~0.5 km to a locally sheared contact between OCC metabasalt and chert and OCC peridotite (UTM 10T, 433453 E, 467677 N). For the next 0.5–1.25 km, the trail passes through a sparsely vegetated, open terrain that characterizes the serpentinized peridotite unit of the OCC. The unit contains outcrops of thoroughly serpentinized peridotite cut by numerous

dikes that range in lithology from rodingite (hydrogarnet replacing a mafic dike), websterite, gabbro and hornblende gabbro (locally pegmatitic), plagiogranite, diabase/basalt, and acicular hornblende diorite. Antigorite (high-temperature serpentine) bake zones commonly border the late-stage dikes. Dikes cannot be followed laterally for >10 m and often occur as boudins in sheared serpentinite. Dike orientations are highly variable, suggesting multiple episodes of emplacement and/or deformation. The rodingite dikes are highly altered and must have been emplaced prior to complete serpentinization of the peridotite, with alteration of the dike to rodingite occurring during the serpentinization of the peridotite. The fact that many other dikes are not altered and have antigorite reaction rinds suggests that they were emplaced once serpentinization of the OCC peridotite was complete.

U-Pb zircon analyses of two plagiogranite dikes yielded concordant ages of 175 and 173 Ma (Yule et al., 2006). The OCC peridotite is therefore at least Middle Jurassic in age and probably much older considering that complete serpentinization occurred prior to intrusion of the plagiogranite dikes. Age data from the plagiogranite dikes and the red chert (Stop 3.7), in combination with striking lithologic similarities, support a correlation of the OCC with the late Triassic to Middle Jurassic ages of the Rattlesnake Creek terrane. If correct, the OCC therefore represents a rift-fragment of pre–Middle Jurassic Klamath accreted terranes, in support of the model for opening of the paired Josephine ophiolite and Rogue-Chetco arc as a marginal ocean basin along western North America in the Late Jurassic (Snoke, 1977; Saleeby et al., 1982; Harper and Wright, 1984; Yule et al., 2006).

At ~1.25 km from the trailhead (UTM 10T, 433048 E, 4677130 N), leave the trail as it bends north and hike west to a small knob (UTM 10T, 432811 E, 4677128 N), where a contact separates OCC peridotite on the east from medium- to thickbedded volcaniclastic strata of the Rogue Formation on the west. The contact is crossed as one ascends the knob, ~\frac{1}{3} of the way above the saddle immediately to the east of the knob. Outcrops show strata that strike NNW and dip 45°-50° ENE, parallel to the contact with the OCC peridotite. Graded beds, local cross stratification, and Bouma-like sequences indicate that the beds are overturned and interlayered with thick beds of volcanic breccia (Fig. 16). About 1.5 km to the west, NW-striking, NE-dipping beds of the Rogue Formation again unconformably overlie OCC peridotite, but sedimentary features show that these beds are upright. The map relations therefore define a shallowly north-plunging, inclined, overturned syncline developed in the Rogue turbidites (Figs. 4 and 18). Retrodeformation of the fold reveals a section with distal turbidites of the Rogue Formation deposited upon a substrate of OCC peridotite (Fig. 14). This contact here is locally broken by NW-SE cross faults, but can be traced for ~50 km to the NE (to the Rogue River), parallel to the regional strike of the belt (Fig. 5).

The view from the top of the knob offers a full panorama view of the Western Klamath terrane, and the destruction of the Biscuit Fire. Points of geologic interest include the following:

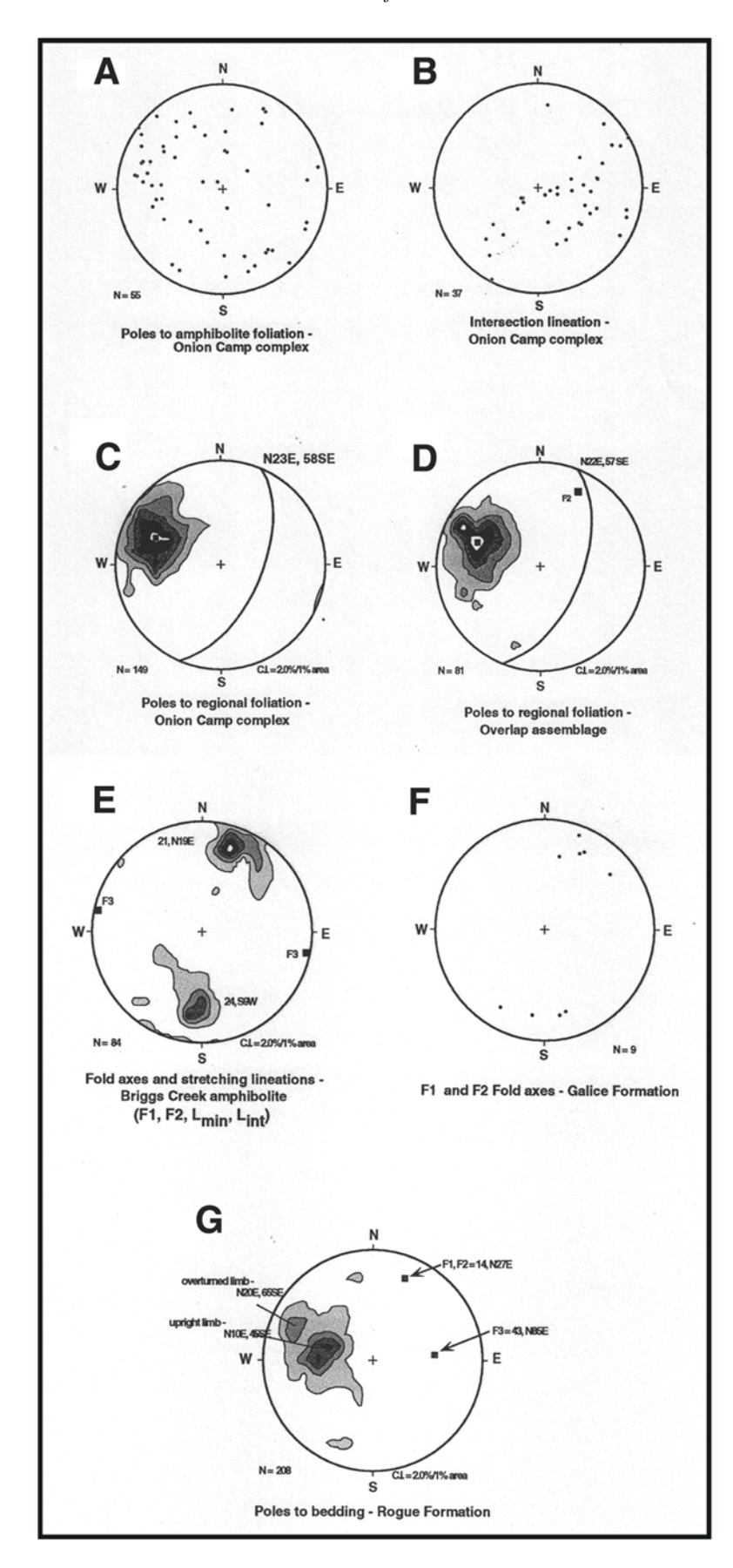


Figure 18. Lambert equal-area stereonet plots from the geologic map area of Figure 2. (A, B) Onion Camp complex (OCC): poles to foliations and intersection lineations in amphibolite bodies that show considerable spread in orientations, an indication of polyphase deformation in the unit. (C, D) Poles to greenschist facies foliation in the OCC and Fiddler Mountain-Rogue-Galice units showing that the same fabric has been imposed on both the OCC substrate and overlap assemblage. (E) Shallow NE- or SW-plunging fold hinges and stretching lineations from the Briggs Creek amphibolite. (F) Scarce fold hinges in the Galice Formation with shallow NE- or SW-plunging fold hinges. (G) Poles to bedding from the Rogue Formation showing the average orientation of limbs of tight, overturned folds, with NE-SW-striking and steeply SE-dipping axial planar foliation that is parallel to the regional foliation in C and D. The equal area stereonet plots are from Yules (1996, fig. 2-35), and modified from Yule et al. (2006, fig. 7).

The highest peaks to the west are Vulcan Peak (~15 km to the SW) and Pearsoll Peak (~6 km to the NNW). Both peaks consist of orange-weathering, unaltered Josephine peridotite that is in shallow contact with gabbros of the Illinois River plutonic complex. (We will visit this rock type at Stop 4.2.) The contacts with underlying units are low-angle features that place peridotite on top of Franciscan rocks and Chetco complex plutonic rocks to the west of Vulcan and Pearsoll peaks, respectively. The contacts are interpreted as Nevadan age thrusts and are named the Valen Lake and Pearsoll Peak thrusts, respectively (Harper et al. 1994).

Eagle Mountain, an intermediate peak halfway between our location and Pearsoll Peak, consists of sheeted mafic dikes that cut OCC peridotite. Serpentitite-clast breccias are exposed along the western margin of the mafic dikes. The unit at Eagle Peak is interpreted to be a block/outlier of Josephine ophiolite-related crust.

The highest peak to the northeast is Squaw Mountain (~15 km away, across the Illinois River Valley). It is a partly barren peak that exposes folded OCC peridotite and amphibolite, and is the location of Stop 4.1.

The highest peak to the east is Fiddler Mountain (~4 km away and consists of the Fiddler Mountain olistostrome; Stop 3.6). Barely visible beyond Fiddler Mountain is Eight Dollar Mountain, located to the east of the Josephine peridotite (Stop 3.5). The accommodations for this trip are located at the base of the northern flank of Eight Dollar Mountain.

Babyfoot Lake, ~2.5 km to the south sits in a small glacial cirque carved from red chert and metabasalt of the OCC (Stop 3.7). The cirque is the northernmost and lowest elevation glacial feature in the Klamath Mountains.

Return to vehicles. Time permitting, drive to Optional Stop 3.9.

Mileage	Description
15.5	Drive SE on USFS 4201 for 0.2 mi and turn left onto USFS 142.
15.7	Drive north on USFS 142 for 0.2 mi and park on the left. Walk to roadcut.

Stop 3.9 (Optional). Late Triassic Chert (UTM 10T, 434425 E, 4676830 N)

Refer to Figures 4 and 5B for location. The outcrop to the north of the road exposes well-bedded red chert layers that dip moderately to the northwest (Fig. 17). Roure and DeWever (1983) report a Triassic age for a chert sample possibly collected from this locality. Note: The precise location of their sample is unknown. However, this is the only easily accessible chert outcrop in the area in the vicinity of their reported, approximately located sample locality. Yule (1996) collected samples from this locality. One sample yielded mostly amorphous radiolarian forms with the exception of a few possible Late Triassic radiolarian forms (*Canoptum* sp.). Two other samples yielded scarce Jurassic and no Triassic forms. The possible Late Triassic to Jurassic radiolarian age ranges from this location agree with the

chert ages from the RCT elsewhere in the Klamath Mountains (Irwin et al., 1982).

End Day 3. Return to vehicles, drive 0.2 miles back to USFS 4201, turn left and drive 15.1 miles to U.S. Hwy 199. Turn left and return to Siskiyou Field Institute.

Day 4

Today we will focus on amphibolite-grade metamorphosed rocks of the Onion Camp complex (Stop 4.1) and the plutonic roots and wallrocks of the Rogue arc (Stops 4.2–4.5). Time-permitting, the final stops will examine Josephine pillow lavas and sheeted mafic dikes, and Galice flysch (Stops 4.6–4.7).

Depart Siskiyou Field Institute and drive east on the Illinois River Road to U.S. Hwy 199. Reset odometers to zero.

	•
Mileage	Description
0.0	Selma, Oregon. Intersection of U.S. Hwy 199 and Illinois River Road. Drive north toward Grants Pass, Oregon.
3.8	Turn left onto Swede Basin Road, USFS 25.
5.6, 6.0,	Illinois Valley fault (IVF). The road thrice
and 6.3	crosses a contact between Galice flysch on the
	SE from sheared serpentinite with a subvertical
	foliation on the NW. This shear zone marks the
	surface trace of the Illinois Valley fault. Slaty
	argillite and siltstone of the Galice Formation
	occur on both sides of the serpentinite-cored
	shear zone.
8.7	The road crosses a sheared boundary between
	Galice Formation on the SE against Josephine
0.0	peridotite and a fault sliver of basalt to the NW.
9.0	Road crosses a high-angle contact separating
	rocks of probable Josephine ophiolite equivalent
	on the SE from peridotite of the Onion Camp complex on the NW.
9.1	Roadcut exposes mafic dikes and gabbro of
7.1	probable Josephine ophiolite equivalent.
9.5	Road crosses a high-angle contact separating
	rocks of probable Josephine ophiolite equivalent
	on the SE from peridotite of the Onion Camp
	complex on the NW.
10.3	Road crosses a high-angle contact separating
	OCC peridotite on the SE from OCC basaltic
	rocks on the NW.
11.3	Unincorporated community of Four Corners
	(Jackson County), Oregon. Turn left onto USFS
	2524 (Serpentine Road). A north-south fault tra-
	verses the saddle at Four Corners and separates
	basaltic rocks of the OCC on the east from inter-
	layered argillite and volcanogenic turbidites of
12.2	the Rogue Formation on the west. Bear left onto USFS 015.
12.2	Dear left offto USFS 013.

12.3	Road crosses a contact between interlayered argillite and volcanogenic turbidites of the
	Rogue Formation on the NW from the serpentinite of the OCC on the SE.
13.4	Road crosses a contact between the serpentinite of the OCC on the NW from the amphibolite of
14.0	the OCC on the SE. Turn right onto an unmarked logging road. Follow a hairpin turn uphill to a logging pad at the
14.4	end of the road. Park and hike to Squaw Peak (150 m distance and 40 m climb from the parking area).

Stop 4.1. Polydeformed Amphibolite and Serpentinite of OCC (UTM 10T, 445277 E, 4688226 N)

Refer to Figures 4 and 5B for location. A short hike west to the peak leads to outcrops exposing amphibolite-grade metamorphosed rocks of the OCC, including gneissic amphibolite with subordinate hornblende schist, massive meta-gabbro, and rare quartzite. The typical amphibolite gneiss contains 60%–80% brown hornblende; the remaining 20%–40% of the rock is composed of plagioclase (untwined albite and oligoclase), epidote, titanite, and opaque oxides (mostly ilmenite). Quartzites are impure and contain 60%–90% quartz with cummingtonite, almandine, biotite, white mica, and opaque oxides making up the remaining 10%–40%. Retrograde alteration is common (chlorite, epidote, clinozoisite, prehnite, green amphibole, white mica, and quartz).

The foliation is defined by flattened hornblende in the schist and 1–3-cm-thick layering in the gneisses. The foliation is folded and contains an intersection lineation that is best developed in the schists. Two styles of folds are present: syn-metamorphic, tight to isoclinal folds, often with attenuated and/or truncated limbs; and late stage open, similar folds. The intersection lineation parallels the isoclinal fold hinges.

The foliation in the amphibolite is parallel to a contact with amphibolite-grade metamorphosed peridotite contact at Squaw Peak. The contact is marked by a sudden vegetation change that rims the peak to the north and west; the amphibolite supports a flora with conifers, madrone, and manzanita, whereas the peridotite is barren of trees and supports ground-hugging shrubs and succulents. The mapped contacts between the amphibolite and the serpentinized peridotite defines map-scale folded, isoclinal folds in these units (Fig. 5B). In support of this map relation, scarce foliations in the serpentinite (Fig. 17) are parallel to the amphibolite-serpentinite contact. This amphibolite-grade metamorphic fabric in the serpentinite is difficult to detect because much of the serpentinite now contains greenschist-facies mineral assemblages, presumably related to a lower-greenschist grade metamorphic event interpreted to relate to the Nevada orogeny.

The serpentinite is brecciated in some outcrops (Fig. 17), with no evidence of the penetrative fabric that exists along the boundary with the amphibolites. The fragmentation probably relates to rifting of older Klamath terranes to form the Josephine

ophiolite (Yule et al., 2006), and bolsters the correlation of OCC rocks with the RCT.

Two samples collected in roadcuts below Squaw Peak yield 40 Ar/ 39 Ar cooling ages of 169.6 \pm 0.7 Ma and 173 \pm 0.6 Ma from brown hornblende in two different amphibolite gneiss samples (Yule et al., 2006) and place a minimum age for metamorphism of the OCC. This Middle Jurassic age correlates with the timing of the "Siskiyou orogeny" elsewhere in the Klamath Mountains, a period of terrane accretion and arc growth (e.g., Cannat and Boudier, 1985; Wright and Fahan, 1988; Hacker et al., 1995). Interestingly, Middle Jurassic cooling ages like those obtained at Squaw Mountain are a rare occurrence in the Klamath Mountains. The Siskiyou orogeny is defined mainly from crystallization ages (zircon ages) from volcanic and plutonic rocks. Ages from metamorphic rocks that are cut by Middle Jurassic plutons (e.g., the Condrey Mountain schist, visited on Day 2 of this trip) yield Late Jurassic ages. One possible explanation is that the metamorphic rocks inferred to have formed during the Middle Jurassic event have also experienced the Late Jurassic Nevadan event that has reset their metamorphic cooling ages. Thus, the relations at Squaw Peak document relatively low-grade Nevadan metamorphic conditions for this part of the OCC.

Complexly folded amphibolite and serpentinite belts are common throughout the Triassic to Middle Jurassic Rattlesnake Creek terrane (RCT). The cooling ages and the polydeformed nature of the amphibolite-serpentinite body observed at Squaw Peak and throughout the OCC further strengthens the correlation of the OCC with RCT found elsewhere in the Klamath Mountains. This correlation crosses a major terrane-bounding thrust—the Orleans thrust—that experienced tens of km, if not > 100 km, of displacement and links the WKT to the overriding Klamath Mountains thrust sheet containing the RCT, broadly known as the western Paleozoic and Triassic belt (e.g., Irwin, 1994).

Return to vehicles and drive back to Four Corners. Reset odometers to zero.

Mileage	Description
0.0	Four Corners. Turn left (north) and proceed on USFS 25 (now referred to as Onion Mountain
	Road).
6.8	The road crosses the contact with a thin sliver of sheared serpentinite separating volcanogenic turbidites of the Rogue Formation on the west from basaltic rocks and scarce chert of the OCC.
10.7	The poorly exposed, approximate location of the informally named Chetco Pass fault (Yule et al., 2006; Fig. 5). The fault separates the Rogue Formation on the east from the Briggs Creek amphibolite on the west. The fault is a crustal-scale discontinuity separating the Illinois River plutonic complex and its amphibolite-grade metamorphic wallrocks on the west from the greenschist-grade metamorphosed Rogue Formation and OCC rock types on the east.

12.1 Turn left (west) onto USFS 2512. Sam Brown Campground is located nearby.

Pull off to the left at a turnout across from the west end of a road metal quarry.

Stop 4.2. Briggs Creek Amphibolite (BCA) (UTM 10T, 441275 E, 4698953 N)

Refer to Figures 4 and 5A for location. The quarry exposes amphibolitic rocks that are distinct from those observed at Stop

4.1. The BCA amphibolites (Fig. 19) are not polydeformed, and they have experienced only local retrograde greenschist-facies metamorphism. Their foliation strikes NE-SW with steep NW to SE dips folded about shallowly plunging NE- and SW-trending folds (both syn- and post-metamorphic folds; Fig. 18). Mineral elongation as well as intersection lineations trend parallel to fold hinge lines. The structural uniformity throughout the BCA indicates deformation controlled by WNW-ESE-directed compression along with NNE-SSW-directed elongation.

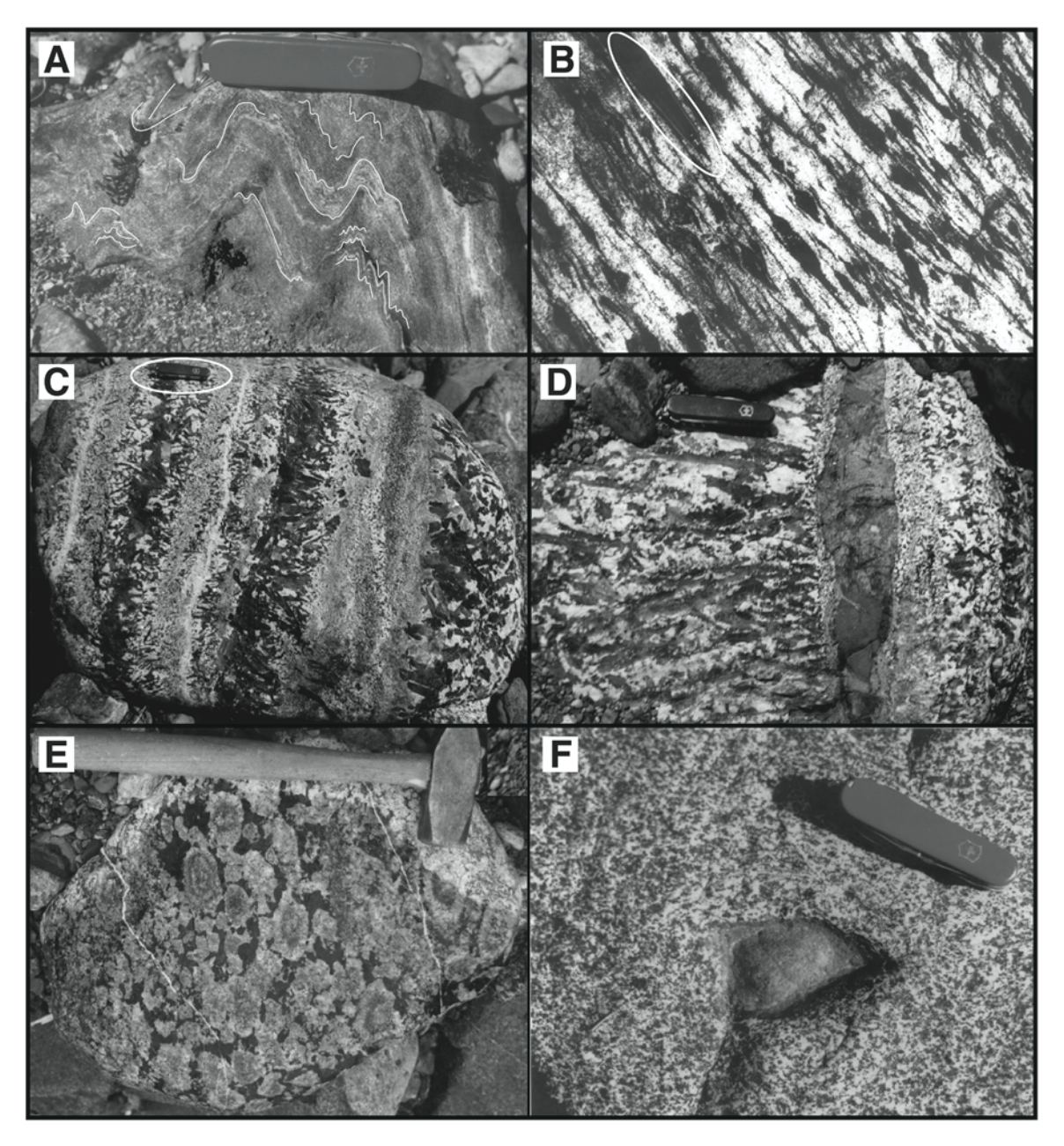


Figure 19. (A) Briggs Creek amphibolite with lines added to highlight folding. (B–F) Rock types of the Illinois River batholith: (B) flaser gabbro; (C) comb-structure hornblende gabbro; (D) comb-structure hornblende gabbro with serpentinized peridotite screen; (E) orbicular norite; (F) diorite with peridotite xenolith. Swiss army knife in A, C, D, and F is 8 cm long. Tip of the pencil in B is 3 cm long. Rock hammer handle in E is 30 cm long.

The BCA cooling ages are younger than OCC amphibolites. The ⁴⁰Ar/³⁹Ar cooling ages from BCA rocks range from 156 to 158 Ma (Hacker and Ernst, 1993; Hacker et al., 1995; Yule et al., 2006). These cooling ages overlap with U-Pb zircon ages obtained from the Illinois River plutonic complex (IRPC) (Stop 4.3). The BCA therefore appears to have annealed following amphibolite-grade dynamothermal metamorphism related to the emplacement of the IRPC.

The protolith material for the BCA is debatable. Coleman and Lanphere (1991) hypothesize that crustal rocks of the Josephine ophiolite provided the protolith for the BCA. However, lithologic and geochemical evidence (MORB and WPB signatures, Coleman and Lanphere, 1991) suggests that the RCT served as the protolith for at least parts of the BCA (Yule et al., 2006).

Return to vehicles, reset odometers to zero, and proceed west on USFS 2512 to Stop 4.3. Note: mileage is cumulative.

Mileage	Description
0.2, 1.2,	The road makes three crossings of the boundary
and 1.7	between the BCA and peridotite.
2.6	Park at the small pullout on the right.

Stop 4.3. Peridotite of Chrome Ridge (UTM 10T, 439665 E, 4697852 N)

Refer to Figures 4 and 5A for location. The roadcut here and outcrops uphill expose relatively pristine harzburgite and dunite, informally referred to as the Chrome Ridge peridotite. Spinel locally defines a weak foliation and strong lineation. The latter dips shallowly to the north or south. Foliations tend to be steeply dipping. Locally, small bodies of podiform chromite occur, similar to the peridotite body exposed at Pearsoll Peak, and the much larger Josephine peridotite massif. These similarities suggest the Josephine, Pearsoll Peak, and Chrome Ridge bodies once formed the mantle lithosphere during Josephine/rogue interarc basin formation.

Return to vehicles, reset odometers to zero, and proceed to Stop 4.4 on USFS 2512.

ileage	Description
1.8	The road crosses a poorly exposed contact
	between the IRPC and Chrome Ridge peridotite.
	Tonalite/trondhjemite, locally garnetiferous, is
	the dominant rock type along this boundary.
4.1	Park at pullout on the left.
4.1	,,

Stop 4.4. Gabbro and Tonalite/Trondhjemite of the Illinois River Batholith (UTM 10T, 435033 E, 4697276 N)

Refer to Figures 4 and 5A for location. This area provides similar relations to those depicted as the "Chetco River plutonic suite" in Figure 14.

The ~150 km² Illinois River batholith (IRB) extends from the upper Chetco River area on the south, across the Illinois River drainage, and north into the southern reaches of the Rogue River drainage. Thus the IRB comprises the westernmost part of the WKT. It consists of intermediate to ultramafic plutonic rocks with numerous meta-gabbro and meta-peridotite screens.

Exposures in the roadcut at Stop 4.4 show tonalite/trond-jhemite dikes cutting cumulate-textured norite, two-pyroxene gabbro, and troctolite (unit Jcm of Hotz, 1971, and Page et al., 1981; also see Jorgenson, 1970; Dick, 1976; Loney and Himmelberg, 1977; Garcia, 1979, 1982; Coleman and Lanphere, 1991; Yule, 1996).

U-Pb zircon ages from localities along the Illinois River to the south yield 157 ± 1 Ma from a tonalite sample and 160 ± 1 Ma from a hornblende-biotite quartz diorite (Yule et al., 2006). 40 Ar/ 39 Ar cooling ages on hornblende from gabbros and dikes that intrude the wallrocks yield ages of 156–155 Ma (Yule et al., 2006). The cooling ages agree with results of previous studies (Dick, 1976; Hotz, 1971).

The IRB is reversely zoned. The core region (immediately to the west) is composed of coarsely crystalline layered troctolite, norite, and hornblende gabbro (Fig. 19). The outer portion consists of massive norite, hornblende gabbro and diorite, and sparse biotite-hornblende quartz diorite. Late-stage units include: (1) a sill-like hornblende pegmatite body, with cockscomb megacrysts up to 60 cm in length, that occurs in the upper Chetco River drainage and appears to have collected at the roof of the complex beneath the Madstone Cabin and Pearsoll Peak thrusts; and (2) tonalite-trondhjemite sills and dikes along the margins of the complex in contact with the Pearsoll Peak and Chrome Ridge peridotite bodies, and along the Illinois River upstream from Oak Flats.

The IRB is similar in age to the plutons that cut the RCT to the east, including the Grayback pluton (Barnes et al., 1995) and the Wooley Creek suite (Barnes, 1983; Barnes et al., 1986a, 1995; Gribble et al., 1990). However, the IRB has lower K₂O and lower LREE abundances, and overall is much more mafic than the eastern plutons. The IRB ages also overlap with the magmatic ages from the Josephine ophiolite (Harper et al., 1994).

Cumulate textures are common in the core of the IRB, and transition to xenomorphic- to hypidiomorphic-granular outward from the core. Compositional layering in the core rocks is defined by varying proportions and sizes of mafic and felsic minerals. Cumulus phases are orthopyroxene and clinopyroxene, hornblende, and labradorite. Kelyphytic rims are common, surrounding spinel and olivine. Normally zoned plagioclase is rare in the cumulus rocks, but common in the marginal gabbros and diorites (cores of An₇₀₋₉₅ and rims of An₅₀₋₇₅). Recrystallized textures are common throughout the complex and include granoblastic textures with subgrain development, undulose extinction, and bent twinning lamellae.

Strain progressively increases from the relatively undeformed core region outward toward the margins where some outcrops show flaser textures (L, and L > S tectonites; Fig. 19). These strongly deformed rocks display a variable foliation where present and a uniform moderate- to shallow-plunging, NE–SW-trending lineation (elongation), parallel to the lineations observed

in the BCA (Stop 4.2). The general structure of the IRPC can be defined as an elongate dome that gently plunges NNE and SSW with steeply dipping SE and NW margins.

Return to vehicles, reset odometers to zero, and drive west to Optional Stop 4.5. Otherwise, drive east, back to the intersection of USFS 2512 and USFS 25 at Sam Brown Campground.

Mileage	Description
0.3	To continue on to Optional Stop 4.5, at the four-way intersection, head west (straight ahead) on USFS 091.
5.3	Park at turnout on right.

Stop 4.5 (Optional). Valen Lake Thrust (UTM 10T, 428568 E, 4697092 N)

See Figures 4 and 5A for location. The drive west from Stop 4.4 follows a ridgeline that marks the northern boundary of the Kalmiopsis Wilderness. Extensive salvage logging of impressive stands of old-growth pine and cedar forest occurred along this northern boundary following the 2002 Biscuit Fire.

Roadcut exposures en route to Stop 4.5 consist of various rock types of the IRB, including coarse pyroxene gabbro and pegmatitic hornblende gabbro, with subordinate meta-gabbro screens and cross-cutting quartz porphyry.

From the stop, note "Chinaman Hat" (elevation 3465 ft) to the north across South Fork Silver Creek and "Bald Mountain" (elevation 3890 ft) to the west, and look south into the Illinois River gorge. The confluence of the Illinois and Rogue rivers is ~20 km due northwest from this location.

Though poorly exposed here, this stop sits at the mapped location of the Valen Lake thrust (northern continuation of the South Fork thrust) and forms the western limit of the KMP. The thrust separates a hanging wall composed of IRB rocks on the east from a footwall composed of Dothan Formation on the west (Franciscan complex equivalent rocks). The thrust strikes N-S and dips ~30 degrees east. An exposure of the thrust can be viewed along the Illinois River trail, to the south and ~200 m below the ridgeline at this stop, where Page et al. (1981) have recorded a 33° dip to the east.

Return to vehicles and drive 14.1 miles back to the intersection of USFS 2512 and USFS 25 at Sam Brown Campground. At intersection, reset odometers to zero.

Mileage	Description
0.0	At four-way intersection of USFS routes 2512
	and 25, turn right (south) on USFS 25.
5.3	Sheared serpentinite separating Rogue Forma-
	tion volcaniclastic strata and subordinate meta-
	argillite from metabasalt and chert of the OCC.
7.	Turn left onto USFS 2509.
8.5	Turn right onto USFS 2706.
9.1	Sheared serpentinite of OCC.
9.7	Sheared boundary between OCC metabasalt to
	the west and serpentinized peridotite to the east.

10.5	Boundary between serpentinized peridotite to the west and sheeted mafic dikes and gabbro to
	the east.
12.3	Approximate location of overturned fold hinge
	in slaty argillite of Galice Formation.
13.8	Park at small turnout on right, at base of outcrop.

Stop 4.6. Pillow Lavas (UTM 10T, 455510 E, 4701398 N)

Refer to Figures 4 and 5A for location. This area provides the stratigraphic relations depicted as the "Shan Creek" columnar section in Figure 14. The roadcut exposes the dip surface of a set of N43°E-striking, 73°SE-dipping basaltic pillow lava (Fig. 15). Lava tubes are "entwined" and individual lava tubes can be followed for up to 3 m. A conformable contact can be inferred between the pillow lavas and slaty argillite of the Galice Formation, exposed in roadcuts a few hundred meters to the south, and in the stream below the road to the west.

The map relations reveal that the lavas here are steeply overturned in the limb of a regional, overturned, tight syncline cored by the Galice Formation. One encounters basalt, sheeted mafic dikes, and bits of gabbro both to the southeast (overturned) and northwest (upright) of the hinge region (Figs. 4, 5, and 18). Thus, the map relations reveal a tightly folded ophiolite sequence, overlain by the Galice Formation, interpreted as a northern extension of the Josephine ophiolite.

This stop is analogous to the basal Galice/pillow lava contact seen at Stop 3.3, along the Smith River.

Return to vehicles, and proceed to Stop 4.7 (Optional). Otherwise, drive 2.5 miles to Riverbanks Road, turn left, and follow signs to Merlin, Oregon, and then follow signs to Interstate-5 and return to Portland, Oregon.

End of field trip.

Mileage	Description
15.2	Park and follow a short trail leading to outcrops along Shan Creek.

Stop 4.7 (Optional). Sheeted Mafic Dikes (UTM 10T, 457129 E, 4700541 N)

Refer to Figures 4 and 5A for location. Stream exposures of mafic dikes, often with chilled margins and occasional gabbro screens, suggest this location occupies a stratigraphically deeper position beneath the pillow lavas at Stop 4.5.

Return to vehicles. Drive 1.1 miles to Riverbanks Road. Turn left, and follow signs to Merlin, Oregon, and then follow signs to Interstate-5 and return to Portland, Oregon.

End of field trip.

ACKNOWLEDGMENTS

This guide is dedicated to the memory of R.G. Coleman (1923–2020), whose research greatly advanced our understanding of the tectonic and petrologic development of the Klamath Mountains Province. This effort benefitted from field and lab

assistance by J. Anderson, A. Bleeker, R. Ceesay, J. Coons, J. Grischuk, M. Klapper, N. Sponseller, and B. Yule; discussions with R. Alexander, C. Barnes, W. Behr, C. Blome, B. Coleman, A. Coulton, T. Dumitru, W.G. Ernst, K. Gates, B. Hacker, G. Harper, M. Helper, F. Hladkey, W. Irwin, J. MacDonald, L. Ramp, J. Saleeby, M. Silk, K. Surpless, T. Wiley, and A. Yoshinobu; insights from reviewers C. Barnes and J. Wakabayashi; and editorial handling by A. Grunder and the GSA editorial staff. D. Yule gives special thanks to J. Saleeby, whose keen observation that "something did not make geologic sense" while kayaking the Illinois River led to the suggestion of Yule's dissertation project, and to A. Snoke who "passed" on working in the Illinois River area and chose the Preston Peak instead for his dissertation project. This work was supported by NSF grant EAR-1846811 (to A.D. Chapman). The Siskiyou Field Institute is thanked for providing a home base for this field trip.

REFERENCES CITED

- Aalto, K.R., 1989, Sandstone petrology and tectonostratigraphic terranes of the northwest California and southwest Oregon Coast Ranges: Journal of Sedimentary Research, v. 59, no. 4, p. 561–571, https://doi.org/10 .1306/212F8FE9-2B24-11D7-8648000102C1865D.
- Aalto, K.R., 2014, Examples of Franciscan Complex mélanges in the northernmost California Coast Ranges, a retrospective: International Geology Review, v. 56, no. 5, p. 555–570, https://doi.org/10.1080/00206814.2013.879841.
- Alberts, D., Gehrels, G.E., and Nelson, J., 2021, U-Pb and Hf analyses of detrital zircons from Paleozoic and Cretaceous Strata on Vancouver Island, British Columbia: Constraints on the Paleozoic tectonic evolution of southern Wrangellia: Lithosphere, https://doi.org/10.2113/2021/7866944.
- Alexander, R.J., and Harper, G.D., 1992, The Josephine ophiolite: An ancient analog for slow- to intermediate-spreading oceanic ridges, *in* Parsons, B., Murton, B.J., and Browning, P., eds., Ophiolites and Their Modern Oceanic Analogues: Geological Society, London, Special Publication 60, p. 3–38, https://doi.org/10.1144/GSL.SP.1992.060.01.02.
- Allen, C.M., and Barnes, C.G., 2006, Ages and some cryptic sources of Mesozoic plutonic rocks in the Klamath Mountains, California and Oregon, in Snoke, A.W., and Barnes, C.G., eds., Geological Studies in the Klamath Mountains Province, California and Oregon: A Volume in Honor of William P. Irwin: Geological Society of America Special Paper 410, p. 223–245, https://doi.org/10.1130/2006.2410(11).
- Anczkiewicz, R., Platt, J.P., Thirlwall, M.F., and Wakabayashi, J., 2004, Franciscan subduction off to a slow start; evidence from high-precision Lu/Hf garnet ages on high-grade blocks: Earth and Planetary Science Letters, v. 225, p. 147–161, https://doi.org/10.1016/j.epsl.2004.06.003.
- Apen, F.E., Wakabayashi, J., Day, H.W., Roeske, S.M., Souders, A.K., and Dumitru, T.A., 2021, Regional-scale correlations of accreted units in the Franciscan Complex, California, USA: A record of long-lived, episodic subduction accretion, *in* Wakabayashi, J., and Dilek, Y., eds., Plate Tectonics, Ophiolites, and Societal Significance of Geology: A Celebration of the Career of Eldridge Moores: Geological Society of America Special Paper 552, p. 233–255, https://doi.org/10.1130/2021.2552(11).
- Bailey, E.H., Irwin, W.P., and Jones, D.L., 1964, Franciscan and related rocks, and their significance in the geology of western California: California Division of Mines and Geology Bulletin, v. 183, 177 p.
- Barnes, C.G., 1983, Petrology and upward zonation of the Wooley Creek batholith, Klamath Mountains, California: Journal of Petrology, v. 24, p. 495– 537, https://doi.org/10.1093/petrology/24.4.495.
- Barnes, C.G., and Barnes, M.A., 2020, The western Hayfork terrane: Remnants of the Middle Jurassic arc in the Klamath Mountain province, California and Oregon: Geosphere, v. 16, no. 4, p. 1058–1081, https://doi.org/10.1130/GES02229.1.
- Barnes, C.G., Allen, C.M., and Saleeby, J.B., 1986a, Open- and closed-system characteristics of a tilted plutonic system, Klamath Mountains, California: Journal of Geophysical Research, v. 91, p. 6073–6090, https://doi.org/10.1029/JB091iB06p06073.

- Barnes, C.G., Rice, J.M., and Gribble, R.F., 1986b, Tilted plutons in the Klamath Mountains of California and Oregon: Journal of Geophysical Research, v. 91, p. 6059–6071, https://doi.org/10.1029/JB091iB06p06059.
- Barnes, C.G., Petersen, S.W., Kistler, R.W., Prestvik, T., and Sundvoll, B., 1992, Tectonic implications of isotopic variation among Jurassic and Early Cretaceous plutons, Klamath Mountains: Geological Society of America Bulletin, v. 104, p. 117–126, https://doi.org/10.1130/0016-7606 (1992)104<0117:TIOIVA>2.3.CO;2.
- Barnes, C.G., Donato, M.M., Barnes, M.A., Yule, J.D., Hacker, B.R., and Helper, M.A., 1995, Geochemical compositions of metavolcanic and metasedimentary rocks, western Jurassic and western Paleozoic and Triassic belts, Klamath Mountains, Oregon and California: U.S. Geological Survey Open-File Report 95-227-A, 63 p., https://doi.org/10.3133/ ofr95227A.
- Barnes, C.G., Petersen, S.W., Kistler, R.W., Murray, R., and Kays, M.A., 1996, Source and tectonic implications of tonalite-trondhjemite magmatism in the Klamath Mountains: Contributions to Mineralogy and Petrology, v. 123, p. 40–60, https://doi.org/10.1007/s004100050142.
- Barrow, W.M., and Metcalf, R.V., 2006, A reevaluation of the paleotectonic significance of the Paleozoic Central Metamorphic terrane, eastern Klamath Mountains, California: New constraints from trace element geochemistry and 40Ar/39Ar thermochronology, in Snoke, A.W., and Barnes, C.G., eds., Geological Studies in the Klamath Mountains Province, California and Oregon: A Volume in Honor of William P. Irwin: Geological Society of America Special Paper 410, p. 393–410, https://doi.org/10.1130/2006.2410(19).
- Barrows, A.G., 1969, Geology of the Hamburg-McGuffy Creek area Siskiyou County, California, and petrology of the Tom Martin ultramafic complex [Ph.D. thesis]: Los Angeles, University of California, 301 p.
- Batt, G.E., Harper, G.D., Heizler, M., and Roden-Tice, M., 2010a, Cretaceous sedimentary blanketing and tectonic rejuvenation in the western Klamath Mountains: Insights from thermochronology: Central European Journal of Geosciences, v. 2, p. 138–151, https://doi.org/10.2478/v10085-009-0041-4.
- Batt, G.E., Casman, S.M., Garver, J., and Bigelow, J.J., 2010b, Thermotectonic evidence for the consequences of two-stage extension on the Trinity detachment surface, Eastern Klamath Mountains: American Journal of Science, v. 310, p. 261–281, https://doi.org/10.2475/04.2010.02.
- Beaulieu, J.D., and Hughes, P.W., 1976, Land-use geology of western Curry County, Oregon (No. 90): Portland, Oregon Department of Geology and Mineral Industries Bulletin no. 90, 148 p., https://ngmdb.usgs.gov/Prodesc/proddesc_33006.htm.
- Behr, W.M., and Platt, J.P., 2013, Rheological evolution of a Mediterranean subduction complex: Journal of Structural Geology, v. 54, p. 136–155, https://doi.org/10.1016/j.jsg.2013.07.012.
- Berkland, J.O., Raymond, L.A., Kramer, J.C., Moores, E.M., and O'Day, M., 1972, What is Franciscan?: AAPG Bulletin, v. 56, p. 2295a–2302, https://doi.org/10.1306/819A421A-16C5-11D7-8645000102C1865D.
- Bestland, E.A., 1987, Volcanic stratigraphy of the Oligocene Colestin Formation in the Siskiyou Pass area of southern Oregon: Oregon Geology, v. 49, p. 79–86.
- Blake, M.C., Irwin, W.P., and Coleman, R.G., 1967, Upside-down metamorphic zonation, blueschist facies, along a regional thrust in California and Oregon, in Geological Survey Research 1967, Chapter C: U.S. Geological Survey Professional Paper 575, p. C1–C9, https://pubs.usgs.gov/pp/0575c/report.pdf.
- Blake, M.C., Jr., Irwin, W.P., and Coleman, R.G., 1969, Blueschist-facies metamorphism related to regional thrust faulting: Tectonophysics, v. 8, p. 237–246, https://doi.org/10.1016/0040-1951(69)90100-0.
- Blake, C., Howell, D.G., and Jones, D.L., 1982, Preliminary tectonostratigraphic terrane map of California: U.S. Department of the Interior Geological Survey Open-File Report 82-593, 9 p.
- Blake, M.C., Jr., Howell, D.G., and Jayko, A.S., 1984, Tectonostratigraphic terranes of the San Francisco Bay region: Pacific Section S.E.P.M., v. 43, p. 5–22.
- Blake, M.C., Jr., Engebretson, D.C., Jayko, A.S., and Jones, D.L., 1985, Tectonostratigraphic terranes in southwest Oregon, in Howell, D.G., ed., Tectonostratigraphic Terranes of the Circum-Pacific Region: Houston, Texas, Circum-Pacific Council for Energy and Mineral Resources, Earth Science Series, p. 147–157.
- Blakey, R.C., and Ranney, W.D., 2018, Ancient Landscapes of Western North America: Cham, Switzerland, Springer, 228 p., https://doi.org/ 10.1007/978-3-319-59636-5.

Bourgeois, J., 1980, A transgressive shelf sequence exhibiting hummocky stratification; the Cape Sebastian Sandstone (Upper Cretaceous), southwestern Oregon: Journal of Sedimentary Research, v. 50, no. 3, p. 681–702, https://doi.org/10.1306/212F7AC2-2B24-11D7-8648000102C1865D.

- Bourgeois, J., and Dott, R.H., Jr., 1985, Stratigraphy and sedimentology of Upper Cretaceous rocks in coastal southwest Oregon: Evidence for wrench-fault tectonics in a postulated accretionary terrane: Geological Society of America Bulletin, v. 96, no. 8, p. 1007–1019, https://doi.org/10.1130/0016-7606(1985)96<1007:SASOUC>2.0.CO;2.
- Bourgeois, J., and Leithold, E.L., 1983, Sedimentation, tectonics and sea-level change as reflected in four wave-dominated shelf sequences in Oregon and California, *in* Larue, D.K., and Steel, R.J., eds., Cenozoic Marine Sedimentation, Pacific Margin, U.S.A.: Los Angeles, Pacific Section, Society of Economic Paleontologists and Mineralogists, p. 1–17.
- Bröcker, M., and Day, H.W., 1995, Low-grade blueschist facies metamorphism of metagreywackes, Franciscan Complex, northern California: Journal of Metamorphic Geology, v. 13, p. 61–78, https://doi.org/10.1111/j.1525-1314.1995.tb00205.x.
- Brown, E.H., and Blake, M.C., Jr., 1987, Correlation of early Cretaceous blueschists in Washington, Oregon and northern California: Tectonics, v. 6, no. 6, p. 795–806, https://doi.org/10.1029/TC006i006p00795.
- Brown, E.H., and Ghent, E.D., 1983, Mineralogy and phase relations in the blueschist facies of the Black Butte and Ball Rock areas, northern California Coast Ranges: The American Mineralogist, v. 68, no. 3–4, p. 365–372.
- Burchfiel, B.C., Cowan, D.S., and Davis, G.A., 1992, Tectonic overview of the Cordilleran orogen in the western United States, in Burchfiel, B.C., Lipman, P.W., and Zoback, M.L., eds., The Cordilleran Orogen: Conterminous U.S.: Boulder, Colorado, Geological Society of America, Geology of North America, v. G3, p. 407–414, https://doi.org/10.1130/DNAG -GNA-G3.407.
- Burton, W.C., 1982, Geology of the Scott Bar Mountains, northern California [M.S. thesis]: Eugene, University of Oregon, 120 p.
- Bushey, J.C., Snoke, A.W., Barnes, C.G., and Frost, C.D., 2006, Geology of the Bear Mountain intrusive complex, Klamath Mountains, California, in Snoke, A.W., and Barnes, C.G., eds., Geological Studies in the Klamath Mountains Province, California and Oregon: A Volume in Honor of William P. Irwin: Geological Society of America Special Paper 410, p. 287–315, https://doi.org/10.1130/2006.2410(14).
- Cannat, M., and Boudier, F., 1985, Structural study of intra-oceanic thrusting in the Klamath Mountains, northern California: Implications on accretion geometry: Tectonics, v. 4, no. 5, p. 435-452, and correction in v. 4, no. 6, p. 597-601.
- Cashman, S.M., and Elder, D.R., 2002, Post-Nevadan detachment faulting in the Klamath Mountains, California: Geological Society of America Bulletin, v. 114, p. 1520–1534, https://doi.org/10.1130/0016-7606(2002)114 <1520:PNDFIT>2.0.CO:2.
- Cashman, S.M., Cashman, P.H., and Longshore, J.D., 1986, Deformational history and regional tectonic significance of the Redwood Creek schist, northwestern California: Geological Society of America Bulletin, v. 97, no. 1, p. 35–47, https://doi.org/10.1130/0016-7606(1986)97<35 :DHARTS>2.0.CO;2.
- Chamberlain, K.R., Snoke, A.W., Barnes, C.G., and Bushey, J.C., 2006, New U-Pb radiometric dates of the Bear Mountain intrusive complex, Klamath Mountains, California, in Snoke, A.W., and Barnes, C.G., eds., Geological Studies in the Klamath Mountains Province, California and Oregon: A Volume in Honor of William P. Irwin: Geological Society of America Special Paper 410, p. 317–332, https://doi.org/10.1130/2006.2410(15).
- Chapman, A.D., 2017, The Pelona–Orocopia–Rand and related schists of southern California: A review of the best-known archive of shallow subduction on the planet: International Geology Review, v. 59, no. 5–6, p. 664–701, https://doi.org/10.1080/00206814.2016.1230836.
- Chapman, A.D., Jacobson, C.E., Ernst, W.G., Grove, M., Dumitru, T., Hourigan, J., and Ducea, M.N., 2016, Assembling the world's type shallow subduction complex: Detrital zircon geochronologic constraints on the origin of the Nacimiento block, central California Coast Ranges: Geosphere, v. 12, no. 2, p. 533–557, https://doi.org/10.1130/GES01257.1.
- Chen, J.H., and Moore, J.G., 1982, Uranium-lead isotopic ages from the Sierra Nevada batholith, California: Journal of Geophysical Research, v. 87, p. 4761–4784, https://doi.org/10.1029/JB087iB06p04761.
- Clennett, E.J., Sigloch, K., Mihalynuk, M.G., Seton, M., Henderson, M.A., Hosseini, K., Mohammadzaheri, A., Johnston, S.J., and Müller, R.D., 2020, A quantitative tomotectonic plate reconstruction of western North

- America and the eastern Pacific basin: Geochemistry, Geophysics, Geosystems, v. 20, https://doi.org/10.1029/2020GC009117.
- Cloos, M., 1983, Comparative study of melange matrix and metashales from the Franciscan subduction complex with the basal Great Valley Sequence, California: The Journal of Geology, v. 91, no. 3, p. 291–306, https://doi.org/10.1086/628772.
- Cloos, M., 1985, Thermal evolution of convergent plate margins: Thermal modeling and reevaluation of isotopic Ar-ages for blueschists in the Franciscan Complex of California: Tectonics, v. 4, no. 5, p. 421–433, https://doi.org/10.1029/TC004i005p00421.
- Coint, N., Barnes, C.G., Yoshinobu, A.S., Chamberlain, K.R., and Barnes, M.A., 2013, Batch-wise assembly and zoning of a tilted calc-alkaline batholith: Field relations, timing, and compositional variation: Geosphere, v. 9, p. 1729–1746, https://doi.org/10.1130/GES00930.1.
- Coleman, R.G., 1972, The Colebrooke Schist of southwestern Oregon and its relation to the tectonic evolution of the region: U.S. Geological Survey Bulletin 1339, 61 p.
- Coleman, R.G., and Lanphere, M.A., 1971, Distribution and age of high-grade blueschists, associated eclogites, and amphibolites from Oregon and California: Geological Society of America Bulletin, v. 82, no. 9, p. 2397–2412, https://doi.org/10.1130/0016-7606(1971)82[2397:DAAOHB]2.0.CO;2.
- Coleman, R.G., Helper, M.D., and Donato, M.M., 1983, Geologic map of the Condrey Mountain Roadless area, Siskiyou County, California: U.S. Geological Survey Miscellaneous Field Studies Map 1540A, https://doi.org/ 10.3133/mf1540A.
- Coleman, R.G., Manning, C.E., Mortimer, N., Donato, M.M., and Hill, L.B., 1988, Tectonic and regional metamorphic framework of the Klamath Mountains and adjacent Coast Ranges, California and Oregon, in Ernst, W.G., ed., Metamorphism and Crustal Evolution of the Western United States—Rubey Volume VII: Englewood Cliffs, New Jersey, Prentice Hall, p. 1059–1097.
- Coleman, R.G., and Lanphere, M.A., 1991, The Briggs Creek amphibolite, Klamath Mountains, Oregon: Its origin and dispersal: New Zealand Journal of Geology and Geophysics, v. 34, p. 271–284, https://doi.org/10.1080/00288306.1991.9514465.
- Collins, W.J., 2002, Hot orogens, tectonic switching, and creation of continental crust: Geology, v. 30, p. 535–538, https://doi.org/10.1130/0091-7613(2002)030<0535:HOTSAC>2.0.CO;2.
- Coons, J., 2017, Structural and U-Pb detrital zircon geochronologic constraints on the origin of the Condrey Mountain Schist, California-Oregon [M.S. thesis]: Rolla, Missouri University of Science and Technology, 49 p.
- Cornwall, H.R., 1981, Chromite deposits in the Seiad Valley and Scott Bar quadrangles, Siskiyou County, California: U.S. Geological Survey Bulletin 1382-D, p. Dl-D17.
- Dailey, S.R., Barnes, C.G., Leib, S.E., and Schoene, B., 2019, Evidence for the initiation of the Nevadan orogeny from partial melting of Rattlesnake Creek amphibolite, Klamath Mountains: Geological Society of America Abstracts with Programs, v. 51, no. 5, https://doi.org/10.1130/ abs/2019AM-336495.
- Darby, B.J., Wyld, S.J., and Gehrels, G.E., 2000, Provenance and paleogeography of the Black Rock terrane, northwestern Nevada, in Soreghan, M.J., and Gehrels, G.E., eds., Paleozoic and Triassic Paleogeography and Tectonics of Western Nevada and Northern California: Geological Society of America Special Paper 347, p. 77–88, https://doi.org/10.1130/0-8137-2347-7.77.
- Davis, G.A., 1968, Westward thrust faulting in the south-central Klamath Mountains, California: Geological Society of America Bulletin, v. 79, p. 911–934, https://doi.org/10.1130/0016-7606(1968)79[911:WTFITS]2.0.CO;2.
- Dick, H.J.B., 1976, The origin and emplacement of the Josephine Peridotite of southwestern Oregon [Ph.D. dissertation]: New Haven, Connecticut, Yale University, 409 p.
- Dickinson, W.R., 1970, Relations of andesites, granites, and derivative sandstones to arc-trench tectonics: Reviews of Geophysics and Space Physics, v. 8, p. 813–860, https://doi.org/10.1029/RG008i004p00813.
- Dickinson, W.R., 2000, Geodynamic interpretation of Paleozoic tectonic trends oriented oblique to the Mesozoic Klamath-Sierran continental margin in California, in Soreghan, M.J., and Gehrels, G.E., eds., Paleozoic and Triassic Paleogeography and Tectonics of Western Nevada and Northern California: Geological Society of America Special Paper 347, p. 209–245, https://doi.org/10.1130/0-8137-2347-7.209.
- Dickinson, W.R., 2004, Evolution of the North American Cordillera: Annual Review of Earth and Planetary Sciences, v. 32, p. 13–45, https://doi.org/ 10.1146/annurev.earth.32.101802.120257.

- Dickinson, W.R., and Gehrels, G.E., 2003, U-Pb ages of detrital zircons from Permian and Jurassic eolian sandstones of the Colorado Plateau, USA: Paleogeographic implications: Sedimentary Geology, v. 163, p. 29–66, https://doi.org/10.1016/S0037-0738(03)00158-1.
- Dickinson, W.R., and Gehrels, G.E., 2008, U-Pb ages of detrital zircons in Jurassic eolian and associated sandstones of the Colorado Plateau: Evidence for transcontinental dispersal and intraregional recycling of sediment: Geological Society of America Bulletin, v. 121, p. 408–433, https:// doi.org/10.1130/B26406.1.
- Dickinson, W.R., and Gehrels, G.E., 2009, Use of U-Pb ages of detrital zircons to infer maximum depositional ages of strata: A test against a Colorado Plateau Mesozoic database: Earth and Planetary Science Letters, v. 288, p. 115–125, https://doi.org/10.1016/j.epsl.2009.09.013.
- Dickinson, W.R., Hopson, C.A., and Saleeby, J.B., 1996, Alternate origins of the Coast Range ophiolite (California): Introduction and implications: GSA Today, v. 6, no. 2, p. 1–10.
- Diller, J.S., 1914, Mineral resources of southwestern Oregon: U.S. Geological Survey Bulletin 546, 147 p.
- Donato, M., Coleman, R., and Kays, M., 1980, Geology of the Condrey Mountain Schist, northern Klamath Mountains, California and Oregon: Oregon Geology, v. 42, no. 2, p. 125–129.
- Donato, M.M., Barnes, C.G., and Tomlinson, S.L., 1996, The enigmatic Applegate Group of southwestern Oregon: Age, correlation, and tectonic affinity: Oregon Geology, v. 58, p. 79–91.
- Dott, R.H., 1971, Geology of the Southwestern Oregon Coast West of the 124th Meridian: Portland, Oregon Department of Geology and Mineral Industries Bulletin, no. 69, 63 p.
- Ducea, M.N., and Chapman, A.D., 2018, Sub-magmatic arc underplating by trench and forearc materials in shallow subduction systems: A geologic perspective and implications: Earth-Science Reviews, v. 185, p. 763–779, https://doi.org/10.1016/j.earscirev.2018.08.001.
- Dumitru, T.A., Wright, J.E., Wakabayashi, J., and Wooden, J.L., 2010, Early Cretaceous transition from nonaccretionary behavior to strongly accretionary behavior within the Franciscan subduction complex: Tectonics, v. 29, TC5001, https://doi.org/10.1029/2009TC002542.
- Dumitru, T.A., Ernst, W.G., Wright, J.E., Wooden, J.L., Wells, R.E., Farmer, L.P., Kent, A.J., and Graham, S.A., 2013, Eocene extension in Idaho generated massive sediment floods into the Franciscan trench and into the Tyee, Great Valley, and Green River basins: Geology, v. 41, no. 2, p. 187–190, https://doi.org/10.1130/G33746.1.
- Dumitru, T.A., Ernst, W.G., Hourigan, J.K., and McLaughlin, R.J., 2015, Detrital zircon U–Pb reconnaissance of the Franciscan subduction complex in northwestern California: International Geology Review, v. 57, p. 767–800, https://doi.org/10.1080/00206814.2015.1008060.
- Dumitru, T.A., Hourigan, J.K., Elder, W.P., Ernst, W.G., Joesten, R., Ingersoll, R.V., Lawton, T.F., and Graham, S.A., 2018, New, much younger ages for the Yolla Bolly terrane and a revised time line for accretion in the Franciscan subduction complex, California, in Ingersoll, R.V., Lawton, T.F., and Graham, S.A., eds., Tectonics, Sedimentary Basins, and Provenance: A Celebration of William R. Dickinson's Career: Geological Society of America Special Paper 540, p. 339–366, https://doi.org/10.1130/2018.2540(15).
- Engebretson, D.C., Cox, A., and Thompson, G.A., 1984, Correlation of plate motions with continental tectonics: Laramide to Basin-Range: Tectonics, v. 3, no. 2, p. 115–119, https://doi.org/10.1029/TC003i002p00115.
- Ernst, W.G., 1970, Tectonic contact between the Franciscan mélange and the Great Valley sequence—Crustal expression of a late Mesozoic Benioff zone: Journal of Geophysical Research, v. 75, p. 886–901, https://doi.org/10.1029/JB075i005p00886.
- Ernst, W.G., 1971, Metamorphic zonations on presumably subducted lithospheric plates from Japan, California and the Alps: Contributions to Mineralogy and Petrology v. 34, p. 43–59, https://doi.org/10.1007/bf00376030.
- Ernst, W.G., 1975, Systematics of large-scale tectonics and age progressions in Alpine and Circum-Pacific blueschist belts: Tectonophysics, v. 26, p. 229–246, https://doi.org/10.1016/0040-1951(75)90092-X.
- Ernst, W.G., 1990, Accretionary terrane in the Sawyers Bar area of the Western Triassic and Paleozoic Belt, central Klamath Mountains, northern California, *in* Harwood, D. S., and Miller, M.M., eds., Paleozoic and Early Mesozoic Paleogeographic Relations: Sierra Nevada, Klamath Mountains, and Related Terranes: Geological Society of America Special Paper 225, p. 297–306, https://doi.org/10.1130/SPE255-p297.

- Ernst, W.G., 2013, Earliest Cretaceous Pacificward offset of the Klamath Mountains salient, NW California–SW Oregon: Lithosphere, v. 5, p. 151–159, https://doi.org/10.1130/L247.1.
- Ernst, W.G., 2017, Geologic evolution of a Cretaceous tectonometamorphic unit in the Franciscan Complex, western California: International Geology Review, v. 59, no. 5–6, p. 563–576, https://doi.org/10.1080/00206814.2016.1201440.
- Ernst, W.G., Martens, U., and Valencia, V., 2009, U-Pb ages of detrital zircons in Pacheco Pass metagraywackes: Sierran-Klamath source of mid-Cretaceous and Late Cretaceous Franciscan deposition and underplating: Tectonics, v. 28, no. 6, https://doi.org/10.1029/2008TC002352.
- Ernst, W.G., Wu, C., Lai, M., and Zhang, X., 2017, U-Pb ages and sedimentary provenance of detrital zircons from eastern Hayfork meta-argillites, Sawyers Bar area, northwestern California: The Journal of Geology, v. 125, p. 33–44, https://doi.org/10.1086/689186.
- Evitt, W.R., and Pierce, S.T., 1975, Early Tertiary ages from the coastal belt of the Franciscan complex, northern California: Geology, v. 3, no. 8, p. 433–436, https://doi.org/10.1130/0091-7613(1975)3<433:ETAFTC>2 .0.CO;2.
- Festa, A., Pini, G.A., Dilek, Y., and Codegone, G., 2010, Mélanges and mélange-forming processes: A historical overview and new concepts: International Geology Review, v. 52, no. 10–12, p. 1040–1105, https://doi.org/10.1080/00206810903557704.
- Frost, C.D., Barnes, C.G., and Snoke, A.W., 2006, Nd and Sr isotopic data from argillaceous rocks of the Galice Formation and Rattlesnake Creek Terrane, Klamath Mountains: Evidence for the input of Precambrian sources, in Snoke, A.W., and Barnes, C.G., eds., Geological Studies in the Klamath Mountains Province, California and Oregon: A Volume in Honor of William P. Irwin: Geological Society of America Special Paper 410, p. 103–120, https://doi.org/10.1130/2006.2410(05).
- Garcia, M.O., 1979, Petrology of the Rogue and Galice formations, Klamath Mountains, Oregon: Identification of a Jurassic island-arc sequence: The Journal of Geology, v. 87, p. 29–41, https://doi.org/10.1086/628389.
- Garcia, M.O., 1982, Petrology of the Rogue River island-arc complex, south-west Oregon: American Journal of Science, v. 282, p. 783–807, https://doi.org/10.2475/ajs.282.6.783.
- Garlick, S.R., Medaris, L.G., Jr., Snoke, A.W., Schwartz, J.J., and Swapp, S.M., 2009, Granulite- to amphibolite-facies metamorphism and penetrative deformation in a disrupted ophiolite, Klamath Mountains, California: A deep view into the basement of an accreted oceanic arc, in Miller, R.B., and Snoke, A.W., eds., Crustal Cross Sections from the Western North American Cordillera and Elsewhere: Implications for Tectonic and Petrologic Processes: Geological Society of America Special Paper 456, p. 151–186, https://doi.org/10.1130/2009.2456(06).
- Gaschnig, R., Macho, A.S., Fayon, A., Schmitz, M., Ware, B.D., Vervoort, J., Kelso, P., LaMaskin, T.A., Kahn, M.J., and Tikoff, B., 2017, Intrusive and depositional constraints on the Cretaceous tectonic history of the southern Blue Mountains, eastern Oregon: Lithosphere, v. 9, p. 265–282 https:// doi.org/10.1130/L554.1.
- Gates, K., Yoshinobu, A., Barnes, C.G., Dailey, S.R., and Leib, S., 2019, Inverted metamorphic gradients and cryptic contacts surrounding the enigmatic Condrey Mountain dome, Klamath Mountain province, CA and OR: Geological Society of America Abstracts with Programs, v. 51, no. 4, https://doi.org/10.1130/abs/2019CD-329660.
- Gehrels, G.E., and Miller, M.M., 2000, Detrital zircon geochronologic study of Upper Paleozoic strata in the eastern Klamath terrane, northern California, in Soreghan, M.J., and Gehrels, G.E., eds., Paleozoic and Triassic Paleogeography and Tectonics of Western Nevada and Northern California: Geological Society of America Special Paper 347, p. 99–108, https:// doi.org/10.1130/0-8137-2347-7.99.
- Gehrels, G.E., and Pecha, M., 2014, Detrital zircon U-Pb geochronology and Hf isotope geochemistry of Paleozoic and Triassic passive margin strata of western North America: Geosphere, v. 10, p. 49–65, https://doi.org/10.1130/GES00889.1.
- Goodge, J.W., 1989, Polyphase metamorphic evolution of a Late Triassic subduction complex, Klamath Mountains, northern California: American Journal of Science, v. 289, p. 874–943, https://doi.org/10.2475/ ajs.289.7.874.
- Gray, G.G., 1985, Structural, geochronologic, and depositional history of the western Klamath Mountains, California and Oregon: Implications for the early to middle Mesozoic tectonic evolution of the western North American Cordillera [Ph.D. dissertation]: Austin, University of Texas, 224 p.

Gray, G.G., 1986, Native terranes of the central Klamath Mountains, California: Tectonics, v. 5, p. 1043–1054, https://doi.org/10.1029/TC005i007p01043.

- Gray, G.G., 2006, Structural and tectonic evolution of the western Jurassic belt along the Klamath River corridor, Klamath Mountains, California, in Snoke, A.W., and Barnes, C.G., eds., Geological Studies in the Klamath Mountains province, California and Oregon: A Volume in Honor of William P. Irwin: Geological Society of America Special Paper 410, p. 141–151, https://doi.org/10.1130/2006.2410(07).
- Gribble, R.F., Barnes, C.G., Donato, M.M., Hoover, J.D., and Kistler, R.W., 1990, Geochemistry and intrusive history of the Ashland pluton, Klamath Mountains, California and Oregon: Journal of Petrology, v. 31, p. 883– 923, https://doi.org/10.1093/petrology/31.4.883.
- Grove, M., Gehrels, G.E., Cotkin, S.J., Wright, J.E., and Zou, H., 2008, Non-Laurentian cratonal provenance of Late Ordovician eastern Klamath blue-schists and a link to the Alexander terrane, in Wright, J.E., and Shervais, J.W., eds., Ophiolites, Arcs, and Batholiths: A Tribute to Cliff Hopson: Geological Society of America Special Paper 438, p. 223–250, https://doi.org/10.1130/2008.2438(08).
- Hacker, B., and Ernst, W.G., 1993, Jurassic orogeny in the Klamath Mountains: A geochronological analysis, in Dunn, G., and McDougall, K., eds., Mesozoic Paleogeography of the Western United States–II: California, Society of Economic Paleontologists and Mineralogists, Pacific Section 71, p. 37–60.
- Hacker, B.R., Donato, M.M., Barnes, C.G., McWilliams, M.O., and Ernst, W.G., 1995, Timescales of orogeny: Jurassic construction of the Klamath Mountains: Tectonics, v. 14, p. 677–703, https://doi.org/10.1029/94TC02454.
- Harms, T., Jayko, A.S., and Blake, M.C., 1992, Kinematic evidence for extensional unroofing of the Franciscan complex along the Coast Range fault, northern Diablo Range, California: Tectonics, v. 11, p. 228–241, https://doi.org/10.1029/91TC01880.
- Harper, G.D., 1980, The Josephine ophiolite-remains of a late Jurassic marginal basin in northwestern California: Geology, v. 8, p. 333–337, https://doi. org/10.1130/0091-7613(1980)8<333:TJOOAL>2.0.CO;2.
- Harper, G.D., 1982, Evidence for large-scale rotations at spreading centers from the Josephine ophiolite: Tectonophysics, v. 82, p. 25–44.
- Harper, G.D., 1984, The Josephine ophiolite: Geological Society of America Bulletin, v. 95, p. 1009–1026, https://doi.org/10.1130/0016-7606 (1984)95<1009:TJONC>2.0.CO;2.
- Harper, G.D., 1989, Field guide to the Josephine ophiolite and coeval island arc complex, Oregon-California, in Aalto, K.R., and Harper, G.D., eds., Geologic Evolution of the Northernmost Coast Ranges and Western Klamath Mountains, California, 28th Geological Congress Field Trip Guidebook T308: Washington, D.C., American Geophysical Union, p. 2–21.
- Harper, G.D., 2003, Fe-Ti basalts and propagating rift tectonics in the Josephine ophiolite: Geological Society of America Bulletin, v. 115, p. 771–787, https://doi.org/10.1130/0016-7606(2003)115<0771:FBAPTI>2.0.CO;2.
- Harper, G.D., 2006, Structure of syn-Nevadan dikes and their relationship to deformation of the Galice Formation, western Klamath terrane, northwestern California, in Snoke, A.W., and Barnes, C.G., eds., Geological Studies in the Klamath Mountains Province, California and Oregon: A Volume in Honor of William P. Irwin: Geological Society of America Special Paper 410, p. 121–140, https://doi.org/10.1130/2006.2410(06).
- Harper, G.D., and Wright, J.E., 1984, Middle to Late Jurassic tectonic evolution of the Klamath Mountains, California-Oregon: Tectonics, v. 3, p. 759– 772, https://doi.org/10.1029/TC003i007p00759.
- Harper, G.D., Bowman, J.R., and Kuhns, R., 1988, Field, chemical, and isotopic aspects of submarine hydrothermal metamorphism of the Josephine ophiolite, Klamath Mountains, California-Oregon: Journal of Geophysical Research, v. 93, p. 4625–4657.
- Harper, G.D., Saleeby, J.B., and Heizler, M., 1994, Formation and emplacement of the Josephine ophiolite, and the age of the Nevadan orogeny in the Klamath Mountains, California-Oregon: U/Pb zircon and ⁴⁰Ar/³⁹Ar geochronology: Journal of Geophysical Research, v. 99, p. 4293–4321, https://doi.org/10.1029/93JB02061.
- Harper, G.D., Giaramita, M.J., and Kosanke, S.B., 2002, Josephine and Coast Range Ophiolites, Oregon and California, in Moore, G.W., ed., Field Guide to the Geologic Processes in Cascadia: Field Trips to Accompany the 98th Annual Meeting of the Cordilleran Section of the Geological Society of America: Portland, Oregon Department of Geology and Mineral Industries Special Paper 36, p. 1–22.
- Helper, M., 1985, Structural, metamorphic and geochronologic constrains on the origin of the Condrey Mountain Schist, north central Klamath Moun-

- tains, northern California [Ph.D. dissertation]: University of Texas at Austin, 209 p.
- Helper, M.A., 1986, Deformation and high P/T metamorphism in the central part of the Condrey Mountain window, north-central Klamath Mountains, California and Oregon, *in* Evans, B.W., and Brown, E.H., eds., Blueschists and Eclogites: Geological Society of America Memoir 164, p. 125–141, https://doi.org/10.1130/MEM164-p125.
- Hill, L.B., 1984, A tectonic and metamorphic history of the north-central Klamath Mountains, California [Ph.D. thesis]: Stanford University, 248 p.
- Hopson, C.A., and Pessagno, E.A., Jr., 2005, Tehama-Colusa serpentinite mélange: A remnant of Franciscan Jurassic oceanic lithosphere, northern California: International Geology Review, v. 47, p. 65–100, https://doi.org/10.2747/0020-6814.47.1.65.
- Hopson, C.A., Mattinson, J.M., Pessagno, E.A., Jr., and Luyendyk, B.P., 2008, California Coast Range ophiolite: Composite Middle and Late Jurassic oceanic lithosphere, in Wright, J.E., and Shervais, J.W., eds., Ophiolites, Arcs, and Batholiths: A Tribute to Cliff Hopson: Geological Society of America Special Paper 438, p. 1–101, https://doi.org/ 10.1130/2008.2438(01).
- Hotz, P.E., 1971, Geology of lode gold districts in the Klamath Mountains, California and Oregon: U.S. Geological Survey Bulletin, v. 1290, 91 p.
- Hotz, P.E., 1977, Geology of the Yreka quadrangle, Siskiyou County, California: U.S. Geological Survey Bulletin 1436, 72 p.
- Hotz, P.E., 1979, Regional metamorphism in the Condrey Mountain quadrangle, north-central Klamath Mountains, California: U.S. Geological Survey Professional Paper 1086, 25 p., https://doi.org/10.3133/pp1086.
- Hsü, K.J., 1968, The principles of melanges and their bearing on the Franciscan-Knoxville paradox: Geological Society of America Bulletin, v. 79, p. 1063–1074, https://doi.org/10.1130/0016-7606(1968)79[1063:POMATB]2.0.CO;2.
- Imlay, R.W., Dole, H.M., Peck, D.L., and Wells, F.G., 1959, Relations of certain Upper Jurassic and Lower Cretaceous formations in southwestern Oregon: The American Association of Petroleum Geologists Bulletin, v. 43, p. 2770–2785.
- Ingersoll, R.V., 1982, Initiation and evolution of the Great Valley forearc basin of northern and central California, USA, in Leggett, J.K., ed., Trenchforearc Geology: Sedimentation and Tectonics on Modern and Ancient Active Plate Margins: Geological Society, London, Special Publications 10, p. 459–467.
- Ingersoll, R.V., and Dickinson, W.R., 1990, Great Valley Group (Sequence), Sacramento, California, in Ingersoll, R.V., and Nilsen, T.H., eds., Sacramento Valley Symposium and Guidebook: Pacific Section, Society of Economic Paleontologists and Mineralogists, p. 183–215.
- Ingersoll, R.V., Rich, E.I., and Dickinson, W.R., 1977, Field Guide: Great Valley Sequence, Sacramento Valley, Field Trip no. 8: Geological Society of America, Cordilleran Section, Guidebook for Field Trips, 73rd annual meeting, Sacramento, California, 5–7 April, 72 p.
- Irwin, W.P., 1960, Geological reconnaissance of the northern Coast Ranges and Klamath Mountains, California, with a summary of the mineral resources: California Division Mines Bulletin 179, 80 p.
- Irwin, W.P., 1966, Geology of the Klamath Mountains province, in Bailey, E.H., ed., Geology of Northern California: California Division of Mines Bulletin 190, p. 19–38.
- Irwin, W.P., 1972, Terranes of the western Paleozoic and Triassic belt in the southern Klamath Mountains, California, in Geological Survey Research, 1972, Chapter C: U.S. Geological Survey Professional Paper 800-C, p. C103–C111, https://doi.org/10.3133/pp800C.
- Irwin, W.P., 1994, Geologic map of the Klamath Mountains, California and Oregon: U.S. Geological Survey Miscellaneous Field Investigations I-2148, scale 1:500,000.
- Irwin, W.P., 1997, Preliminary map of selected post-Nevadan geologic features of the Klamath Mountains and adjacent areas, California and Oregon: U.S. Geological Survey Open-File Report 97-465, scale 1:500,000, with 29 p. pamphlet.
- Irwin, W.P., 2003, Correlation of the Klamath Mountains and Sierra Nevada: U.S. Geological Survey Open-File Report 02-490, 2 map sheets, https://pubs.usgs.gov/of/2002/0490/.
- Irwin, W.P., 2010, Reconnaissance geologic map of the Hyampom 15' quadrangle, Trinity County, California: U.S. Geological Survey Scientific Investigations Map 3129, scale 1:50,000, 1 map sheet.
- Irwin, W.P., and Blome, C.D., 2004, Fossil Localities of the Rattlesnake Creek, Western and Eastern Hayfork, and North Fork Terranes of the Klamath

- Mountains: U.S. Geological Survey Open-File Report 2004-1094, 1 sheet, 50 p.
- Irwin, W.P., and Wooden, J.L., 1999, Plutons and accretionary episodes of the Klamath Mountains, California and Oregon: U.S. Geological Survey Open-File Report 99-374, 1 sheet, https://pubs.usgs.gov/of/1999/0374/.
- Irwin, W.P., Jones, D.L., and Blome, C.D., 1982, Map showing sampled radiolarian localities in the western Paleozoic and Triassic belt, Klamath Mountains, California: U.S. Geological Survey Miscellaneous Field Studies Map 1399, scale 1:250,000, https://doi.org/10.3133/mf1399.
- Irwin, W.P., Yule, J.D., Court, B.L., Snoke, A.W., Stern, L.A., and Copeland, W.B., 2011, Reconnaissance geologic map of the Dubakella Mountain 15' Quadrangle, Trinity, Shasta, and Tehama Counties, California: U.S. Geological Survey Scientific Investigations Map 3149, scale 1:50,000, 1 map sheet, https://doi.org/10.3133/sim3149.
- Jayko, A.S., 1996, Reconnaissance geologic map of the Lane Mountain 7.5' quadrangle, Oregon: U.S. Geological Survey Open-File Report 95-20, 1 plate.
- Jayko, A.S., and Blake, M.C., Jr., 1989, Deformation of the Eastern Franciscan belt, northern California: Journal of Structural Geology, v. 11, no. 4, p. 375–390, https://doi.org/10.1016/0191-8141(89)90016-3.
- Jayko, A.S., and Blake, M.C., Jr., 1993, Northward displacements of forearc slivers in the Coast Ranges of California and southwest Oregon during the late Mesozoic and early Cenozoic, in Dunne, G.C., and McDougall, K.A., eds., Mesozoic Paleogeography of the Western United States–II: Los Angeles, Pacific Section, Society of Economic Paleontologist and Mineralogists, Book 71, p. 19–36.
- Jayko, A.S., Blake, M.C., Jr., and Brothers, R.N., 1986, Blueschist metamorphism of the Eastern Franciscan belt, northern California, in Evans, B.W., and Brown, E.H., Blueschists and Eclogites: Geological Society of America Memoir 164, p. 107–124, https://doi.org/10.1130/MEM164-p107.
- Jayko, A.S., Blake, M.C., and Harms, T., 1987, Attenuation of the Coast Range ophiolite by extensional faulting, and nature of the Coast Range "thrust," California: Tectonics, v. 6, no. 4, p. 475–488, https://doi.org/10.1029/TC006i004p00475.
- Johnston, S.T., and Borel, G.D., 2007, The odyssey of the Cache Creek terrane, Canadian Cordillera: Implications for accretionary orogens, tectonic setting of Panthalassa, the Pacific superwell, and break-up of Pangea: Earth and Planetary Science Letters, v. 253, p. 415–428, https://doi.org/10.1016/j.epsl.2006.11.002.
- Jones, D.L., 1969, Buchia zonation in the Myrtle Group, southwestern Oregon: Geological Society of America Abstracts with Programs, v. 65, p. 31–32.
- Jones, D.L., and Irwin, W.P., 1971, Structural implications of an offset Early Cretaceous shoreline in northern California: Geological Society of America Bulletin, v. 82, p. 815–822, https://doi.org/10.1130/0016-7606 (1971)82[815:SIOAOE]2.0.CO;2.
- Jorgenson, D.B., 1970, Petrology and origin of the Illinois River Gabbro, a part of the Josephine Peridotite-Gabbro Complex, Klamath Mountains, southwestern Oregon [Ph.D. dissertation]: University of California, Santa Barbara, 195 p.
- Katrib, J., 2005, Source of meta-igneous blocks and structure of the Colebrooke Schist in the Snowcamp Peak area, Pickett Peak terrane, southwestern Oregon [Master's thesis]: University at Albany, State University of New York, 125 p.
- Kays, M.A., 1968, Zones of alpine tectonism and metamorphism, Klamath Mountains, southwestern Oregon: The Journal of Geology, v. 76, p. 17–36, https://doi.org/10.1086/627306.
- Kays, M.A., and Ferns, M.L., 1980, Geologic field trip guide through the northcentral Klamath Mountains: Oregon Geology, v. 42, no. 2, p. 23–35.
- Kelsey, H.M., and Bockheim, J.G., 1994, Coastal landscape evolution as a function of eustasy and surface uplift rate, Cascadia margin, southern Oregon: Geological Society of America Bulletin, v. 106, no. 6, p. 840–854, https://doi.org/10.1130/0016-7606(1994)106<0840:CLEAAF>2.3.CO;2.
- Klapper, M., and Chapman, A., 2017, Inverted metamorphism of the Condrey Mountain schist (northern California/southern Oregon): A ~30 myr record of subduction initiation and maturation beneath a cooling upper plate: Geological Society of America Abstracts with Programs, v. 49, no. 4, https://doi.org/10.1130/abs/2017CD-292952.
- Klein, C.W., 1977, Thrust plates of the north-central Klamath Mountains near Happy Camp, California: California Division of Mines and Geology, Special Publication, v. 28, p. 23–26.
- Knittel, U., Suzuki, S., Nishizaka, N., and Lee, Y.-H., 2014, U-Pb ages of detrital zircons from the Sanbagawa Belt in western Shikoku: Additional evidence for the prevalence of Late Cretaceous protoliths of the Sanbagawa Metamorphics: Journal of Asian Earth Sciences, v. 96, p. 148–161, https:// doi.org/10.1016/j.jseaes.2014.09.001.

- Koch, J.G., 1966, Late Mesozoic stratigraphy and tectonic history, Port Orford-Gold Beach area, southwestern Oregon coast: American Association of Petroleum Geologists Bulletin, v. 50, no. 1, p. 25–71.
- Krueger, S.W., and Jones, D.L., 1989, Extensional fault uplift of regional Franciscan blueschists die to subduction shallowing during the Laramide orogeny: Geology, v. 17, no. 12, p. 1157–1159, https://doi.org/10.1130/0091-7613(1989)017<1157:EFUORF>2.3.CO;2.
- Lanphere, M.A., Irwin, W.P., and Hotz, P.E., 1968, Isotopic age of the Nevadan orogeny and older plutonic and metamorphic events in the Klamath Mountains, California: Geological Society of America Bulletin, v. 79, p. 1027–1052, https://doi.org/10.1130/0016-7606(1968)79[1027:IAOTNO]2.0.CO;2.
- Lanphere, M.A., Blake, M.C., and Irwin, W.P., 1978, Early Cretaceous metamorphic age of the South Fork Mountain schist in the northern Coast Ranges of California: American Journal of Science, v. 278, no. 6, p. 798– 815, https://doi.org/10.2475/ajs.278.6.798.
- LaMaskin, T.A., Vervoort, J.D., Dorsey, R.J., and Wright, J.E., 2011, Early Mesozoic paleogeography and tectonic evolution of the western United States: Insights from detrital zircon U-Pb geochronology, Blue Mountains Province, northeastern Oregon: Geological Society of America Bulletin, v. 123, p. 1939–1965, https://doi.org/10.1130/B30260.1.
- LaMaskin, T.A., Rivas, J.A., Barbeau, D.L., Schwartz, J.J., Russell, J.A., and Chapman, A.D., 2021, A crucial geologic test of Late Jurassic exotic collision versus endemic re-accretion in the Klamath Mountains province, western United States, with implications for the assembly of western North America: Geological Society of America Bulletin, https://doi.org/ 10.1130/B35981.1.
- Liner, N., 2005, A paleomagnetic paleolatitude determination from the Upper Cretaceous units of the Gold Beach Terrane, southwest coastal Oregon [Master's thesis]: Bellingham, Western Washington University, 101 p.
- Loney, R.A., and Himmelberg, G.R., 1977, The geology of the gabbroic complex along the northern border of the Josephine peridotite, Vulcan Peak area, southwestern Oregon: Journal of Research of the U.S. Geological Survey, v. 5, p. 761–781.
- Lund, K., and Snee, L.W., 1988, Metamorphism, structural development, and age of the continent-island arc juncture in west-central Idaho, in Ernst, W.G., ed., Metamorphism and Crustal Evolution of the Western United States—Rubey Volume III: Englewood Cliffs, New Jersey, Prentice Hall, p. 297–331.
- MacDonald, J.H., Jr., Harper, G.D., and Zhu, B., 2006, Petrology, geochemistry, and provenance of the Galice Formation, Klamath Mountains, Oregon and California, in Snoke, A.W., and Barnes, C.G., eds., Geological Studies in the Klamath Mountains Province, California and Oregon: A Volume in Honor of William P. Irwin: Geological Society of America Special Paper 410, p. 77–101, https://doi.org/10.1130/2006.2410(04).
- Manuszak, J.D., Satterfield, J.I., and Gehrels, G.E., 2000, Detrital-zircon geochronology of Upper Triassic strata in western Nevada, in Soreghan, M.J., and Gehrels, G.E., eds., Paleozoic and Triassic Paleogeography and Tectonics of Western Nevada and Northern California: Geological Society of America Special Paper 347, p. 109–118, https://doi.org/10.1130/0-8137-2347-7.109.
- Mattinson, J.M., 1986, Geochronology of high-pressure-low-temperature Franciscan metabasites: A new approach using the U-Pb system, in Evans, B.W., and Brown, E.H., eds., Blueschists and Eclogites: Geological Society of America Memoir 164, p. 95–105, https://doi.org/10.1130/ MEM164-p95.
- Mauel, D.J., Lawton, T.F., González-León, C., Iriondo, A., and Amato, J.M., 2011, Stratigraphy and age of Upper Jurassic strata in north-central Sonora, Mexico: Southwestern Laurentian record of crustal extension and tectonic transition: Geosphere, v. 7, p. 390–414, https://doi.org/10.1130/ GES00600 1
- Maxwell, J.C., 1974, Anatomy of an orogen: Address as retiring president of the Geological Society of America, Dallas, Texas, November 1973: Geological Society of America Bulletin, v. 85, no. 8, p. 1195–1204, https://doi.org/10.1130/0016-7606(1974)85<1195:AOAO>2.0.CO;2.
- McClaughry, J.D., Ma, L., Jones, C.B., Mickelson, K.A., and Wiley, T.J., 2013, Geologic map of the southwestern Oregon coast between Crook Point and Port Orford, Curry County, Oregon: Oregon Department of Geology and Mineral Industries, Open-file Report O-13-21, scale 1:24,000.
- McClelland, W.C., Gehrels, G.E., and Saleeby, J.B., 1992, Upper Jurassic–lower Cretaceous basinal strata along the Cordilleran margin: Implications for the accretionary history of the Alexander-Wrangellia-Peninsular terrane: Tectonics, v. 11, p. 823–835, https://doi.org/10.1029/92TC00241.

McDougall, I., and Harrison, T.M., 1999, Geochronology and Thermochronology by the ⁴⁰Ar/³⁹Ar Method, 2nd edition: New York, Oxford University Press, 288 p.

- McDowell, F.W., Lehman, D.H., Gucwa, P.R., Fritz, D., and Maxwell, J.C., 1984, Glaucophane schists and ophiolites of the northern California Coast Ranges: Isotopic ages and their tectonic implications: Geological Society of America Bulletin, v. 95, no. 11, p. 1373–1382, https://doi.org/10.1130/0016-7606(1984)95<1373:GSAOOT>2.0.CO;2.
- McKnight, B.K., 1984, Stratigraphy and sedimentology of the Payne Cliffs Formation, southwestern Oregon, in Nilsen, T.H., ed., Geology of the Upper Cretaceous Hornbrook Formation, Oregon and California: Pacific Section, Society of Economic Paleontologists and Mineralogists, v. 42, p. 187–194.
- McLachlin, B.R., 2011, Petrology of the Chetco Complex, Klamath Mountains, Oregon [Master's thesis]: Lubbock, Texas Tech University, 101 p.
- Medaris, L.G., Jr., 1966, Geology of the Seiad Valley area, Siskiyou County, California, and petrology of the Seiad ultramafic complex [Ph.D. thesis]: University of California, Los Angeles, 333 p.
- Medaris, L.G., Jr., 1972, High-pressure peridotites in southwestern Oregon: Geological Society of America Bulletin, v. 83, no. 1, p. 41–58, https://doi.org/10.1130/0016-7606(1972)83[41:HPISO]2.0.CO;2.
- Miller, J.S., Miller, R.B., Wooden, J.L., and Harper, G.D., 2003, Geochronologic links between the Ingalls Ophiolite, North Cascades, Washington and the Josephine Ophiolite, Klamath Mts., Oregon and California: Geological Society of America Abstracts with Programs, v. 35, no. 6, p. 113.
- Miller, M.M., and Saleeby, J.B., 1995, U-Pb geochronology of detrital zircon from Upper Jurassic synorogenic turbidites, Galice Formation, and related rocks, western Klamath Mountains: Correlation and Klamath Mountains provenance: Journal of Geophysical Research, v. 100, B9, p. 18,045–18,058, https://doi.org/10.1029/95JB00761.
- Moores, E.M., 1970, Ultramafics and orogeny, with models of the US Cordillera and the Tethys: Nature, v. 228, p. 837–842, https://doi.org/10.1038/228837a0.
- Mortimer, N., and Coleman, R.G., 1985, A Neogene structural dome in the Klamath Mountains, California: Geology, v. 13, p. 253–256, https://doi.org/10.1130/0091-7613(1985)13<253:ANSDIT>2.0.CO;2.
- Mulcahy, S.R., Starnes, J.K., Day, H.W., Coble, M.A., and Vervoort, J.D., 2018, Early onset of Franciscan subduction: Tectonics, v. 37, no. 5, p. 1194– 1209, https://doi.org/10.1029/2017TC004753.
- Murchey, B.M., and Blake, M.C., Jr., 1993, Evidence for subduction of a major ocean plate along the California margin during the middle to early late Jurassic, in Dunn, G., and McDougall, K., eds., Mesozoic Paleogeography of the Western United States–II: Los Angeles, California, Pacific Section, Society of Economic Paleontologists and Mineralogists, v. 71, p. 1–18.
- Nilsen, T.H., ed., 1984, Geology of the Upper Cretaceous Hornbrook Formation, Oregon and California: Pacific Section, Society of Economic Paleontologists and Mineralogists, v. 42, p.129–132.
- Norman, E.A.S., 1984, The structure and petrology of the Summit Valley area, Klamath Mountains, California [M.S. thesis]: Salt Lake City, University of Utah. 148 p.
- Ohr, M., 1987, Geology, geochemistry and geochronology of the Lems Ridge olistostrome, Klamath Mountains, California [M.S. thesis]: State University of New York, Albany, 278 p.
- Page, N.J., Gray, F., Cannon, J.K., Foose, M.P., Lipin, B., Moring, B.C., Nicholson, S.W., Sawline, M.G., Till, A., and Ziemianski, W.P., 1981, Geologic map of the Kalmiopsis wilderness area, Oregon: U.S. Geological Survey Miscellaneous Field Studies Map 1240A, scale 1:62,500, https://doi.org/10.3133/mf1240A.
- Pearce, J.A., Lippard, S.J., and Roberts, S., 1984, Characteristics and tectonic significance of suprasubduction zone ophiolites, *in* Kokelaar, B.P., and Howells, M.F., eds., Marginal Basin Geology: Geological Society, London, Special Publication 16, p. 77–94.
- Pessagno, E.A., Jr., 2006, Faunal evidence for the tectonic transport of Jurassic terranes in Oregon, California, and Mexico, in Snoke, A.W., and Barnes, C.G., eds., Geological Studies in the Klamath Mountains Province, California and Oregon: A Volume in Honor of William P. Irwin: Geological Society of America Special Paper 410, p. 31–52, https://doi.org/10.1130/2006.2410(02).
- Pessagno, E.A., Jr., and Blome, C.D., 1990, Implications of new Jurassic stratigraphic, geochronometric, and paleolatitudinal data from the western Klamath terrane (Smith River and Rogue Valley subterranes): Geology,

- v. 18, p. 665–668, https://doi.org/10.1130/0091-7613(1990)018<0665 :IONJSG>2.3.CO:2.
- Plake, T.D., 1989, Structure and Petrology of the Colebrooke Schist, Southwestern Oregon [Ph.D. thesis]: Bellingham, Western Washington University.
- Platt, J.P., 1975, Metamorphic and deformational processes in the Franciscan Complex, California: Some insights from the Catalina Schist terrane: Geological Society of America Bulletin, v. 86, no. 10, p. 1337–1347, https://doi.org/10.1130/0016-7606(1975)86<1337:MADPIT>2.0.CO;2.
- Platt, J.P., 1986, Dynamics of orogenic wedges and the uplift of high-pressure metamorphic rocks: Geological Society of America Bulletin, v. 97, no. 9, p. 1037–1053, https://doi.org/10.1130/0016-7606(1986)97<1037:DOOWAT>2.0.CO;2.
- Ramp, L., 1961, Chromite in southwestern Oregon: Oregon Department of Geology and Mineral Industries Bulletin 52, 169 p.
- Ramp, L., 1977, Geology, mineral resources, and rock material of Curry County, Oregon: Oregon Department of Geology and Mineral Industries Bulletin, v. 88, 47 p.
- Ramp, L., 1984, Geologic map of the southeast quarter of the Pearsoll Peak quadrangle, Curry and Josephine Counties, Oregon: Oregon Department of Geology and Mineral Industries, Geologic Map Series GMS-30, scale 1:24,000.
- Ramp, L., 1986, Geologic map of the northwest quarter of the Cave Junction quadrangle, Josephine County, Oregon: Oregon Department of Geology and Mineral Industries Geologic Map Series GMS-38, scale 1:24,000,
- Ramp, L., and Peterson, N.V., 1979, Geology and mineral resources of Josephine County, Oregon: Oregon Department of Geology and Mineral Industries Bulletin, v. 100, 45 p.
- Raymond, L.A., 2015, Designating tectonostratigraphic terranes versus mapping rock units in subduction complexes: Perspectives from the Franciscan Complex of California, USA: International Geology Review, v. 57, no. 5–8, p. 801–823, https://doi.org/10.1080/00206814.2014.911124.
- Raymond, L.A., 2018, What is Franciscan?: Revisited: International Geology Review, v. 60, no. 16, p. 1968–2030, https://doi.org/10.1080/00206814 2017 1396933
- Raymond, L.A., 2019, Origin of melanges of the Franciscan Complex, Diablo Range and northern California: An analysis and review: Geosciences, v. 9, no. 8, p. 338, https://doi.org/10.3390/geosciences9080338.
- Ring, U., 2008, Deformation and Exhumation at Convergent Margins: The Franciscan Subduction Complex: Geological Society of America Special Paper 445, 61 p., https://doi.org/10.1130/SPE445.
- Roure, F., and Blanchet, R., 1983, A geological transect between the Klamath Mountains and the Pacific Ocean (southwestern Oregon): A model for paleosubductions: Tectonophysics, v. 91, no. 1–2, p. 53–72, https://doi.org/10.1016/0040-1951(83)90057-4.
- Roure, F., and DeWever, P., 1983, Découverte de radiolarites du Trias dans l'unité occidentale des Klamath, sud-ouest de l'Oregon, U.S.A.: Consequences sur l'age des peridotited de Josephine: Comptes Rendus de l'Académie des Sciences (Paris), v. 297, p. 161–164.
- Rynearson, G.A., and Smith, C.T., 1940, Chromite deposits in the Seiad quadrangle, Siskiyou County, California: U.S. Geological Survey Bulletin 922-J, p. 281–306.
- Saleeby, J.B., 1984, Pb/U zircon ages from the Rogue River area, western Jurassic belt, Klamath Mountains, Oregon: Geological Society of America Abstracts with Programs, v. 16, p. 331.
- Saleeby, J.B., and Harper, G.D., 1993, Tectonic relations between the Galice Formation and the schists of Condrey Mountain, Klamath Mountains, northern California, in Dunne, G., and McDougall, K., eds., Mesozoic Paleography of the Western United States–II: Los Angeles, California, Pacific Section, Society of Economic Paleontologists and Mineralogists, p. 61–80.
- Saleeby, J.B., Harper, G.D., Snoke, A.W., and Sharp, W.D., 1982, Time relations and structural-stratigraphic patterns in ophiolite accretion, west central Klamath Mountains, California: Journal of Geophysical Research, v. 87, p. 3831–3848, https://doi.org/10.1029/JB087iB05p03831.
- Sambridge, M.S., and Compston, W., 1994, Mixture modeling of multicomponent data sets with application to ion-probe zircon ages: Earth and Planetary Science Letters, v. 128, p. 373–390, https://doi.org/ 10.1016/0012-821X(94)90157-0.
- Scherer, H.H., and Ernst, W.G., 2008, North Fork terrane, Klamath Mountains, California: Geologic, geochemical, and geochronologic evidence for an

- early Mesozoic forearc, *in* Wright, J.E., and Shervais, J.W., eds., Ophiolites, Arcs, and Batholiths: Geological Society of America Special Paper 438, p. 289–309, https://doi.org/10.1130/2008.2438(10).
- Scherer, H.H., Ernst, W.G., and Wooden, J.L., 2010, Regional detrital zircon provenance of exotic metasandstone blocks, Eastern Hayfork terrane, western Paleozoic and Triassic belt, Klamath Mountains, California: The Journal of Geology, v. 118, p. 641–653, https://doi.org/10.1086/656352.
- Schmidt, W.L., and Platt, J.P., 2018, Subduction, accretion, and exhumation of coherent Franciscan blueschist-facies rocks, northern Coast Ranges, California: Lithosphere, v. 10, no. 2, p. 301–326, https://doi.org/10.1130/ L697.1.
- Schmidt, W.L., and Platt, J.P., 2020, Metamorphic temperatures and pressures across the eastern Franciscan: Implications for underplating and exhumation: Lithosphere, v. 2020, no. 1, https://doi.org/10.2113/2020/8853351.
- Schweickert, R.A., and Cowan, D.S., 1975, Early Mesozoic tectonic evolution of the western Sierra Nevada, California: Geological Society of America Bulletin, v. 86, p. 1329–1336, https://doi.org/10.1130/0016-7606 (1975)86<1329:EMTEOT>2.0.CO;2.
- Schweickert, R.A., and Snyder, W.S., 1981, Paleozoic plate tectonics of the Sierra Nevada and adjacent regions, in Ernst, W.G., ed., Geotectonic Development of California—Rubey Volume I: Englewood Cliffs, New Jersey, Prentice-Hall, p. 182–202.
- Schweickert, R.A., Bogen, N.L., Girty, G.H., Hanson, R.E., and Merguerian, C., 1984, Timing and structural expression of the Nevadan orogeny, Sierra Nevada, California: Geological Society of America Bulletin, v. 95, p. 967–979, https://doi.org/10.1130/0016-7606(1984)95<967:TASEOT >2.0.CO:2.
- Sharman, G.R., Sharman, J.P., and Sylvester, Z., 2018, A Python-based toolset for visualizing and analyzing detrital geo-thermochronologic data: The Depositional Record, v. 4, p. 202–215, https://doi.org/10.1002/dep2.45.
- Shenon, P. J., 1933, Geology and ore deposits of the Takilma-Waldo district, Oregon (including the Blue Creek district): U.S. Geological Survey Bulletin 846-B, p. 141–194.
- Shervais, J.W., 1982, Ti-V plots and the petrogenesis of modern and ophiolitic lavas: Earth and Planetary Science Letters, v. 59, p. 101–118, https://doi.org/10.1016/0012-821X(82)90120-0.
- Shervais, J.W., Murchey, B.L., Kimbrough, D.L., Renne, P.R., and Hanan, B., 2005, Radioisotopic and biostratigraphic age relations in the Coast Range ophiolite, northern California: Implications for the tectonic evolution of the western Cordillera: Geological Society of America Bulletin, v. 117, p. 633–653, https://doi.org/10.1130/B25443.1.
- Sigloch, K., and Mihalynuk, M.G., 2013, Intra-oceanic subduction shaped the assembly of Cordilleran North America: Nature, v. 496, p. 50–56, https:// doi.org/10.1038/nature12019.
- Sigloch, K., and Mihalynuk, M.G., 2017, Mantle and geological evidence for a Late Jurassic-Cretaceous suture spanning North America: Geological Society of America Bulletin, v. 129, p. 1489–1520, https://doi.org/ 10.1130/B31529.1.
- Smith, J.G., Page, N.J., Johnson, M.G., Moring, B.C., and Gray, F., 1982, Preliminary Geologic Map of the Medford I' × 2' Quadrangle, Oregon and California: U.S. Geological Survey Open-File Report 82-955, scale 1:250,000.
- Snoke, A.W., 1977, A thrust plate of ophiolitic rocks in the Preston Peak area, Klamath Mountains, California: Geological Society of America Bulletin, v. 88, p. 1641–1659, https://doi.org/10.1130/0016-7606 (1977)88<1641:ATPOOR>2.0.CO;2.
- Snoke, A.W., and Barnes, C.G., 2006, The development of tectonic concepts for the Klamath Mountains province, California and Oregon, in Snoke, A.W., and Barnes, C.G., eds., Geological Studies in the Klamath Mountains Province, California and Oregon: A Volume in Honor of William P. Irwin: Geological Society of America Special Paper 410, p. 1–29, https:// doi.org/10.1130/2006.2410(01).
- Speed, R.C., 1977, Island-arc and other paleogeographic terranes of late Paleozoic age in the western Great Basin, in Stewart, J.H., Stevens, C.H., and Fritsche, A.E., eds., Paleozoic Paleogeography of the Western United States: Pacific Section, Society of Economic Paleontologists and Mineralogists, p. 349–362.
- Speed, R.C., 1979, Collided Paleozoic microplate in the western U.S.: The Journal of Geology, v. 87, p. 279–292, https://doi.org/10.1086/628417.
- Suppe, J., 1973, Geology of the Leech Lake Mountain–Ball Mountain Region, California: A Cross-section of the Northeastern Franciscan Belt and Its Tectonic Implications: Berkeley, University of California Press, 82 p.

- Suppe, J., and Armstrong, R.L., 1972, Potassium-argon dating of Franciscan metamorphic rocks: American Journal of Science, v. 272, no. 3, p. 217– 233, https://doi.org/10.2475/ajs.272.3.217.
- Surpless, K.D., 2015, Hornbrook Formation, Oregon and California: A sedimentary record of the Late Cretaceous Sierran magmatic flare-up event: Geosphere, v. 11, no. 6, p. 1770–1789, https://doi.org/10.1130/GES01186.1.
- Surpless, K.D., and Beverly, E.M., 2013, Understanding a critical basinal link in Cretaceous Cordilleran paleogeography: Detailed provenance of the Hornbrook Formation, Oregon and California: Geological Society of America Bulletin, v. 125, p. 709–727, https://doi.org/10.1130/B30690.1.
- Tagami, T., and Dumitru, T.A., 1996, Provenance and thermal history of the Franciscan accretionary complex: Constraints from zircon fission track thermochronology: Journal of Geophysical Research, v. 101, p. 11,353– 11,364, https://doi.org/10.1029/96JB00407.
- Tipper, H.W., 1984, The allochthonous Jurassic-Early Cretaceous terranes of the Canadian Cordillera and their relation to correlative strata of the North American craton, in Jurassic-Cretaceous Biochronology and Paleogeography of North America: Geological Association of Canada Special Paper 27, p. 113–120.
- Ukar, E., 2012, Tectonic significance of low-temperature blueschist blocks in the Franciscan mélange at San Simeon, California: Tectonophysics, v. 568–569, p. 154–169, https://doi.org/10.1016/j.tecto.2011.12.039.
- Ukar, E., Cloos, M., and Vasconcelos, P., 2012, First 40 Ar-39 Ar ages from low-T mafic blueschist blocks in a Franciscan mélange near San Simeon: Implications for initiation of subduction: The Journal of Geology, v. 120, no. 5, p. 543–556, https://doi.org/10.1086/666745.
- Underwood, M.B., 1989, Temporal changes in geothermal gradient, Franciscan subduction complex, northern California: Journal of Geophysical Research, Solid Earth, v. 94, no. B3, p. 3111–3125, https://doi.org/10.1029/JB094iB03p03111.
- Wagner, D.L., and Saucedo, G.J., 1987, Geologic map of the Weed Quadrangle: California Division of Mines and Geology, Regional Geologic Map RGM 004, scale 1:250,000.
- Wakabayashi, J., 1992, Nappes, tectonics of oblique plate convergence, and metamorphic evolution related to 140 million years of continuous subduction, Franciscan Complex, California: The Journal of Geology, v. 100, no. 1, p. 19–40, https://doi.org/10.1086/629569.
- Wakabayashi, J., 2015, Anatomy of a subduction complex: Architecture of the Franciscan Complex, California, at multiple length and time scales: International Geology Review, v. 57, no. 5–8, p. 669–746, https://doi.org/10 .1080/00206814.2014.998728.
- Wakabayashi, J., 2017, Structural context and variation of oceanic plate stratigraphy, Franciscan Complex, California: Insight into mélange origins and subduction-accretion processes: Progress in Earth and Planetary Science, v. 4, p. 18, https://doi.org/10.1186/s40645-017-0132-y.
- Wakabayashi, J., and Dumitru, T.A., 2007, 40 Ar/39 Ar ages from coherent, high-pressure metamorphic rocks of the Franciscan Complex, California: Revisiting the timing of metamorphism of the world's type subduction complex: International Geology Review, v. 49, no. 10, p. 873–906, https://doi.org/10.2747/0020-6814.49.10.873.
- Wakabayashi, J., and Unruh, J.R., 1995, Tectonic wedging, blueschist metamorphism, and exposure of blueschists: Are they compatible?: Geology, v. 23, no. 1, p. 85–88, https://doi.org/10.1130/0091-7613(1995)023<0085:TWBMAE>2.3.CO;2.
- Waldien, T.S., and Roeske, S.M., 2019, Revisiting the petrology and age of accretionary complex rocks at Bandon, OR: Geological Society of America Abstracts with Programs, v. 51, no. 4, p. 36, https://doi.org/10.1130/ abs/2019CD-329860.
- Walker, R.G., 1977, Deposition of upper Mesozoic resedimented conglomerates and associated turbidites in southwestern Oregon: Geological Society of America Bulletin, v. 88, no. 2, p. 273–285, https://doi.org/10.1130/0016 -7606(1977)88<273:DOUMRC>2.0.CO;2.
- Wallin, E.T., and Metcalf, R.V., 1998, Supra-subduction zone ophiolite formed in an extensional forearc: Trinity terrane, Klamath Mountains, California: The Journal of Geology, v. 106, p. 591–608, https://doi.org/ 10.1086/516044.
- Wallin, E.T., Noto, R.C., and Gehrels, G.E., 2000, Provenance of the Antelope Mountain Quartzite, Yreka terrane, California: Evidence for large-scale late Paleozoic sinistral displacement along the North American Cordilleran margin and implications for the mid-Paleozoic fringing-arc model, *in* Soreghan, M.J., and Gehrels, G.E., eds., Paleozoic and Triassic

Paleogeography and Tectonics of Western Nevada and Northern California: Geological Society of America Special Paper 347, p. 119–131, https://doi.org/10.1130/0-8137-2347-7.119.

- Weiss, R.B., 2014, Identification of magma compositions using trace element partitioning in augite from the Chetco Complex, Josephine ophiolite and Grayback pluton located in the Klamath Mountains, Oregon and the implications for tectonic setting [Master's thesis]: Lubbock, Texas Tech University, 572 p.
- Wells, F.G., and Walker, G.W., 1953, Geology of the Galice quadrangle, Oregon: U.S. Geological Survey Quadrangle Map GQ-25, scale 1:62,500, https://doi.org/10.3133/gq25.
- Wells, F.G., Hotz, P.E., and Cater, F.W., Jr., 1949, Preliminary description of the geology of the Kerby quadrangle, Oregon: Oregon Department of Geology and Mineral Industries Bulletin 40, 23 p.
- Wernicke, B., and Klepacki, D.W., 1988, Escape hypothesis for the Stikine block: Geology, v. 16, p. 461–464, https://doi.org/10.1130/0091-7613 (1988)016<0461:EHFTSB>2.3.CO;2.
- Wiley, T.J., McClaughry, J.D., and D'Allura, J.A., 2011, Geologic Database and Generalized Geologic Map of Bear Creek Valley, Jackson County, Oregon: Oregon Department of Geology and Mineral Industries Open-File Report O-2011-11, scale 1:24,000.
- Wiley, T.J., McClaughry, J.D., Rivas, J.A., and Schwartz, J.J., 2017, Detrital zircon assemblages in sandstone indicate revised early to late Cretaceous age for the Dothan Formation in southwestern Oregon: Geological Society of America Abstracts with Programs, v. 49, no. 4, https://doi.org/10.1130/abs/2017CD-292968.
- Wise, J.P., 1969, Geology and petrography of a portion of the Jurassic Galice Formation, Babyfoot Lake area, southwestern Oregon [M.S. thesis]: Pocatello, Idaho State University, 108 p.
- Wolf, M.B., and Saleeby, J.B., 1995, Late Jurassic dike swarms in the south-western Sierra Nevada Foothills terrane, California: Implications for the Nevadan orogeny and North American plate motion, in Miller, D.M., and Busby, C., eds., Jurassic Magmatism and Tectonics of the North American Cordillera: Geological Society of America Special Paper 299, p. 203–228, https://doi.org/10.1130/SPE299-p203.
- Worrall, D.M., 1981, Imbricate low-angle faulting in uppermost Franciscan rocks, south Yolla Bolly area, northern California: Geological Society of America Bulletin, v. 92, no. 10, p. 703–729, https://doi.org/10.1130/0016 -7606(1981)92<703:ILFIUF>2.0.CO;2.
- Wright, J.E., 1982, Permo-Triassic accretionary subduction complex, south-western Klamath Mountains, northern California: Journal of Geophysical Research, v. 87, p. 3805–3818, https://doi.org/10.1029/JB087iB05p03805.
- Wright, J.E., and Fahan, M.R., 1988, An expanded view of Jurassic orogenesis in the western United States Cordillera: Middle Jurassic (pre-Nevadan) regional metamorphism and thrust faulting within an active arc environment, Klamath Mountains, California: Geological Society of America Bulletin, v. 100, p. 859–876, https://doi.org/10.1130/0016-7606 (1988)100<0859:AEVOJO>2.3.CO;2.
- Wright, J.E., and Wyld, S.J., 1986, Significance of xenocrystic Precambrian zircon contained within the southern continuation of the Josephine ophio-

- lite: Devils Elbow ophiolite remnant, Klamath Mountains, northern California: Geology, v. 14, p. 671–674, https://doi.org/10.1130/0091-7613 (1986)14<671:SOXPZC>2.0.CO;2.
- Wright, J.E., and Wyld, S.J., 1994, The Rattlesnake Creek terrane, Klamath Mountains, California: An early Mesozoic volcanic arc and its basement of tectonically disrupted oceanic crust: Geological Society of America Bulletin, v. 106, p. 1033–1056, https://doi.org/10.1130/0016 -7606(1994)106<1033:TRCTKM>2.3.CO;2.
- Wright, J.E., and Wyld, S.J., 2006, Gondwanan, Iapetan, Cordilleran interactions: A geodynamic model for the Paleozoic tectonic evolution of the North American Cordillera, in Haggart, J.W., Enkin, R.J., and Monger, J.W.H., eds., Paleogeography of the North American Cordillera: Evidence For and Against Large-Scale Displacements: Geological Association of Canada Special Paper 46, p. 377–408.
- Wyld, S.J., 1985, Geology of the western Jurassic belt, South Fork Trinity River area, Klamath Mountains, California [M.S. thesis]: Berkeley, University of California, 168 p.
- Wyld, S.J., 1991, Permo-Triassic tectonism in volcanic arc sequences of the western U.S. Cordillera and implications for the Sonoman orogeny: Tectonics, v. 10, p. 1007–1017, https://doi.org/10.1029/91TC00863.
- Wyld, S.J., 2002, Structural evolution of a Mesozoic back-arc fold-thrust belt in the U.S. Cordillera: New evidence from northern Nevada: Geological Society of America Bulletin, v. 114, p. 1452–1468, https://doi.org/ 10.1130/0016-7606(2002)114<1452:SEOAMB>2.0.CO;2.
- Wyld, S.J., and Wright, J.E., 1988, The Devils Elbow ophiolite remnant and overlying Galice Formation: New constraints on the Middle to Late Jurassic evolution of the Klamath Mountains, California: Geological Society of America Bulletin, v. 100, p. 29–44, https://doi.org/10.1130/0016 -7606(1988)100<0029:TDEORA>2.3.CO;2.
- Wyld, S.J., Rogers, J.W., and Copeland, P., 2003, Metamorphic evolution of the Luning-Fencemaker fold-thrust belt, Nevada: Illite crystallinity, metamorphic petrology, and ⁴⁰Ar/³⁹Ar geochronology: The Journal of Geology, v. 111, p. 17–38, https://doi.org/10.1086/344663.
- Yule, J.D., 1996, Geologic and tectonic evolution of Jurassic marginal ocean basin lithosphere, Klamath Mountains, Oregon [Ph.D. thesis]: Pasadena, California Institute of Technology, 308 p.
- Yule, J.D., Saleeby, J.B., Jones, D.L., and Silk, M., 1992, Correlation of basement terranes across the Late Jurassic Josephine inter-arc basin, southwestern Oregon and northern California: Geological Society of America Abstracts with Programs, v. 24, p. 93.
- Yule J.D., Saleeby, J.S., and Barnes, C.G., 2006, A rift-edge facies of the Late Jurassic Rogue–Chetco arc and Josephine ophiolite, Klamath Mountains, Oregon, in Snoke, A.W., and Barnes, C.G., eds., Geological Studies in the Klamath Mountains Province, California and Oregon: A Volume in Honor of William P. Irwin: Geological Society of America Special Paper 410, p. 53–76, https://doi.org/10.1130/2006.2410(03).

Manuscript Accepted by the Society 22 July 2021